Tilburg School of Economics and Management

An Empirical Analysis of Cost-of-Carry and Quarterly Futures Prices in the Cryptocurrency Market

A thesis submitted in partial fulfillment of the requirements for the degree of MSc Quantitative Finance and Actuarial Science

S.N.C van Rij
SNR: 2001707
ANR: 618727
s.n.c.vanrij@tilburguniversity.edu

Supervised by:
dr.ir. G.W.P. Charlier

April 13, 2023

Abstract

This thesis aims to find a satisfactory cost-of-carry model that can explain the futures basis for the largest two cryptocurrencies, Bitcoin and Ethereum. Empirical evidence shows Bitcoin and Ethereum expressing a substantial and volatile futures basis, reaching values greater than 10% with a maturity of a maximum of six months. It is investigated in this thesis if a model exists that can explain this volatile futures basis. In order to do so, cost-of-carry models from investment assets and commodities are tested on Bitcoin and Ethereum futures data. The testing procedure is the two-step Engle-Granger test used to establish a cointegrating relationship between actual futures prices and predicted futures prices according to the models. It is found that the cost-of-carry model for investment assets has a cointegrating parameter magnitudes too large to explain the observed futures basis. Under the cost-of-carry model for commodities, all this unexplained futures basis has to be explained by a parameter defined as the net convenience yield. It is concluded that it is unrealistic that the net convenience yield can explain a futures basis greater than 10%. These results imply that the cryptocurrency market is inefficient, and arbitrage opportunities exist. Schmeling et al. (2022) perform similar research to this thesis, and conclude that there is too little capital in the form arbitrageurs to restore efficiency in the futures market. This thesis builds on this conclusion, and shows that arbitrageurs experience high opportunity costs in the form of a profitable alternative: cash-and-carry trades on perpetual futures. Arguments are given to motivate that this opportunity cost in combination with other factors leads to perpetual futures directly influencing quarterly futures. To test this hypothesis, a new cost-of-carry model is proposed, with the perpetual futures funding rate as a native crypto risk-free rate proxy. This proxy is modeled using an $ARIMA(p, d, q)$ model. The proposed model performs significantly better in terms of cointegration, resulting in a cointegration parameter substantially closer to 1. This results in a higher explanation of the Bitcoin and Ethereum futures basis under this new model.

Contents

1 Introduction

The introduction of Bitcoin by Nakamoto (2008) as the first decentralized peer-to-peer digital currency has initiated the interest in a new disruptive type of technology, called blockchain technology. A blockchain is a distributed ledger of transactions on a decentralized computer network. The ledger is public and can be verified independently by the computers that make up the network, without being reliant on a single entity. The decentralized and open-source characteristics of blockchain technology allow everyone who is technically capable to create a new blockchain or build upon an existing one. Cryptocurrencies are digital currencies that reside on a blockchain. White (2015) defines cryptocurrencies as transferable digital assets, secured by cryptography. Due to the increasing popularity of blockchain technology and cryptocurrencies, there are now more than 13000 cryptocurrencies in existence (Coingecko [1]). As cryptocurrencies have become well known, its market has seen explosive growth over the last decade, growing to an asset class with a market capitalization of almost 3 trillion dollars at its peak at the end of 2021 (Coingecko). The cryptocurrency market is characterized by high volatility, leading to fast price increases as well as decreases, being infamous for its bubble-like behavior. Enoksen et al. (2020) conclude that cryptocurrencies have experienced multiple bubble periods, especially in the periods 2017 and 2018. This bubble-like behavior has attracted a large amount of speculative capital, as well as fuelling the desire to hedge against these enormous price fluctuations by parties such as miners, which are entities responsible for securing the network and issuing new Bitcoin in the process. The inflow of speculative capital and the demand for hedging has led to a rapidly growing futures market of cryptocurrencies.

The futures market of cryptocurrencies differs significantly from those of more established asset classes. The markets of cryptocurrencies are never closed, not even during the weekend. Most volume on cryptocurrency futures takes place on native cryptocurrency exchanges, often operating offshore and unregulated. There are regulated ventures where institutional investors can trade on cryptocurrency futures, but these are limited with most notably only the *Chicago Merchantile Exchange (CME)* offering Bitcoin and Ethereum futures. Another noteworthy difference between the futures market of cryptocurrencies and larger asset classes is the high degree of retail investors active in the cryptocurrency futures market. These investors are classified as particularly active. Lammer et al. (2019) report investors in cryptocurrencies logging into their brokerage accounts 9 times per month, compared to other markets where the average tends to be 2 times. In addition to being more active, the degree of risk-tolerance of these retail investors is considered to be greater than observed in other markets. Grobys and Junttila (2020) find a high degree of *lottery-demand*, where investors are drawn to the high volatility in the cryptocurrency market. The potential of high returns due to this volatility is perceived to be attractive, whilst empirical evidence suggests this results in losses more often than gains. The characteristics of the cryptocurrency futures market fit well with this high-risk tolerance, as the markets are never closed and a high degree of *leverage* can be used on cryptocurrency futures. As a result of a high presence of retail investors and a high degree of excessive speculation, an inefficient market structure in cryptocurrency futures is observed. The observed *futures basis* over the last three years has exceeded 10% for futures with a maturity of only a few months. This empirical observation leads to the question whether these futures are efficiently priced, or that the cryptocurrency market is found to be inefficient.

The literature regarding fair pricing of futures for market such as stocks, bonds, currencies or commodities is extensive and dates back several decades. The work of Cox et al. (1981), Jarrow and Oldfield (1981), French (1983) and Cornell and French (1983) regarding the conditions of a no-arbitrage futures price has led to a general class of models used for no-arbitrage futures pricing being developed, called *cost-of-carry models*. These models assume that in a frictionless market, the futures price should be the spot price with any *carry costs* incorporated. The existence of carry costs is due to the deferred payment property of futures contract, a futures contract bought at time t does not have any payment until time T, whilst for spot assets, payment is due immediately.

[1] Retrieved from https://www.coingecko.com on November 2nd 2021

This means that from time t to T capital could be invested at the risk-free rate, making it a so-called carry cost. The exact formulation of the cost-of-carry model are asset-class specific and depends on the carrying variables. In this thesis, widely accepted cost-of-carry models for stocks, bonds, currencies and commodities are discussed.

The testing procedure of cost-of-carry models described by Heany (2001) is akin to testing the market efficiency. This follows from the fact that under the cost-of-carry model there exists a unique no-arbitrage price for a futures contract, given the spot price and the carry factors. Damodaran (2004) tabulates possible profitable arbitrage opportunities originating from a self-financing portfolio if the cost-of-carry models do not hold. In an efficient market, it is therefore expected that an equilibrium around this no-arbitrage price is established. This does not mean that the no-arbitrage price will always hold, Maslyuk and Smyth (2009) describe that short-term deviations may occur, but in an efficient market arbitrageurs will restore equilibrium due to arbitrage opportunities being possible. The testing procedure of these cost-of-carry models therefore comes down to testing for a long-run equilibrium. Similar research as performed in this thesis, such as Quan (1992), Heany (2001), Asche and Guttormsen (2002) and Wu et al. (2021), describe testing for cointegration to be applicable in this type of research. Cointegration is a relatively new concept in econometrics, with the work of Engle and Granger (1987) setting the stage in the literature for research of this particular topic. The motivation behind cointegration lies in the problems that arise when performing statistical analysis on non stationary data. It is well-known in the literature that prices of financial assets consist of a stochastic trend and may therefore be non stationary. As a result, *spurious regressions* may occur. Testing for cointegration ensures that the regression analysis is valid, and it can be tested whether a long-run equilibrium exists.

Despite extensive research regarding fair futures pricing in other markets, little research has been done on this topic for the cryptocurrency market, and most research dates back only a few years, such as Corelli (2018), Lian et al. (2019), Kapar and Olmo (2019), Hu et al. (2020), Wu et al. (2021), Schmeling et al. (2022), and He et al. (2023). This thesis aims to contribute to this rapidly developing field of literature. Specifically, it aims to find a model that can explain the futures basis observed for Bitcoin and Ethereum. This will be done by first testing traditional models on the market data, and later developing a new model. The practical implications of this thesis are mainly a more robust understanding of the cryptocurrency futures market both for researchers and investors. The futures market of cryptocurrencies may not yet be fully understood by researchers wishing to model futures prices. This thesis aims to provide a new benchmark model where future research can elaborate on. The application of this thesis from an investor point of view is a better understanding of the dynamics of the Bitcoin and Ethereum futures market. The extensive explanation of the risks imposed by Coin-M futures, an analysis of historical futures basis, and establishing the connection between perpetual and quarterly futures contribute to a greater understanding of the cryptocurrency futures market. This will hopefully contribute to an industry-standard cost-of-carry model, that will improve the efficiency of the cryptocurrency futures market.

This thesis is structured as follows. Section 2 introduces the theory of futures prices, and derives through possible arbitrage opportunities the fair futures price for a simple asset. This is then extended using a class of *cost-of-carry models* for different asset classes. Section 3 aims to give the reader a thorough introduction of the futures market of cryptocurrencies specifically, and ties the theory given in section 2 to cryptocurrencies. Section 4 provides the theory required for an understanding of the unit root and cointegration tests used later. Section 5 performs all time series analysis and develops a new model to price quarterly futures prices in the cryptocurrency market. Section 6 summarizes all results found in this thesis and proposes recommendations future research for this particular topic.

2 Futures Contracts

This section will give an introduction to futures contracts. Futures are a special type of forward contracts. Therefore, we introduce forward contracts first and then discuss futures contracts.

2.1 Forward Contracts

Before discussing *futures contracts*, it is important to define what *forward contracts* are, since a futures contract is essentially a standardized version of a forward contract. According to Hull (2014), a forward contract is an agreement to acquire or sell an asset at a specific future time for a specified price. A forward contract is considered to be very flexible, and is simply an agreement between two parties to exchange an asset at a specified date for a prespecified price. There are no restrictions on the contract size or maturity date, as long as both the buyer and seller of a contract agree on the terms specified in the contract. An important property of a forward contract is that the cashflow of a forward contract written at time t, with expiration at time T ($t < T$), is zero. Recall that a forward contract at time t is simply an agreement between a buyer and seller upon a transaction which will take place in the future (the delivery date T), and thus initially no money changes hands. Buyers or sellers of forward contracts may have different objectives in mind. The buyer of a forward contract could be a speculator, or a large buyer that wants to minimize price fluctuations of purchases. This would be the case for an airline, who is a large buyer of fuel. The price of fuel for air crafts is highly correlated with the price of oil. The airline could buy oil forwards for next year to minimize price fluctuations on fuel costs in case the spot price of oil rises next year. The seller of a forward contract could be a producer of a commodity, or a party that holds a large quantity of the underlying asset. By selling at a predetermined price in the future, price risk can be minimized. For example, a large Australian wheat farmer who expects to have a large amount of harvest in December may want to sell a December forward contract and 'lock in' a price in the case that the demand of wheat drops in December.

To illustrate forward contracts in more detail, consider the example of the wheat farmer. Suppose the current wheat spot price is \$80. The wheat farmer with harvest in December, 1 year from now, does not want to be exposed to price fluctuations and enters a forward contract for to sell 1 bushel of wheat for a price of \$80.80 in December. The counter party of the wheat farmer, to be called *party A*, bought the contract and has a *long position* for 1 bushel of wheat. The wheat farmer, who will be called *party B* from now on, sold the contract and has a *short position* of 1 bushel of wheat. Party A will buy the bushel of wheat at a *predetermined* price of \$80.80 in December from party B. In other words, the long position of the forward will receive the underlying asset, and the short position will deliver the underlying asset. The payoff of party A corresponding to the price in December is visualized in Figure 1.

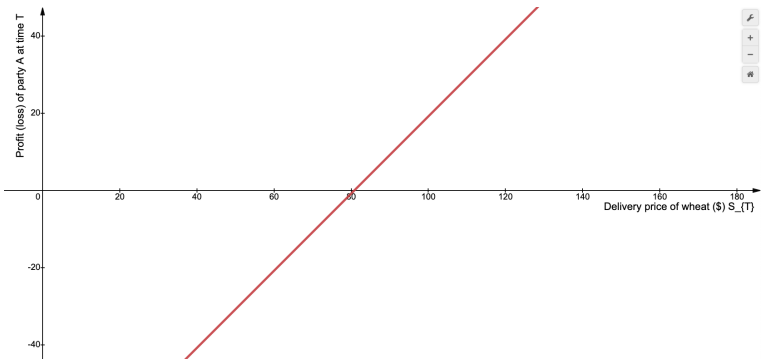

Figure 1: Payoff of party A as a function of the price of wheat at expiration. Graph made using Desmos.

The x-axis shows the spot wheat price at expiration (December), and the y-axis shows the profit or loss in dollars. If the spot price in December is above \$80.80, then party A made a profit since an agreement was made to buy the bushel of wheat for \$80.80. Party B loses an equivalent amount of money since party B agreed to sell to party A for a price of \$80.80. When the contract matures, party B will either physically deliver the bushel of wheat to party A (physical delivery), or the profit is transferred to the party that was in profit (cash settlement). As becomes clear from this example, a forward contract is an agreement between two (physical) parties. Therefore, forward contracts are traded *over-the-counter (OTC)*. This means forward contracts are not listed on any exchanges. In order to engage in the desired contract, buyers or sellers have to find a counter party, since a forward contract requires both a buyer and a seller in order to be written. Despite the existence of OTC brokers [2], finding a counter party for an OTC contract is generally considered to be more difficult than using a centralized venture such as an exchange. As a result, forward contracts are considered to be less liquid than derivatives traded on exchanges, such as futures, which will be discussed in section 2.2.

2.1.1 Pricing and Valuing Forward Contracts

The forward price is the agreed upon price for which the buyer of a forward contract will buy a specific quantity of an underlying asset from the seller at a certain date at delivery date T. Let S_t denote the *spot price* of the underlying asset at time t, and $FO(t,T)$ the time-t *forward price* with expiration at time T. We assume that is it not possible to exit a forward contract before expiration date T. If a buyer (seller) of a forward contract wants to close the position, it is more common to sell (buy) a forward contract with the same delivery date. Cox et al. (1981) set the stage for research in fair forward pricing. In their paper, Cox et al. (1981) show that the fair time-t forward price $FO(t,T)$ can be derived using arbitrage arguments. Let $P(t,T)$ be the time t price of a (zero-coupon) risk-free bond that pays \$1 at time T ($t < T$). When interest rates are positive, $P(t,T) < 1$ [3]. We then perform the following investment strategy:

A long position of 1 forward contract $FO(t,T)$ is taken, at time t, with expiration at time T. We then subsequently invest $FO(t,T)P(t,T)$ amount [4] in risk-free bonds at time t,with a price of $P(t,T)$ and maturity at time T. If we let $\pi_1(t)$ denote the portfolio value of this strategy at time t we have:

$$\pi_1(t) = FO(t,T)P(t,T) \tag{1}$$

This investment strategy at time t only requires a payment of $FO(t,T)P(t,T)$, since taking a long position in a forward contract at time t has a cash flow of zero. Thus, only the $FO(t,T)P(t,T)$ amount invested in risk-free bonds has to be paid at time t. At time T, the forward contracts will have a payoff of $FO(t,T)$. Note that we have the terminal condition $FO(T,T) = S_T$, since the underlying asset will be delivered at time T to the long position of the forward contract. Thus, the time T payoff of the forward contract is $S_T - FO(t,T)$. This is from the perspective of the long position. For the perspective of the short position, the payoff will be the exact opposite, $FO(t,T) - S_T$. To avoid confusion, we will always consider the position of the long position unless stated otherwise. For the payoff of the risk-free bonds, we know each bond $P(t,T)$ pays \$1 at time T. Thus the part of the strategy which invested in risk-free bonds has a payoff at time T of $FO(t,T)P(T,T) = FO(t,T)$. Combining the above, the investment strategy proposed by Cox et al. (1981) of investing $FO(t,T)P(t,T)$ in risk-free bonds and taking a long position in the

[2] OTC brokers are entities which try to match buyers and sellers of OTC traded contracts. This makes finding a counter party of a forward contract easier.

[3] If $P(t,T) \geq 1$ and interest rates are positive, investors would pay more to hold a bond for (T-t) years than the face value of \$1. Meanwhile, depositing money in a bank account earns a positive return. Therefore, in a rational market, there would be no demand for this bond until the price $P(t,T) < 1$. For negative interest rates, the scenario $P(t,T) \geq 1$ would be possible, however.

[4] Suppose the price of 1 forward contract $FO(t,T)$ is \$10. The price of a bond that pays \$1 in (T-t) years is 0.9. We would then invest $10 * 0.9 = \$9$ in risk-free bonds.

forward contract $FO(t,T)$ yields the following portfolio value $\pi_1(T)$ at time T:

$$\pi_1(T) = [S_T - FO(t,T)] + FO(t,T) \tag{2}$$
$$= S_T \tag{3}$$

From (1) and (3) we see that a strategy of investing $FO(t,T)P(t,T)$ at time t yields a payoff of S_T at time T. Now consider the (trivial) investment strategy of buying 1 unit of S_t at time t. This has a payment of S_t at time t, since payment is due immediately. Let $\pi_2(T)$ denote the portfolio value of holding 1 unit of S_t until time T (assuming no payments such as dividends). The portfolio value of this strategy at time T is given by:

$$\pi_2(T) = S_T \tag{4}$$

The second strategy of holding 1 unit of S_t until time T yields the same time T portfolio value as the strategy of taking a long position in a forward contract and buying risk free bonds.(i.e. $\pi_1(T) = \pi_2(T)$). Table 1 shows the time t and T portfolio values for the strategies discussed earlier. Since both strategies do not have inflow or outflow between time t and T, both strategies are said to be *self-financing*. Schumacher (2020) describes a self-financing strategy as a trading strategy with no outside deposits or withdrawals:

Strategy	$\pi(t)$	$\pi(T)$
1	$FO(t,T)P(t,T) + 0$	$FO(t,T) + (S_T - FO(t,T)) = S_t$
2	S_t	S_T

Table 1: Portfolio values at time t and T of strategy 1 (π_1) and strategy 2 (π_2), respectively. Note that the '+0' stems from the fact that taking a long position in forward contract at time t has a deferred payment until time T.

Now suppose that $FO(t,T)P(t,T) < S_t$, or equivalent, $\pi_1(t) < \pi_2(t)$. We know that $\pi_1(T) = \pi_2(T)$. An arbitrageur could make a risk-less profit by selling short 1 unit of S_t, and performing the same procedure as strategy 1. At time T, the profit of the arbitrageur would be $FO(t,T)P(t,T) - S_t > 0$, since the portfolio is self-financing (no in- or outflows). In an arbitrage-free market we must thus have:

$$\pi_1(t) = \pi_2(t) \iff FO(t,T)P(t,T) = S_t \iff FO(t,T) = \frac{S_t}{P(t,T)} \tag{5}$$

Therefore, Cox et al. (1981) state that the time-t forward price is given by: $FO(t,T) = \frac{S_t}{P(t,T)}$. The (no-arbitrage) time t forward price is the current spot price S_t discounted by the return of a risk-free bond. For positive interest rates, the no-arbitrage forward price will be above the spot price, and vise versa for negative interest rates. The notation of Cox et al. (1981) using $P(t,T)$, is not common practice in literature regarding forward pricing. Most literature such as Cornell and French (1983), Gibson and Schwartz (1990), and Pinkdyck (2001) express fair forward prices using the risk-free rate $r_{t,T}$. However, this is equivalent to using a zero-coupon bonds $P(t,T)$. If we assume the zero-coupon bond is continuously compounding and pays \$1 at time T, we have: $P(t,T) = 1 * e^{-r_{t,T}(T-t)} = e^{-r_{t,T}(T-t)}$. Since we discuss zero-coupon bonds here, and the time to maturity $(T-t)$ is known, $r_{t,T}$ is the risk-free rate of holding the bond from time t to time T. According to Cox et al. (1981), the forward price has to be discounted by this risk-free rate. Mathematically,

$$FO(t,T) = \frac{S_t}{P(t,T)} = \frac{S_t}{e^{-r_{t,T}(T-t)}} \tag{6}$$
$$= S_t e^{r_{t,T}(T-t)} \tag{7}$$

The fair forward price is thus given by $FO(t,T) = S_t e^{r_{t,T}(T-t)}$, where $r_{t,T}$ can be derived from a zero-coupon bond. Referring back to the example of 1, the forward price agreed upon by parties A and B was 80.80, $r_{t,T} = 0.01$, and the contract written at time t with maturity in 1 year. The spot price S_t was \$80. It can now be verified that this is a fair forward price, since $FO(t,T) = 80e^{0.01(T-t)} = 80e^{0.01*1} = 80.80$. This form of forward pricing is the most simple form, and describes in a perfect efficient and complete market what the forward price should be. We will see later, however, that certain factors can cause the forward price to deviate from this no-arbitrage price.

Now that an expression for the fair forward price is derived, the *value* of a forward contract is discussed. Confusion often arises between the price and value of a forward contract. Let $s \in \{t, t+1, ..., T\}$. The value of a forward contract at time s, written at time t, with expiration at time T is given by $VO(s,t,T)$[5]. Intuitively, the value of a forward contract can be described as the profit (loss) of the forward contract at any period in time. To start, there are two important boundary conditions for the value of a forward contract. Assume a forward contract is written at time t with expiration at time T. Any forward contract written at time t must satisfy $VO(t,t,T) = 0$. This condition is related to the fair forward price $FO(t,T)$, where it was assumed that a forward price is chosen such that no arbitrage opportunities are possible. This condition also seems intuitive, since when two (rational) parties agree upon a forward contract, the transaction would not take place if $VO(t,t,T) \neq 0$. Both parties have to agree upon a price, and if $VO(t,t,T) \neq 0$, then either the buyer or seller is initiating the contract at a sub-optimal price. Therefore, it should hold that $VO(t,t,T) = 0$. Another boundary condition is $VO(T,t,T) = S_T - FO(t,T)$. At time t (when the contract is written), the buyer and seller of a forward contract agreed upon a price $FO(t,T)$. At time T, this payment is due and the buyer receives the underlying asset S_T for and pays a price of $FO(t,T)$. Therefore, the value of the forward contract at time T $VO(T,t,T) = S_T - FO(t,T)$. Note that this is from the perspective of the buyer (person who has a long position). For the seller (person who has a short position), the value at time T of the forward contract would be $VO(T,t,T) = FO(t,T) - S_T$. To avoid confusion regarding the meaning of $VO(T,t,T)$, we will look at $VO(T,t,T)$ from the perspective of the buyer. The seller of a forward contract is assumed to have a position of -1 forward contracts such that $-VO(T,t,T) = -1 * (S_T - FO(t,T) = FO(t,T) - S_T$. Referring back to the example above, the forward price agreed upon by parties A and B was \$80.80 at time t. So, $VO(T,t,T) = S_T - 80.80$ for party A (the buyer). For party B (the seller), the value of the contract at time T is $-VO(T,t,T) = 80.80 - S_T$. If the price at time T is \$100, $VO(T,t,T) = 100 - 80.8 = 19.2$. Party B has sold one forward contract, and thus 'holds' -1 forward contract, with a loss of $-1 * VO(T,t,T) = -19.2$.

Now that boundary conditions are discussed, we generalize this to a time s setting to determine $VO(s,t,T)$, where $s \in \{t, t+1, ..., T\}$. Note that this implies that it is attempted to value a forward contract that has already been written at time t. Recall that a forward contract can not be closed early. So in order to determine the value of a forward contract at time s (which has already been written at time t), a new forward contract is used.

Time	Action	Price
t	Buy forward	$FO(t,T)$
s	Sell forward	$FO(s,T)$
T	Receive S_T	S_T
T	Deliver S_T	S_T

Table 2: Trading strategy visualized where a trader buys a forward contract at time t (with expiration at time T), and sells a forward contract at time s (also with expiration at time T)

Table 2 shows a trading strategy of first buying a forward contract at time t with expiration at time

[5]The notation $VO(s,t,T)$ might seem odd, however, later we will denote the value of a futures contract as well. Since we have $FO(t,T)$ for the price of a forward contract, $VO(s,t,T)$ is used to remain consistent.

T, and then selling a similar contract at time s. From time t onwards, the exposure of the trader to the underlying asset is zero, since at time T we can use the received S_T from the long position to deliver the S_T for the short position. Therefore, $VO(s,t,T) = FO(s,T) - FO(t,T)$. This is under the assumption that a counter party is willing to buy the forward contract from the trader at the fair forward price $FO(s,T)$ at time s. If so, the trader is always able to artificially close the forward position and thus realize the value of $VO(s,t,T) = FO(s,T) - FO(t,T)$. Making it more concrete, consider the example of the wheat forward contract again. Suppose $s = t+1$, such that time to maturity is 11 months. The spot price of wheat $S_s = 90$. Assume the 1-year interest rate is still 1%. Party A has bought the forward contract for \$80 and wants to realize his profit. The fair forward price at time $s = t+1$ with maturity at T is: $FO(t+1,T) = 90e^{0.01\frac{11}{12}} = 90.82$. Constructing a similar table as 2, we get:

Time	Action	Price
t	Buy forward	80.80
s	Sell forward	90.82
T	Receive S_T	S_T
T	Deliver S_T	S_T

Table 3: Table 2 specified to our example

From table 3, we see that the value of the forward contract at time t is $VO(s,t,T) = FO(s,T) - FO(t,T) = 90.82 - 80.80 = 10.02$.

To conclude this section, it has been shown by arbitrage arguments given by Cox et al. (1981), that the fair forward price at time t is given by $FO(t,T) = \frac{S_t}{P(t,T)} = S_t e^{r_{t,T}(T-t)}$. Consequently, by performing a trading strategy, the time s value of a forward contract is shown to be $VO(s,t,T) = FO(s,T) - FO(t,T)$ with boundary conditions $VO(t,t,T) = 0$ and $VO(T,t,T) = S_T - FO(t,T)$,

2.2 Futures Contacts

Now that the definition and pricing methods of forward contracts have been given, futures contracts can be discussed. To summarize in one sentence: *A futures contract is a standardized version of a forward contract which is marked to market by exchanges.* Forward contracts have been discussed prior to futures contracts, due to the fact that a futures contract is a standardization of the forward contracts

2.2.1 Introduction to Futures Contracts

Forward contracts are exchanged over-the-counter (OTC), whereas futures contracts are standardized versions and traded on exchanges like the *Chicago Mercantile Exchange (CME)*. The exchanges create futures contracts with fixed expiration dates and contract sizes. The exchange on which the futures are traded determines when the futures expire, and what the size of a contract should be. This makes futures contracts less flexible than forward contracts because in a forward contract the two parties engaging in the contracts are free to set the date and size of the contract (as long as both parties agree). For futures contracts, the exchange on which the futures are traded takes care of the settlement. In case of a forward contract, both parties engaged in the contract rely upon each other to make sure the transaction is settled at the end of the contract. This makes a forward contract more vulnerable to *counter party risk*, as the engaging parties in the contract do not know the complete financial position of their counter party, and the other party can default and not fulfill the obligation stated in the forward contract. For futures contracts traded on exchanges, this counter party risk is lower as the exchange acts as a third party. If one of the parties of a contract is at risk of defaulting, the exchange will know this before the contract

is settled and manually close the position for that party. This property of the exchanges taking care of settlement allows for trading futures contract without having to know the counter party. This is different from forward contract, where a (physical) counter party has to be found and kept in contact with whilst in a forward contract.

In order to make sure users of exchanges do not default on the obligations stated in the futures contract, the exchanges settle the futures contract at the end of each trading day. The main difference between forward contracts and futures contracts is the settlement executed by the exchanges. In order to make sure users of exchanges do not default on the obligations stated in the futures contract, the exchanges settle the futures contract at the end of each trading day. This settlement process is called *Mark-to-Market (MTM)*, which entails the adding or subtracting of profit or loss to or from the account balance of the user at the end of each trading day. This addition or subtraction of daily profit and comparison with forward contracts will be discussed in more detail later in Table 5. The process of mark-to-market in addition with the concept of *margin requirements* reduce counter party risk for traders. Futures exchanges use two types of margin requirements: *initial margin* and *maintenance margin*. The initial margin is the amount of capital that is required to open a position, relative to the dollar amount of the futures position size. The maintenance margin is the minimal amount of capital relative to the position size in order to keep the position open after it has already been opened. The process of mark-to-market done by exchanges at the end of each trading day either increases or decreases the collateral of the buyer or seller of the contract. If the collateral of the buyer or seller falls below the maintenance margin, a *margin call* will be made. This is a notice to top-up the collateral back to the maintenance margin level. If this does not happen, the exchange will close the position for the trader. To illustrate the concepts of margin on exchanges, we continue with the example given earlier. Suppose the initial margin is set to 50% and the maintenance margin 25%. Party A posts \$40 in collateral to precisely satisfy the initial margin and proceeds to buy 1 futures contract with a price of \$80. Table 4 shows the process of mark-to-market and when the trader would get a margin-call. Let $F(t,T)$ denote futures price at time t with expiration at time T.

t	F(t,T)	Daily Profit	Collateral	Maintenance Margin
0	80	0	40	20
1	70	-10	30	20
2	90	20	50	20
3	60	-30	20	20
4	**59**	**-1**	**19**	**20**

Table 4: Simulating the evolution of a futures price $F(t,T)$ and the corresponding process of mark to market. The trader posts \$40 of collateral and takes a long position of 1 unit of $F(t,T)$ at t=0.

In Table 4 the process of the futures contract being marked to market at the end of each trading day is visible. The daily profit, i.e. $F(t,T)-F(t-1,T)$ is added or subtracted from the collateral of the trader. Thus, the exchange settles the futures contract at the end of time t, and automatically writes a new futures contract at time $t+1$ with expiration date T. The row in bold, $t=4$, shows the collateral of the trader falling below \$20, the maintenance margin. If this happens, a margin call is made. If the trader does not top-up his collateral to at least the maintenance margin within a certain time frame, the exchange will close the position for the trader. This is called a *liquidation*. This makes sure that the exchange does not incur bad debt and the trader who has the opposite position can always get paid.

2.2.2 Pricing and Valuing of Futures Contracts

In section 2.1, the no-arbitrage forward price was defined as $FO(t,T) = S_t e^{r_{t,T}(T-t)}$. Recall that a forward contract makes no payments during the life of the contract until expiration date T. For

futures contracts, this is different due to the property of daily mark-to-market of exchanges. At the end of each day the daily profit or loss is added to or subtracted from the collateral of the trader on an exchange. Table 5 shows the property of mark-to-market of futures contracts. Each day the price of the futures contract increases by two and is added to the collateral on a daily basis. For the forward contract this does not happen and the payout happens at once at time T. As a result, the value of a futures contract is zero after this mark-to-market payout has been completed. The term mark-to-market essentially means that at the end of each period (in this case day), the futures contract is valued at the market price, and payout is transferred to the holder of the futures contract. For a forward contract, we defined the value as the 'unrealized profit or loss' of a forward contract that could be realized by buying or selling an equivalent contract at time $s \in \{t, ..., T\}$. For futures contracts, the mark to market property does this for us, and the profit (loss) is realized at the interval at which the mark to market takes place.

t	$F(t,T)$	Daily Profit	Collateral	$FO(t,T)$	Daily Profit
0	80	0	40	80	-
1	82	2	42	82	-
2	84	2	44	84	-
3=T	86	2	46	86	6

Table 5: Simulating the evolution of a futures price $F(t,T)$ and forward price $FO(t,T)$ and showing that the futures contract will have a daily payout whilst the forward contracts does not. Note that we have $F(t,T) = FO(t,T)$ here for simplicity. At time T, we have $F(T,T) = FO(T,T) = S_T$.

The property of futures contracts having a daily payout almost always leads to futures contracts having a different price than forward contracts. To illustrate how futures or forward prices may differ, Cox et al. (1981) developed the following trading strategy. Let $r_{t,t+1}$ be the return of a default-free zero-coupon bond coupon, continuously compounding at time t maturing at time $t+1$. This will be referred to as the risk-free rate from time t to $t+1$. Cox et al. (1981) then perform the following trading strategy:

Let $Z = \{t+1, ..., T-1, T\}$. Initially at time t, we invest $F(t,T)$ amount [6] in risk-free bonds with maturity t+1. Then for each $k \in Z$, the bond from $k-1$ matures (since each bond has a maturity of 1 day). We reinvest $F(t,T)$ and the accrued interest for each k except $k = T$ (since the bond would mature at T+1). This procedure is done for each $k = \{t+1, t+2, .., T-1\}$. This will result in the payoff at time T of $F(t,T)\prod_{i=t}^{T-1} e^{r_{i,i+1}}$, the compounded interest rate of investing $F(t,T)$ at time t and reinvesting this on a daily basis. To show how this part of the trading strategy evolves over time, let $\Gamma_{1,1}(k)$ denote the portfolio value of this part of the strategy at each time $k = t, t+1, .., T$ and consider the following table:

[6] Note that $F(t,T)$ is the time-t futures price with expiration at time T. Similar to the strategy of forward contracts, we invest the dollar amount $F(t,T)$ in risk-free bonds.

k	$\Gamma_{1,1}(k)$
t	$F(t,T)$
$t+1$	$F(t,T)\prod_{i=t}^{t} e^{r_{i,i+1}}$
t+2	$F(t,T)\prod_{i=t}^{t+1} e^{r_{i,i+1}}$
...	...
T-1	$F(t,T)\prod_{i=t}^{T-2} e^{r_{i,i+1}}$
T	$F(t,T)\prod_{i=t}^{T-1} e^{r_{i,i+1}}$

Table 6: First part of the futures strategy proposed by Cox et al., 1981. $F(t,T)$ is invested in a risk-free bond with maturity of 1 day at time $k=t$. We then reinvest $F(t,T)$ plus accrued interest for every $k=t+1,..,T-1$. $\Gamma_{1,1}(k)$ denotes the portfolio value for this strategy at each $k=t,..,T$.

In addition to $\Gamma_{1,1}$ described above, Cox et al. (1981) perform an additional trading strategy. Let $Q=\{t,t+1,t+2,..,T-1\}$. For each $k\in Q$, a long futures position of $\prod_{i=t}^{k} e^{r_{i,i+1}}F(t,T)$ contracts is taken. The position size is thus increased (decreased)[7] every day with the one-day risk-free rate. This position is held for one trading day, and at time $k+1$, the position is closed, and the proceeds invested in daily risk-free bonds up until time T. Thus at time $k+1$, we get the payoff $\prod_{i=t}^{k} e^{r_{i,i+1}}[F(k+1,T)-F(k,T)]$. This is then re-invested at the risk-free rate at time $k+1$ until T: $\left(\prod_{i=t}^{k} e^{r_{i,i+1}}[F(k+1,T)-F(k,T)]\right)\prod_{i=k+1}^{T-1} e^{r_{i,i+1}}$. Notice that a negative daily payoff is possible, i.e. $F(k+1,T)<F(k,T)$. In this case we will 'invest' these negative returns in the risk-free rate, which means borrowing at the risk-free rate. It will be shown later that the intra-day payouts being positive or negative will not affect the portfolio value at time T. Let $\Gamma_{1,2}$ denote the second part of the strategy.

k	Position size	$\Gamma_{1,2}(k)$
t	$F(t,T)\prod_{i=t}^{t} e^{r_{i,i+1}}$	0
t+1	$F(t,T)\prod_{i=t}^{t+1} e^{r_{i,i+1}}$	$e^{r_{t,t+1}}[F(t+1,T)-F(t,T)]$
t+2	$F(t,T)\prod_{i=t}^{t+1} e^{r_{i,i+1}}$	$e^{r_{t+1,t+2}}\Gamma_{1,2}(t+1)+\prod_{i=t}^{t+1} e^{r_{i,i+1}}[F(t+2,T)-F(t+1,T)]$
...	...	...
T-1	$F(t,T)\prod_{i=t}^{T-1} e^{r_{i,i+1}}$	$e^{r_{T-2,T-1}}\Gamma_{1,2}(T-2)+\prod_{i=t}^{T-2} e^{r_{i,i+1}}[F(T-2,T)-F(T-1,T)]$
T	0	$S_T\prod_{i=t}^{T-1} e^{r_{i,i+1}}-F(t,T)\prod_{i=t}^{T-1} e^{r_{i,i+1}}$

Table 7: Second part of the futures strategy proposed by Cox et al. (1981). A position of $\prod_{i=t}^{T-1} e^{r_{i,i+1}}$ futures contracts is taken for each $k=t,..,T-1$. This payoff at time $k+1$ is given by $\prod_{i=t}^{k} e^{r_{i,i+1}}[F(k+1,T)-F(k,T)]$. $\Gamma_{1,2}(k)$ denotes the portfolio value for this strategy at each $k=t,..,T$.

Table 7 shows the evolution of the portfolio value for the second part of the futures strategy of Cox et al. (1981). Despite looking quite complex, this investment strategy reduces down to an elegant form. Notice how every day the position size of $F(t,T)$ is increased with the compounded risk-free rate. Meanwhile, all previous payoffs are invested (borrowed) at the risk free rate as well,

[7] If the interest rate is positive, we increase our position size since $e^{r_{i,i+1}}>1$. If the interest rate is negative, we decrease the position size since $e^{r_{i,i+1}}<1$

such that we have at time $t+2$:

$$\Gamma_{1,2}(t+2) = e^{r_{t,t+1}}[F(t+1,T) - F(t,T)]e^{r_{t+1,t+2}} + \prod_{i=t}^{t+1} e^{r_{i,i+1}}[F(t+2,T) - F(t+1,T)] \tag{8}$$

$$= e^{r_{t,t+1}+r_{t+1,t+2}}[F(t+1,T) - F(t,T)] + e^{r_{t,t+1}+r_{t+1,t+2}}[F(t+2,T) - F(t+1,T)] \tag{9}$$

$$= e^{r_{t,t+1}+r_{t+1,t+2}}[F(t+1,T) - F(t,T) + F(t+2,T) - F(t+1,T)] \tag{10}$$

$$= e^{r_{t,t+1}+r_{t+1,t+2}}[F(t+2,T) - F(t,T)] \tag{11}$$

By the property of daily payout of futures contracts, and dynamically adjusting the position size by the daily risk-free rate every day, every term in $\{t+1,..,T-1\}$ can be added and subtracted. This will lead to a dependence only of $F(t,T)$ and $F(T,T) = S_T$ at time T, which will be shown now. Let $\Gamma_1(T) = \Gamma_{1,1}(T) + \Gamma_{1,2}(T)$ denote the time T portfolio value of the strategies combined. We get similar to Cox et al. (1981):

$$\Gamma_1(T) = \Gamma_{1,1}(T) + \Gamma_{1,2}(T) \tag{12}$$

$$= F(t,T)\prod_{i=t}^{T-1} e^{r_{i,i+1}} + \sum_{k=t}^{T-1}\left(\prod_{i=t}^{k} e^{r_{i,i+1}}[F(k+1,T) - F(k,t)]\right)\prod_{i=k+1}^{T-1} e^{r_{i,i+1}} \tag{13}$$

$$= F(t,T)\prod_{i=t}^{T-1} e^{r_{i,i+1}} + \sum_{k=t}^{T-1}\left(\prod_{i=t}^{T-1} e^{r_{i,i+1}}[F(k+1,T) - F(k,t)]\right) \tag{14}$$

$$= F(t,T)\prod_{i=t}^{T-1} e^{r_{i,i+1}} + \left(\prod_{i=t}^{T-1} e^{r_{i,i+1}}[F(t+1,T) - F(t,T) + F(t+2,T) - F(t+1,T) + ... + F(T,T) - F(T-1,T)]\right) \tag{15}$$

$$= \prod_{i=t}^{T-1} e^{r_{i,i+1}}\left(F(t,T) - F(t,T) + F(T,T)\right) \tag{16}$$

$$= S_T\prod_{i=t}^{T-1} e^{r_{i,i+1}} \tag{17}$$

The final portfolio value at time T, $\Gamma_1(T)$ only has dependence on $F(T,T) = S_T$ and the compounded daily risk-free rate, as shown by (13-17). Since an initial investment of $F(t,T)$ is made and a final portfolio value of $S_T\prod_{i=t}^{T-1} e^{r_{i,i+1}}$ is obtained, the fair (no-arbitrage) time t futures price according to Cox et al. (1981) is the discounted value of the payoff $S_T\prod_{i=t}^{T-1} e^{r_{i,i+1}}$ at time t. Notice, however, that in contrast to forward contracts, the compounded daily interest rate here is stochastic and unknown at time t. In order to get the no-arbitrage price, the compounded risk-free rate for all future periods until maturity has to be estimated. For forward contracts, no intermediate cash flows happened, and it was possible to exactly determine the no-arbitrage price at time t, since the risk-free rate of holding a bond from time t to time T is known beforehand. For futures contracts, this is not the case due to the intermediate cash flows arising from the property of mark to market, which are able to be invested at a different risk-free rate each day.

So far, only daily mark-to-market payouts have been discussed. However, this can be extended to smaller time steps. In fact, for cryptocurrency exchanges the mark-to-market payments are done on a very low time frame, almost instantaneous. Despite the time frame being lower, the strategy (13) will still hold. Cox et al. (1981) state that their strategy of rolling over a bond on a daily basis is equivalent to investing in the money market account from time t to T. Let r_s denote

the instantaneous short-rate at time $s \in [t, T]$, and assume continuous mark to market of futures payouts. If we invest \$1 in the money market account at time t, and perform the same strategy as (13), but now in continuous time, a payoff at time T of $S_T e^{\int_t^T r_s ds}$ is obtained. In order to discount this at time t, nformation about the price process of r_s is still required.

Schroder (1999) builds upon the framework of Cox et al. (1981) in the continuous time setting and shows that in a risk-neutral world, we have under the measure $\mathbb{Q}$ that the futures price $F(t, T)$ is a martingale. We can compute the time-t expectation of $F(t, T)$ in a risk-neutral way. Let $M_T = e^{\int_t^T r_s ds}$ denote the value of the money market account at time T, with an initial investment of \$1 at time t, and let F denote the price process of a futures contract. We have that $\frac{F}{M}$ is a martingale under $\mathbb{Q}$ using M as a numeraire, so $\frac{F(t,T)}{M(t)} = E_t^{\mathbb{Q}}[\frac{F(t,T)}{M_T}] = E_t^{\mathbb{Q}}[\frac{S_T}{M_T}]$. Consequently, we have under the risk-neutral measure :

$$\frac{F(t,T)}{M_t} = F(t,T) \tag{18}$$

$$= \mathbb{E}_t^{\mathbb{Q}}\left[\frac{S_T}{M_T}\right] = \mathbb{E}_t^{\mathbb{Q}}\left[\frac{S_T}{M_T} M_t\right] \tag{19}$$

$$= S_t \mathbb{E}_t^{\mathbb{Q}}\left[\frac{1}{M_T}\right] = S_t \mathbb{E}_t^{\mathbb{Q}}\left[e^{-\int_t^T r_s ds}\right] \tag{20}$$

So, under the risk-neutral measure, the no arbitrage futures price is given by: $F(t, T) = S_t E_t^{\mathbb{Q}}[e^{-\int_t^T r_s ds}]$, according to Schroder (1999).

2.2.3 Comparison Futures and Forward Prices

In section 2.2.2, the strategy of Cox et al. (1981) has shown in the discrete case that the fair futures price at time t is the present value of a portfolio that pays $S_t \prod_{i=t}^{T-1} e^{r_{i,i+1}}$ at time T. Due to the fact that the daily risk-free rate in the future is unknown at time t, it is not possible to exactly determine the no-arbitrage futures price at time t. In this section, the results obtained from the no-arbitrage forward and futures contracts will be compared. The no-arbitrage price of a forward contract equals the futures price if and only if:

$$F(t,T) = FO(t,T) \iff = S_t \prod_{i=t}^{T-1} e^{r_{i,i+1}} = S_t e^{r_{t,T}(T-t)} \tag{21}$$

$$\iff (T-t) * r_{i,i+1} = r_{t,T} \quad \forall i \in \{t, t+1, .., T-1\} \tag{22}$$

So, only if the return of continuously investing in daily risk-free on a daily basis up until time T is the same as investing all at once at time t, i.e. under constant interest rates, the forward price equals the futures price. In general, it is expected that $F(t, T) \neq FO(t, T)$, since interest rate in practice are not deterministic and constant. As French (1983) states, the difference arises from the fact that holding a risk-free bond from time t to time T (forward contract) is in general not equal to rolling over a bond on a daily basis (futures contract). We have seen above that futures contracts allows us to invest the profits on a daily basis (due to MTM). If the interest rates fluctuate on a daily basis, these proceeds are invested at a different interest rates. Forward contracts do not have any intermediate payments and thus the forward and futures prices may differ if interest rates are stochastic. Specifically, if $Cov[F(t, T), r_{t,t+1}] > 0$, then $F(t, T) > FO(t, T)$. If the futures price is positively correlated with interest rates, we would expect a daily profit if the interest rate rises, and are able to re-invest the profits at higher and higher interest rates. Therefore the futures price would be higher than the forward price. Similarly, if $Cov[F(t, T), r_{t,t+1}] < 0$, then $F(t, T) < FO(t, T)$. In this case, if the futures position were to have a daily profit, it would be expected to invest profits at a lower interest rate, and if the futures position incurs a loss, borrow at a higher risk-free rate.

Considering expression of the fair futures price $F(t,T) = S_t \prod_{i=t}^{T-1} e^{r_{i,i+1}}$ again, dependence is noted on all daily interest rates from time t to time T, which are not yet known at time t. Levy (1989) shows, however, that in order to determine the fair futures price at time t, only the one-period ahead interest rate needs to be predicted. Suppose the current time is $T-3$, and a forward contract and futures contract are both maturing at time T. The goal of Levy (1989) is to replicate a forward contract with a futures contract. The first (trivial) strategy to do so is the following:

At time $T-3$ one forward contract is bought and held until time T. For the futures contract, one contract at each time $T-3$, $T-2$, $T-1$ is bought and closed the next day. Note here that it is important that both strategies have an initial cash flow at time $T-3$ of zero, since both contracts do not require any payment to be made up front. Table 8 shows that both strategies have the same time T cashflow if $FO(T-3,T) = F(T-3,T)$. However, notice the arbitrage opportunity showing why this should not hold in general. Both strategies have an initial investment of 0, but the futures contract has two intermediate cash flows, which could be invested at the risk-free rate, whilst the forward contract does not. If we would have $FO(T-3,T) = F(T-3,T)$, an arbitrageur could take a short position in the forward contract, a long position in the futures contract, and invest the daily cash flows received of the futures contract at time $T-2$ and $T-1$ at the risk-free rate. At time T, the arbitrageur would be hedged, since $F(T,T) - FO(T,T) = S_T - F(T-3,T) - FO(T-3,T) - S_T = 0$. Thus, if interest rates are nonzero, this simple strategy does not allow us to replicate a forward contract with a futures contract in an efficient market, since arbitrage opportunities would arise.

time	Forward Cashflow	Futures Cashflow
T-3	0	0
T-2	0	$F(T-2,T) - F(T-3,T)$
T-1	0	$F(T-1,T) - F(T-2,T)$
T	$S_T - FO(T-3,T)$	$S_T - F(T-3,T)$

Table 8: A simple strategy which tries to replicate a forward contract with a futures contract.

In order to replicate a forward contract with a futures contract, we have to choose the amount of futures contract such that this arbitrage opportunity does not arise. Levy (1989) shows that this is possible by performing the following trading strategy. At time $T-3$ one forward contract is bought and held it until time T. For the futures contract, let $r_{T-k,T}$ denote the risk-free rate for time $T-k$ to T, $k = 1, 2$. At time $T-3$, we buy $e^{-r_{T-2,T}}$ futures contracts, and at time $T-2$, when we receive the payoff, it is invested until time T, similar to (13). At time $T-2$, we buy $e^{-r_{T-1,T}}$ futures contracts, and at $T-1$ when we get the first payoff, we invest this in the risk-free rate until time T. At time $T-1$ we buy 1 futures contract. The cash flows of this strategy are denoted in Table 9.

time	Forward Cashflow	Futures Cashflow
T-3	0	0
T-2	0	$e^{-r_{T-2,T}}[F(T-2,T) - F(T-3,T)]$
T-1	0	$e^{-r_{T-1,T}}[F(T-1,T) - F(T-2,T)]$
T	$S_T - FO(T-3,T)$	$S_T - F(T-3,T)$

Table 9: Daily cash flows of the forward and futures positions of the strategy as described by Levy (1989).

The result in the last row of table 9 comes is due to the fact we invest the payoffs of $T-2$ and $T-1$ two and one day, respectively, in the risk-free rate, such that at time T we get: $[F(T-2,T) - F(T-3,T) + (F(T-1,T) - F(T-2,T) + S_T - F(T-1,T)] = S_T - F(T-3,T)$. Notice that we perform the 'arbitrage opportunity' that was described in table 8, by investing the daily

payoffs of the futures contract in the risk-free rate. However, due to the smart choice of position sizing, we end up with $S_T - F(T-3, T)$, which essentially replicates a forward contract, since we 'lock' in a price at time $T-3$ for which the underlying asset at can be bought at time T. The key takeaway of this example, and the paper of Levy (1989) in general, is that in order to create a perfect hedge of a forward contract at time t with expiration at time T, with a futures contract with equal maturity, we need to estimate for each $k \in \{t, ..., T-1\}$ the yield of a zero-coupon bond at time $k+1$ maturing at time T. Despite that this needs to be done every period, the yield (i.e. interest rate) of the zero-coupon bond has to be forecasted only one period ahead. Estimating the risk-free rate one-period ahead, k times, might be easier than estimating at time t all interest rates k periods ahead. Levy (1989) states that the variance of estimating the one-period ahead risk-free rate k times is much smaller than forecasting all future risk-free rates at time t. Therefore, it might be reasonable to assume that forward and futures prices are approximately equal to each other, and the price difference between the two insignificant.

In addition to the arguments given by Levy (1989), the contract duration of the futures contract is also important to consider. Hull (2014) states that for contracts with only a few months duration the difference between forward and futures prices is insignificant and can be ignored. This difference arises due to the fact that $e^{r_{t,T}(T-t)} \neq \prod_{i=t}^{T-1} e^{r_{i,i+1}}$, the yield of a bond time to maturity $(T-t)$ is in general not equal to rolling over a daily bond from time t to T. The longer the time to maturity, the bigger this difference is expected to become as the interest rates are stochastic. In this thesis, we will only analyze futures contracts with maturity of 3 or 6 months, which are considered to be of short duration. The arguments given by Levy (1989) and Hull (2014) conclude that it is reasonable to assume $FO(t,T) = F(t,T)$. This provides a more viable expression to work with, since forward contracts do not have future stochastic interest rates which have to be discounted at time t.

In this thesis, we will only futures contracts will be priced because of the absence of forward contracts in the cryptocurrency market. Evidence given above has shown that without loss of generality, it can assumed that forward and futures prices are almost equal to each other, although it is acknowledged that the prices are not perfectly equal. We get the desired expression for a fair time t futures price with expiration at time T as:

$$F(t,T) = S_t e^{r_{t,T}(T-t)} \tag{23}$$

, where r_t is the risk-free rate of holding a zero-coupon bond from time t to T, in other words a time to maturity of $T-t$.

2.2.4 Contango and Backwardation

A futures contract can express *contango* and *(normal)*[8] *backwardation*. Rau-Bredow (2022) describes contango as the event where the futures price for a given asset with delivery some months ahead is above the spot price. Backwardation is the inverse, where the futures price trades below the spot price. Supply and demand for certain delivery dates can shift these futures prices higher or lower than the spot price. Using a similar example as earlier, an airline may want to pay a premium for price stability in the summer months, thus buying July oil futures which trade at contango. Figure 2 visualizes what contango and backwardation look like. Note that we have convergence of the futures price and the spot price close to maturity. This follows from the fact that at time T, the boundary condition $F(T,T) = S_T$ hold. If this convergence does not happen, arbitrage opportunities will arise.

[8]Normal backwardation and backwardation are two equivalent terms and describe the same phenomenon. Throughout this thesis the term 'backwardation' will be used.

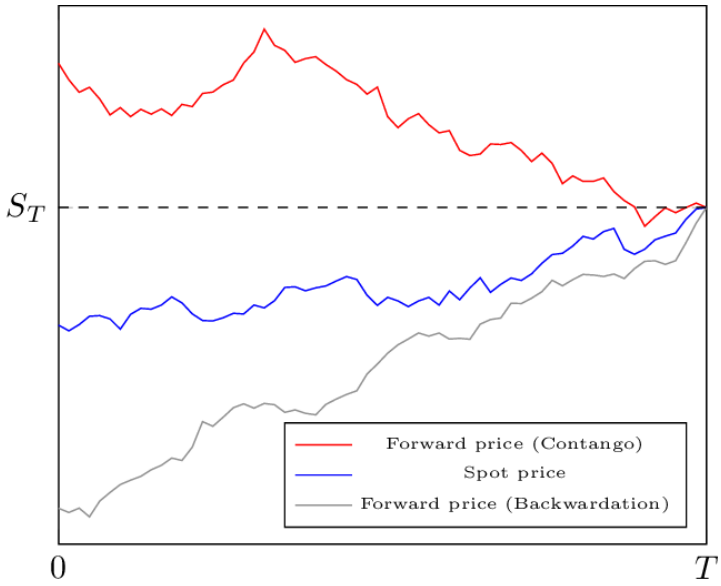

Figure 2: Contango and backwardation visualized. Retrieved from Fahim (2019).

2.2.5 Cost-of-Carry Models

In section 2.2.3 a fair futures price expression (23) has been derived. This was done for an asset with no intermediate payments such as dividends. As one can expect, the expression derived in (23) does not have to hold for every type of asset. As we will see later, some assets have benefits associated with holding the underlying asset instead of a futures contract, and other assets have costs incurred with holding the underlying asset. This section aims to give an overview of existing models of fair (no-arbitrage) futures prices throughout different asset classes. Once this overview is complete, it can attempted to extend this to a new asset class, that of cryptocurrencies.

The expression derived in (23) is the most simple version of the *cost-of-carry model*. Riley (2014) explains that the name of this model stems from the associated cost of carrying an asset until expiration. The cost-of-carry model simply states the fair futures price is the spot price adjusted by all costs (benefits) of carrying [9]an asset from time t to T. Recall that buying a futures contract does not require payment at time t, whilst buying the underlying asset does require a payment at time t. It has been shown earlier that for forward contracts, it is possible to invest money at the risk-free rate at time t and end up with the underlying asset and a risk-free return at time T. This is not possible for buying the underlying asset and carrying it until time T. Therefore the (opportunity) cost of carrying the underlying asset S_t, i.e. holding it from time t to time T, has to be incorporated into the fair futures price at time t. This (opportunity) cost is the risk-free rate from time t to T, $e^{r_{t,T}(T-t)}$. As a result, the fair futures price at time t will be greater than the spot price if interest rates are positive. In order for the cost-of-carry model to hold, however, certain assumptions need to be made. The cost-of-carry model operates in a friction less market[10], under which the *Law of One Price (LoOP)* holds. According to Corradin and Rodriguez-Moreno (2016), the LoOP states that two assets that produce an identical cash flow should trade at the same price, in other words absence of arbitrage. If the LoOP does not hold, arbitrage opportunities are possible. In addition to the LoOP, a few additional assumptions are formulated under which the cost-of-carry models should hold. The assumptions are derived from Cornell and French (1983) and are as follows:

[9]The term carrying means holding an asset for a certain period of time. Specifically in the case of futures pricing, the underlying asset is carried from time t to time T.

[10]A friction less market assumes that there are no costs associated with making transactions.

- There are no taxes and transaction costs, assets are perfectly divisible, and short-selling is allowed
- The costs of risk-free lending and borrowing are constant and equal
- Dividends (if any) are paid continuously at a rate of D dollars per period

The above assumptions will be refered to as a perfect market. Under the perfect market assumptions, the fair futures price for an investment asset with no intermediate payments should equal the cost-of-carry model stated in (23). To see why this should hold, consider the following table where the equality does not hold:

time	$\mathbf{F(t,T) > S_t e^{r_{t,T}(T-t)}}$	Cashflow	*time*	$\mathbf{F(t,T) < S_t e^{r_{t,T}(T-t)}}$	Cashflow
t	Short/sell $F(t,T)$	0	t	Buy/long $F(t,T)$	0
t	Borrow S_t amount	S_t	t	Short/sell S_t	S_t
t	Buy S_t	$-S_t$	t	Lend out S_t amount	$-S_t$
		0			**0**
T	Deliver $F(t,T)$	$F(t,T)$	T	Take delivery on $F(t,T)$	$-F(t,T)$
T	Pay back loan	$-S_t e^{r_{t,T}(T-t)}$	T	Collect loan	$S_t e^{r_{t,T}(T-t)}$
Profit		$\mathbf{F(t,T) - S_t e^{r_{t,T}(T-t)} > 0}$		$\mathbf{S_t e^{r_{t,T}(T-t)} - F(t,T) > 0}$	

Table 10: Simulating an arbitrage strategy if the simple cost-of-carry model does not hold in a frictionless market. Based upon Damodaran (2004).

Table 10 shows two potential arbitrage opportunities if the simple cost-of-carry model does not hold. To clarify the table further, consider the left scenario ($F(t,T) > S_t e^{r_{t,T}(T-t)}$). Borrowing is done at the risk-free rate to buy the underlying asset at time t for a price of S_t. At time T, the underlying asset which is held is used to deliver the futures obligation, since being short on a futures contract means delivering the underlying asset at time T. The payoff of a short futures contract at time T is $F(t,T) - S_T$. The resulting payoff is $F(t,T) - S_T + S_T = F(t,T)$. Finally, the loan is paid back loan to receive a total profit of $F(t,T) - S_t e^{r(T-t)} > 0$. Such a trade is often called a *cash-and-carry*. This name is derived from the fact that one buys an asset at time t, carries it until the end of the maturity and uses it to deliver the futures contract.The same scenario in reverse holds for the right hand side of Table 10, which is sometimes referred to as the *reverse cash-and-carry*.

So far, only an investment asset with no intermediate payments such as dividends, or assets that require a payment such as storage costs have been discussed. Cornell and French (1983) build upon the work of Cox et al. (1981) and extend this standard no-arbitrage futures price, to the case of dividend paying stocks. This is done under the assumptions stated above of a perfect market. In addition, Cornell and French (1983) make the same assumption as in this thesis, that forward and futures prices are equal. Let S_t denote the stock price at time t paying continuous dividends at a constant rate of D dollars per period. Cornell and French (1983) assume a constant risk-free rate r. This is equivalent to the assumption in thesis that the risk-free rate from time t to T is known at time t. It has been shown earlier how to derive this risk-free rate by using a zero-coupon bond with maturity at time T. The trading strategy proposed by Cornell and French (1983) is to invest all dividends (paid continuously) in risk-free bonds and receiving the risk-free rate. The initial portfolio value at time t of this strategy[11]is given by:

$$\Pi_1(t) = S_t \tag{24}$$

[11]Since two strategies are discussed here, $\Pi_1(t)$ represents the portfolio value of strategy 1 at time t.

The portfolio value of this strategy at time T is then obtained by investing dividend continuously in risk-free bonds:

$$\Pi_1(T) = S_T + D\int_t^T e^{r_{t,T}(T-w)}dw \tag{25}$$

$$= S_T + \frac{D}{r}[e^{r_{t,T}(T-t)} - 1] \tag{26}$$

So, (26) is the payoff at time T of investing in the stock at time t and investing dividends continuously in risk-free bonds with maturity T. Cornell and French (1983) show that this payoff can be replicated using forward contracts. Let $FO(t,T)$ denote the time t forward price with expiration date T. The investor takes a long position in one forward contract $FO(t,T)$ and invests $\left(FO(t,T) + \frac{D}{r}[e^{r_{t,T}(T-t)} - 1]\right)e^{-r_{t,T}(T-t)}$ in risk free bonds. The initial value of this portfolio at time t is given by:

$$\Pi_2(t) = \left(FO(t,T) + \frac{D}{r}[e^{r_{t,T}(T-t)} - 1]\right)e^{-r_{t,T}(T-t)} \tag{27}$$

This is held risk-free bonds until time T, which gives a portfolio value of:

$$\Pi_2(T) = S_T + \frac{D}{r}[e^{r_{t,T}(T-t)} - 1] \tag{28}$$

Note that (26) and (28) representing the portfolio values are equal at time T. So, since Π_1 and Π_2 are both self-financing portfolios with $\Pi_1(T) = \Pi_2(T)$, we must have $\Pi_1(t) = \Pi_2(t)$. Tabulating for comparison purposes gives:

Strategy	$\Pi(t)$	$\Pi(T)$
1	S_t	$S_T + \frac{D}{r}[e^{r_{t,T}T-t)} - 1]$
2	$\left(FO(t,T) + \frac{D}{r}[e^{r_{t,T}(T-t)} - 1]\right)e^{-r(T-t)}$	$S_T + \frac{D}{r}[e^{r_{t,T}(T-t)} - 1]$

Similarly to the strategy proposed by Cox et al. (1981), to avoid arbitrage, the following must hold:

$$S_t = \left(FO(t,T) + \frac{D}{r}[e^{r_{t,T}(T-t)} - 1]\right)e^{-r_{t,T}(T-t)} \tag{29}$$

$$\iff S_t e^{r_{t,T}(T-t)} = FO(t,T) + \frac{D}{r}[e^{r_{t,T}(T-t)} - 1] \tag{30}$$

$$\iff FO(t,T) = S_t e^{r_{t,T}(T-t)} - \frac{D}{r}[e^{r_{t,T}(T-t)} - 1] \tag{31}$$

Notice that for a non-dividend paying stock, i.e. $D = 0$, we get $F(t,T) = S_t e^{r_{t,T}(T-t)}$, equivalent to (23). The sign of the dividend payments, in (31) is negative, resulting in a negative effect of dividends on the futures price. This follows from the fact that the stock itself pays dividends, whilst the futures contract does not. Equivalently, but more common in the literature is to let d denote the dividend yield, which is paid on a continuous basis, similar to the risk-free rate being continuously compounding. Using (31) with the dividend yield continuously paying, i.e. e^d, as a result:

$$F(t,T) = S_t e^{(r_{t,T} - d_t)(T-t)} \tag{32}$$

Equation 32 is the cost-of-carry model for a stock with a dividend yield of d_t annually. Again, we have the minus sign of dividend yield in the expression here.

The cost-of-carry model can be extended for asset classes beyond stocks. Hull (2014) states the cost of carry model for foregin currencies as:

$$F(t,T) = S_t e^{(r_{t,T} - r^f_{t,T})(T-t)} \tag{33}$$

, where $r_{t,T}$ is the risk free rate in the local currency from time t to T, and $r^f_{t,T}$ the risk free rate in the foreign currency. To explain the signs in (33) more clearly, suppose an European investor buys a futures contract of EUR/USD. The yearly interest rate in Europe is 2% and in the US is 3%. Similarly as in the (dividend-paying) investment asset, the European investor could buy the desired dollars at time t, but the property of deferred payment of futures contracts allow the investor to delay the purchase until time T, and meanwhile invest the euro's at the risk-free rate of 2%. This has a positive effect on the futures price. However, the interest rate in the US is 3%. If the investor would have bought spot dollars at time t, it could have been invested at a higher risk-free rate of 3%. This therefore has a negative effect on the futures price, since it is the risk-free return that could be earned on the spot asset at time t.

Commodities are an asset class which can be categorized as both investment and consumption assets. Gold is considered an investment, whilst oil or natural gas are consumption assets. In addition, commodities are, in contrast to all assets we have talked about so far, physically stored. Storage of commodities incurs costs to the holders of the underlying commodity. Aïd et al. (2015) state therefore that the cost of carrying commodities is not the interest rate alone and thus for commodities another model has to be used. In other words, commodities have a higher carry cost than investment assets, where we have seen in (23) that the cost of carry only consists of the risk-free rate. Pinkdyck (2001) formulates the cost-of-carry model for commodities as:

$$F(t,T) = S_t e^{(r_{t,T} + k_t - \Psi_t)(T-t)} \tag{34}$$

For commodities, two new parameters in the cost-of-carry model are introduced. The first one, k_t, is the storage cost associated with storing the commodity. Notice that this is expressed as a yield (percentage), not in absolute terms. The reason k_t has a plus sign, which implies a positive effect on the futures price, is since the physical commodity incurs storage costs at an rate of k_t per unit of the commodity. Holding a long position in a futures contract does not have storage costs, so the futures price has to be adjusted for this. To illustrate this, suppose $r_{t,T} = 0$, $\Psi_t = 0$. If we omit the term k_t in the cost of carry model (34), then we would have $F(t,T) = S_t e^{0(T-t)} = S_t$. However, if the physical commodity is carried from time t until T, a cost of k_t (in percentage, i.e. negative yield) is incurred. Holding the futures contract does not have this cost. Thus, at time T holding the physical commodity gives us $(1 - k_t)S_T$ and holding the futures contract gives us S_T. This would give rise to an arbitrage opportunity similar to Table 10, hence the term k_t has to be included in the cost of carry model for commodities and has a positive sign, as it benefits the futures contract holder, which leads to a higher futures price.

The other term Ψ_t in the cost of carry model for commodities is the *convenience yield*, which is the benefit of holding the physical commodity instead of the futures contract. Pinkdyck (2001) states that the convenience yield obtained by holding a commodity is similar to that of dividend yield of holding a stock, such that it has a negative effect on the futures price as seen in (34). The convenience yield is intangible and is found through market prices. To illustrate the role of Ψ_t, suppose we omit the term from the cost of carry model, such that we have:

$$F(t,T) = S_t e^{(r_{t,T} + k_t)(T-t)} \tag{35}$$

In a perfect, frictionless market we would expect (35), the theoretical price of commodities to hold due to the similar arbitrage arguments given in Table 10, with additional storage costs. In practice, this parity rarely holds, however. Emperical evidence shows that the observed futures price for commodities often deviates from the theoretical futures price given in (35). Litzenberger and Rabinowitz (1995) find that oil futures between 1984 and 1992 were in strong backwardation

77% of the time. This is a surprising result, since oil has a positive cost of carry, and we would expect $F(t,T) > S_t$. In other commodity markets the same phenomenon is found. Movassagh and Modjtahedi (2005) report significant backwardation for the market of natural gas between 1991 and 2003. As a result of this emperical evidence, the cost-of-carry model for commodities introduces an intangible parameter Ψ_t called the convenience yield.

To illustrate the concept of convenience yield, consider the market of natural gas. Suppose an unexpectedly cold winter occurs. Market participants are expecting a shortage of natural gas due to increased demand for natural gas. This shortage occurs short-term, and will lead to spot prices of natural gas rising. Despite this, it may happen that the prices of futures contracts expiring in June may not rise as much as the spot price. The market expects that the shortage of natural gas will disappear after the winter, and that demand in June may be lower, resulting in expected spot price in June to be lower. For producers holding the actual natural gas, this means that it is possible to sell the natural gas on the spot market when shortage occurs. A futures contract has a fixed delivery date, which does not give this flexibility. Net buyers of commodities such as energy companies may also be worried that this cold winter will lead to a shortage of natural gas as demand increases. They may choose to rather buy the natural gas on the spot market now to cope with the increasing demand instead of buying a futures contract with a later delivery, as the energy company needs the commodities in the short term. This perceived benefit of having the actual commodity over a derivative is called the convenience yield. If the convenience yield is positive, market participants prefer to hold the actual underlying commodity instead of a derivative. The natural gas example demonstrates why the sign of the convenience yield Ψ_t is negative in (34), holding the actual underlying asset has a benefit relative to the futures contract, which makes the futures contract cheaper relative to the spot price. Girard (2010) explains that the value of the convenience yield can be interpreted as the expectation of future supply and demand changes. If market participants expect a shortage of the commodity to occur, it will be more worthwhile to hold the actual commodity instead of a futures contract with a fixed delivery date. This will lead to a high convenience yield, and a backwardated market as a result. Since the convenience yield reflects expectations regarding future supply and demand, it follows that the convenience yield is not constant over time. This is why Ψ_t has dependence on t. To illustrate this, Pinkdyck (2001) presents the following figure:

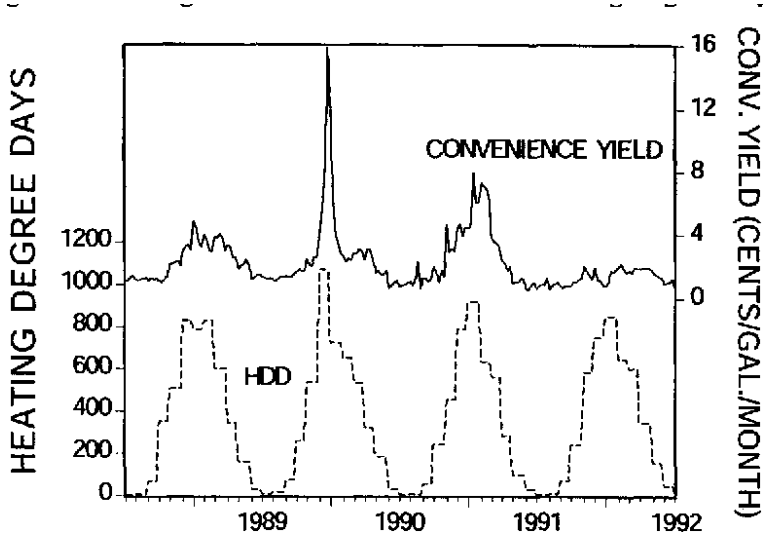

Figure 3: Convenience yield visualized, retrieved from Pinkdyck (2001)

Figure 3 shows the relationship between heating degree days and the convenience yield of heating oil. Heating degree days represent the amount of heating needed given the outside temperature. It becomes visible from Figure 3 that the convenience yield is highly cyclical and spikes in winter

months, when demand is high. This follows from the example of natural gas given earlier, where in winter months market participants expect more demand and would rather hold the actual commodity than a future, since a shortage short-term could occur. This becomes even more clear if we consider the spike in convenience yield in 1989 in Figure 3, as a result of the heating degree days reaching a high level. This is due to a cold winter, skyrocketing the demand for heating oil in the short-term and causing the convenience yield to rise accordingly. In the summer months we see the convenience yield approaching zero as demand for heating oil is lower.

A recent example where convenience yield spiked was the surge in oil and natural gas prices in the beginning of 2022 as a result of the war in Ukraine and the boycot of Russian oil and gas. The spot price of oil and gas jumped during the start of the war as the short-term supply was expected to dry up. However, the futures market for long dated futures traded lower than the spot price, and was in significant backwardation. The reason behind this was similar to what Girard (2010) described, a significant change in expectation of future supply and demand. The boycot of the largest supplier of oil and natural gas to Europe meant that the short-term supply of oil and natural gas was going to dry up. Long-dated futures jumped less in price, as Europe would have more time to find supply of oil and gas elsewhere, and equalling the supply and demand to normal levels. The convenience yield of holding the physical commodity (oil, gas) thus experienced high levels in early 2022.

The convenience yield is intangible and can be found through market prices. This is since it is the aggregate expectation of market participants, and not some deterministic value that we can plug into (34). The convenience yield thus represents the difference between the theoretical futures price state in (35) and observed market price. The reason this difference is not arbitraged away as quickly in the case of investment assets is due to the physical storage of commodities. Girard (2010) states that in a backwardated market for commodities, which we often see, it is not always possible to sell a lot of inventory of the commodity and long the futures contract. This is due to physical constraints, as well as producers always needing to keep a certain level of storage. If we let $\hat{F}(t,T)$ denote the theoretical futures price as predicted by 35 and $F(t,T)$ the true market prices, we have $ln\left(\frac{F(t,T)}{\hat{F}(t,T)}\right) = ln\left(\frac{1}{e^{-\Psi_t}}\right) = \Psi_t$. So, under the cost of carry model for commodities, we find this intangible parameter Ψ_t through market prices and we solve for Ψ_t.

The parameters k_t and Ψ_t combined together, $k_t - \Psi_t$ is called the net convenience yield by Girard (2010). If the net convenience yield is negative, it means that the costs of holding the underlying commodity exceed the benefits of holding the commodity. In other words, it is not expected that a shortage will occur, and we have a futures market in contango. Similarly, for a positive convenience yield, we will have a market in backwardation. The cost-of-carry model with the term δ_t is given by:

$$F(t,T) = S_t e^{(r_{t,T} - \delta_t)(T-t)} \tag{36}$$

The net convenience yield is found using market prices, and may have a cyclical nature and thus dependence on t.

Despite (34) being widely used for determining the no-arbitrage commodities futures price, there are cases where this model has been challenged. An example of this are commodities with no storage costs, or cannot be stored. The electricity market does not have storage costs, since electricity cannot be stored. Therefore, the benefit of having the 'physical' electricity should not exist. Despite that, Viehmann (2011) showed that the futures market of electricity experienced levels of contango and backwardation. This has caused some debate in the literature about the notion of convenience yield.

3 Futures in the cryptocurrency market

In the previous section, futures pricing through several cost-of-carry models was discussed, to find a no-arbitrage futures price. The cryptocurrency market has different characteristics and products than established futures markets. The first difference is the property of the underlying spot market never closing. The spot market is open 24/7, which leads to the futures market never closing as a result. In addition, new terms such as *perpetual futures* or *coin-margined* futures are specific to the cryptocurrency market. This section aims to introduce the dynamics of the cryptocurrency futures market, and sets the stage to test the cost-of-carry models on market data later on. The empirical results of the Bitcoin and Ethereum futures basis will also be presented to motivate why cost-of-carry models will be applied. Throughout this thesis, data from the cryptocurrency exchange *Binance* will be used. Binance is the largest cryptocurrency exchange and has a market share of approximately 63% in the cryptocurrency futures market (Bitcoinfuturesinfo) [12]. In this section the ticker symbol for Bitcoin (BTC) and for Ethereum (ETH) will at times be used for shorter notation. The two assets Bitcoin and Ethereum are chosen is since these are the largest two cryptocurrencies and are the most frequently traded on the quarterly futures market.

3.1 Futures in the cryptocurrency market

In the cryptocurrency market the term 'futures contract' does not have a universal interpretation, due to different types of futures contracts being available for trading. So far in this thesis, futures in the traditional market have been discussed, which have an expiration date T. In the cryptocurrency market, two different types of futures contracts are frequently traded, ones with an expiration date and ones without an expiration date. A futures contract without an expiration date is called a *perpetual futures* contract, and is native to the cryptocurrency market, with its name giving away the property of no settlement. In this thesis, it will not be attempted to price these futures, but its effect on futures with an expiration date will be studied. Since two types of futures contracts are discussed here, using the term 'futures' alone can give ambiguity about which type of futures contract is described. Futures with an expiration date in the cryptocurrency market are often referred to as *quarterly futures*. This term arises from the fact that futures contracts traded in the cryptocurrency market only have maturity at the end of a certain quarter. Consequently, the term *quarterly futures* will be used throughout this thesis when talking about a future with an expiration date, similar to those discussed in section 2.2. Futures without an expiration date will be referred to as *perpetual futures* in the remainder of this thesis.

3.1.1 Quarterly Futures

Quarterly futures in the cryptocurrency market are split into two types based on the type of collateral used. These two types are called *Coin-Margined (Coin-M)* and *USD-Margined (USD-M)* quarterly futures. Coin-Margined (Coin-M) quarterly futures allow for cryptocurrencies such as Bitcoin (BTC) and Ethereum (ETH) to be used as collateral, whilst USD-Margined (USD-M) quarterly futures allow only USD[13] collateral. The underlying collateral being of a different type leads to different levels of exposure. Table 11 illustrates these properties. Suppose that 1 BTC is trading at \$10000, and the quarterly futures price $F(t,T)$ is also \$10000, i.e. $S_t = F(t,T) = 10000$. For Coin-M quarterly futures, the trader holds 1 BTC as collateral, and for USD-M quarterly futures, the trader holds \$10000 as collateral. Note that the dollar amount of collateral is the same at time t (\$10000). Table 11 shows the different net exposure for each type of contract when a long or short trade is being made. Note that the column 'Position Size' represents being long or short one BTC worth of quarterly futures, that means buying or selling 1 BTC worth of $F(t,T)$.

[12] https://bitcoinfuturesinfo.com/market-share-and-futures-curve, retrieved on 5th of December 2022

[13] This collateral is in the form of 'stablecoins'. These are tokens on the Blockchain which have underlying Dollars backing it. This causes the token to have a value of \$1. The most well-known stablecoins are USDT and USDC.

Futures Type	Collateral	Position Type	Position Size	Net exposure
Coin-M	1 BTC	Long	1 BTC	2 BTC
Coin-M	1 BTC	Short	-1 BTC	0
USD-M	\$10000	Long	1 BTC	1 BTC
USD-M	\$10000	Short	-1 BTC	-1 BTC

Table 11: Illustrating the net exposure of a trader when taking a long or short position on Coin-M and USD-M quarterly futures, respectively.

Table 11 illustrates that Coin-M quarterly futures always have a larger net exposure relative to the underlying asset (in this case BTC) than USD-M quarterly futures, assuming they hold the same quarterly futures position. This follows naturally from the fact that the trader already has an underlying long position from holding the spot asset, instead of holding cash. In the first row, the trader takes a long position of 1 BTC on quarterly futures, and already has 1 BTC as collateral. This results in a net exposure of 2 BTC, i.e. for every \$1 move in BTC, the trader gains or loses \$2. In the second row, having a short position in $F(t,T)$ of 1 BTC (selling 1 BTC worth of $F(t,T)$), is equivalent to holding a cash position, since the positions approximately offset one another[14]. For USD-M quarterly futures, buying 1 BTC worth of $F(t,T)$ results in a net exposure of 1 BTC, and selling one BTC worth of $F(t,T)$ results in a negative exposure of approximately 1 BTC. Table 11 thus shows that for long positions, Coin-M quarterly futures are twice as sensitive to price movements of the underlying asset than USD-M quarerly futures. Any long exposure to the Coin-M quarterly futures is thus leveraged exposure. For USD-M this is not the case since the collateral is held in USD.

Before illustrating the additional risk of a long position on Coin-M quarterly futures, it is necessary to discuss another difference between Coin-M and USD-M quarterly futures. Coin-M quarterly futures are denominated and settled in the underlying asset, whilst USD-M quarterly futures settle in USD. This means that for Coin-M quarterly futures, the profit-and-loss (PnL) is added to or subtracted from the underlying asset, whilst for USD-M quarterly futures this is added to or subtracted from the USD balance posted as collateral. Another difference between Coin-M and USD-M quarterly futures is the contract size. As explained in section 2.2, futures contracts size are standardized, and it is up to the discretion of an exchange to determine this contract size. Binance has different contract sizes for Coin-M and USD-M quarterly futures. For Coin-M quarterly futures on Binance, each asset has a standard size in dollar amounts. For Bitcoin (BTC) this contract size is \$100, and for Ethereum (ETH) this is \$10. Binance calls this price of the contract the *multiplier*. The fact that one contract is a pre-determined specified dollar amount, instead of one unit of the underlying asset, might arise confusion. So, far it was assumed that $F(t,T)$ is the price of a futures contract of one unit of the underlying asset. To remain consistent, the notation $F(t,T)$ will remain the quarterly futures price of one unit of the underlying asset, and the property of a multiplier given by Binance allows traders to buy fractions of $F(t,T)$. Figure 25 in the Appendix shows what this looks like in the Binance user-interface (UI). Since Coin-M quarterly futures are denominated in the native asset, the price of one contract is a function of the multiplier and the current quarterly futures price $F(t,T)$. If we let $C(F(t,T)$ denote the price of one quarterly futures contract denominated in the underlying asset, and M the multiplier of the given asset, then:

$$C(F(t,T)) = \frac{M}{F(t,T)} \tag{37}$$

M is deterministic here, hence C is a function only of $F(t,T)$. Suppose the price of one BTC is

[14]Being short 1 BTC worth of a quarterly futures position of BTC approximately offsets the native BTC exposure. During the contract, we may see the BTC quarterly futures contract $F(t,T)$ trade at different levels of contango and backwardation, but at time T we have convergence to the spot price ($S_T = F(T,T)$).

$10000, and it is known that for BTC $M = 100$. The price of one contract $C(10000)$ is given by: $\frac{100}{10000} = 0.01$. If the BTC price were to be higher, $12500 for example, one contract denominated in BTC would be lower, $C(12500) = \frac{100}{12500} = 0.008$. Now suppose the price of one Ethereum (ETH) is $920. A trader wants to replicate one ETH of exposure in quarterly futures. If M were to be 100 we would get: $C(920) = \frac{100}{920} = 0.1087$. Buying 10 contracts $C(920)$ would give an exposure of 1.087 ETH, and buying 9 contracts would give an exposure of 0.978 ETH. With such a high multiplier relative to $F(t,T)$ it becomes very hard to replicate an exact amount of ETH. Since the price of BTC is a lot higher than ETH, it does not have this problem which allows for a higher multiplier.

USD-M quarterly futures do not have this standardized contract size property (multiplier). However, it is possible to buy fractions of $F(t,T)$ similarly to Coin-M quarterly futures. Figure 26 in the Appendix, shows a screenshot of the Binance quarterly futures UI, showing the possibility to buy any fraction of $F(t,T)$, as long as the minimal quantity bought is above 0.001 BTC. Thus, for USD-M quarterly futures there is no standardized contract size as there is for Coin-M quarterly futures.

Now that different levels of exposure, denomination and contract size have been discussed, an example is given where the concepts will become more clear. To be consistent with earlier examples in this section, Bitcoin (BTC) quarterly futures will be used. Consider two traders, trader 1 and trader 2. Both have a starting capital of $10000 at time t. Assume for simplicity that $S_t = F(t,T) = 10000$. Suppose trader 1 is bullish on BTC and wants exposure in the December 2022 USD-M quarterly futures contract. Trader 1 uses his $10000 in collateral to take a long position of 1 BTC ($10000) worth of $F(t,T)$. His payoff during the lifespan of the contract for different prices of $F(t,T)$ is given by:

t	$F(t,T)$	Futures Type	Position Size (Units)	Position Size (USD)	Collateral	PnL
0	10000	USD-M	1 BTC	10000	10000	0
1	12500	USD-M	1 BTC	12500	12500	2500
2	9000	USD-M	1 BTC	9000	9000	-1000
3	7500	USD-M	1 BTC	7500	7500	-2500
4	5000	USD-M	1 BTC	5000	5000	-5000

Table 12: Profit-and-loss (PnL) of a USD-M position

Table 12 shows that the profit-and-loss (PnL) is added or subtracted from the deposited collateral in a linear way. Now, consider trader 2, who is more bullish on BTC than trader 1. The starting capital for trader 2 is also $10000. Trader 2 uses the $10000 to buy 1 BTC on the spot market. This purchased BTC on the spot market is used as collateral to open 1 BTC worth of Coin-M quarterly futures contracts. A common goal to use Coin-M quarterly futures is to gain additional units of the underlying asset. In the case of the example, it can be the case that trader 2 wants to earn additional BTC, because of a positive outlook on the Bitcoin price. Using Coin-M quarterly futures allows trader 2 to hold spot BTC, and use it as collateral to buy a quarterly futures of BTC. If the price of BTC goes up and subsequently $F(t,T)$ goes up, the trader gains additional BTC and the price of BTC is higher, resulting in large profits.

Table 13 shows trader 2 initially buying 100 contracts with a total size of $C(F(t,T)) * 100 = 1$ BTC. Notice how $C(F(t,T))$ decreases as $F(t,T)$ increases. This causes the position size of trader 2 to get smaller denominated in BTC as $F(t,T)$ rises, and larger as $F(t,T)$ decreases in price. This is also reflected in the PnL of trader 2, a gain of 25% (10000 to 12500) in $F(t,T)$ gives the trader an additional 0.2 BTC, and a 25% (10000 to 7500) decrease in price results in a loss of -0.33 BTC. The payoff of trader 2 denominated in the underlying asset is thus non-linear. This follows directly from the negative relationship between $F(t,T)$ and $C(F(t,T))$. If the price of $F(t,T)$ rises, the price of 100 contracts $C(F(t,T))$ becomes less when denominated in $F(t,T)$. Similarly, if $F(t,T)$

t	F(t,T)	C(F(t,T))	Size (BTC)	Size (USD)	Collateral	PnL (BTC)
0	10000	$(\frac{100}{10000} =)0.01$	(0.01*100 =)1	10000	10000	0
1	12500	$(\frac{100}{12500} =)$ 0.008	(0.008*100 =) 0.8	12500	15000	0.2
2	9000	$(\frac{100}{9000} =)0.011$	(0.011 * 100 =) 1.1	9000	8000	-0.11
3	7500	$(\frac{100}{7500} =)0.0133$	(0.0133 * 100 =)1.33	7500	5000	-0.33
4	5000	$(\frac{100}{5000} =)$ 0.02	(0.02*100 =) 2	5000	0	-1

Table 13: Profit-and-loss (PnL) in BTC terms of a Coin-M position. Note that we make the assumption here that $F(t,T) = S_t$ for $t = 0, 1, 2, 3, 4$

decreases, the 100 contracts become worth more when denominated in the underlying asset. This non-linear payoff function has *negative convexity*, which means that the profit-and-loss function denominated in the underlying asset is more sensitive on the downside than on the upside. Figure 4 shows this neagtive convexity.

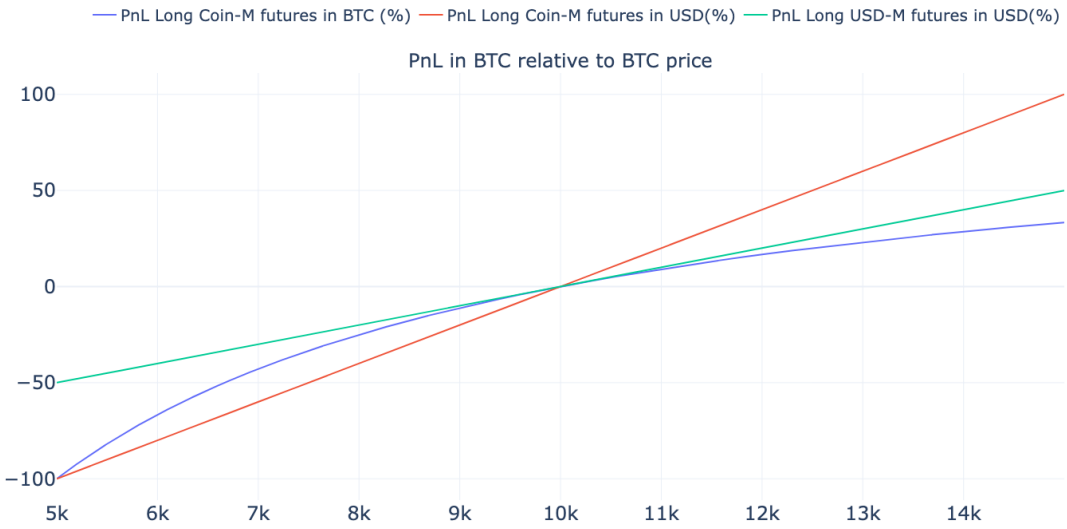

Figure 4: PnL curve of the returns in BTC and USD of longing 1 BTC worth of Coin-M quarterly futures and holding 1 BTC as collateral. The y-axis is the return in percentage, the x-axis is the corresponding BTC price.

The purple line demonstrates a convex loss function for Coin-M futures when dominated in the underlying asset. This shows that a long position on Coin-M quarterly futures has a high downside risk, since it is denominated in the underlying asset. Despite this, Coin-M quarterly futures are frequently used as leveraged speculation, with the goal of obtaining additional units of the underlying asset. The potential to gain high returns in short periods of time attracts speculators to this type of contract, usually unaware of significantly more downside risk. This is something we may see back in the levels of contango or backwardation of futures contracts later, where the Coin-M futures may see more euphoria in certain periods, but also deeper drawdown as a result of this leverage property. The linear USD-denominated payoff of trader 2 can be found in Table 25 in the appendix.

3.1.2 Perpetual Futures

Despite more participation by institutional investors via ventures as CBOE and CME, which offer regulated Bitcoin futures, most volume and open interest is dominated by a type of futures contract which has not seen a lot of usage in other markets. This contract is called a *perpetual futures contract*, or often also called a *perpetual swap*, traded on crypto-specific exchanges. With a daily volume of over 250 billion USD (Coingecko [15]), there certainly is a lot of interest in speculating on cryptocurrencies through these perpetual contracts. Perpetual futures are more frequently traded than quarterly futures. Table 14 shows a comparison.

Asset	Type	24h Spot Vol ($B)	24h Perpetual Vol ($B)	24h Quarterly Vol ($B)
BTC	Coin-M	6.098	1.421	0.135
BTC	USD-M	6.098	9.735	0.062
ETH	Coin-M	1.216	1.336	0.149
ETH	USD-M	1.216	8.880	0.057

Table 14: 24-hour volume for Bitcoin (BTC) and Ethereum (ETH) spot, perpetual futures (perpetual), and quarterly futures (quarterly), respectively, on the Binance exchange (Coingecko). Retrieved from https://www.coingecko.com/en/exchanges/binance_futures on 17th of December, 2022. Abbreviation 'Vol' means volume.

Shiller (1993) originally proposed the idea for perpetual futures contracts, using it to price illiquid assets or quantities such as the consumer price index or human capital. As the name suggests, the length of the futures contract is perpetual, and it has no expiration date. The benefit for speculators is that no rollover is required if a speculator desires to hold the contract for a longer period of time. The property of no expiration date does arise questions as to how these contracts are priced and kept in-line with the spot price. The property of convergence of the futures price to the spot price does not exist, since the futures are perpetual and no expiration date exists. In order to overcome this and stimulate the convergence of the perpetual futures contract to the spot price there is a mechanism called the *funding rate*. Nimmagadda and Ammanamanchi (2019) describe the funding rate as a mechanism to anchor the perpetual futures to the spot price. The funding rate is a periodic payment, usually every 8 hours, from one side of market participant to the other side, given the price difference between the perpetual futures and spot price. In general, if the perpetual futures price is greater than the spot price, the funding rate is positive. This implies that participants who have a long position in a perpetual futures contract have to pay the participants who have a short position. If the funding rate is negative (i.e. the perpetual futures price is below the spot price), then participants who are short pay participants who are long. To illustrate how the funding rate stimulates the perpetual futures price to converge back to the spot price, consider the following example where the perpetual futures price is given by $F_p(t)$:

$F_p(t)$	S_t	$FR(t)$
15100	15000	0.1%

Table 15: Scenario where the perpetual futures price at time t $F_p(t)$ is greater than the spot price S_t the funding rate is 0.1%

First of all, note how we only have parameter t in the expression for the perpetual futures price. This is since no expiration date is present, and therefore we do not have the T in the expression as for quarterly futures. The perpetual futures price $F_p(t)$ in table 15 is 15100, whilst the spot price S_t is 15000. An arbitrageur could take a short position in the perpetaul futures contract, buy the underlying asset S_t and collect the funding rate $FR(t)$, and receive 0.1%. In an efficient

[15] Retrieved from https://www.coingecko.com/en/exchanges/derivatives, on the 16th of Feb 2023

and frictionless market, we would expect arbitrageurs to exploit this opportunity until the two prices are equal again. However, performing this arbitrage is not fully risk-less. He et al. (2023) state that since the futures contract is perpetual, there is no date at which convergence of the spot price will happen and the trade will be closed out. It could happen that the gap between the perpetual futures price and the spot price will only widen further. Despite this hypothetical scenario of diverging prices, the arbitrageur will get paid the funding rate every 8 hours for which the perpetual futures price is above the spot price, which mitigates some of the price risk.

The exact calculation of the funding rate consists of two components. The first one is called the *premium index*, which is a time weighted premium of the perpetual futures price relative to the spot price. Since all data used in this thesis is from the cryptocurrency exchange Binance, we will stick to the premium index calculation performed by Binance. The premium index Z_t is given by:

$$Z_t = \frac{[Max(0, I_{b,t} - \bar{S}_t) - Max(0, \bar{S}_t - I_{a,t})]}{\bar{S}_t} \tag{38}$$

The premium index described in 38 consists of 3 variables. The first one $\bar{S}_t$ is a spot price index of several crypto exchanges weighted by volume, to give a fair indication of what the current spot price is. This prevents price manipulation to alter the funding rate. $I_{b,t}$ is the *Impact Bid Price*. This is the average price to execute a sell order for a predetermined amount. This is again done to avoid price manipulation. If the market of the perpetual futures is very liquid, the $I_{b,t}$ will be very close to the actual price. $I_{a,t}$ is the *Index Ask Price*, this is the opposite of the $I_{b,t}$, the average ask price for filling a market buy order of a predetermined size. By using a weighted spot price and a fair way to determine the price of the perpetual future by the $I_{b,t}$ and $I_{a,t}$, Z_t is a fair representation of the premium or discount of the perpetual future relative to the spot price. Terminology often used for the perpetual futures price is the *mark price*, and the weighted spot index $\bar{S}_t$ is often called the *index price*. Binance does the calculation of (38) every 5 seconds for a total period of 8 hours. This comes down to 5760 premium index calculations for every funding payment interval. So, (38) describes how much of an average premium or discount the perpetual futures market has relative to the spot price over a period of 8 hours. Let $\bar{Z}_t = \frac{\sum_{t=1}^{5760} tZ_t}{\sum_{t=1}^{5760} t}$. The funding rate is then calculated as:

$$\text{Funding Rate } (FR_t) = \bar{Z}_t + C(r - \bar{Z}_t, 0.05, -0.05) \tag{39}$$

, where r is the predetermined interest rate set by binance, and $\bar{Z}_t$ the average premium index over the 8 hour period, $C(.)$ is the *clamp* function which acts as a damper:

$$C(x, min, max) = \begin{cases} min & \text{if x} < min \\ max & \text{if x} > max \\ x & \text{if } x \in [min, max] \end{cases}$$

To see how the clamp function acts as a damper, consider the following figure:

From (39) we see that if $r - Z_t \in (-0.05, 0.05)$, then $FR_t = \bar{Z}_t + r - \bar{Z}_t = r$. If there is a very high premium, say 0.1%, and $r = 0.01$ then $FR_t = 0.1 + C(-0.09.0.05, -0.05) = 0.05$. The funding rate is therefore a function of the premium index and damped to some extent.

The interpretation of the height of the funding rate can be interpreted as the level of sentiment in the cryptocurrency market. This arises due to the property that the funding rate is paid peer-to-peer, meaning that longs pay shorts or shorts pay long. In (38) and (39), it has been shown that the funding rate is mainly determined by the height of the premium index. A high premium index $\bar{Z}_t$ is a result of the perpetual futures price $FR(t)$ trading above the spot price S_t for the duration of the 8 hour period. The perpetual future is therefore in higher demand for traders which pushes the price above the spot price. A sustained period of strong positive funding rates thus implies that market participants are willing to pay a premium for the perpetual futures contract, and a

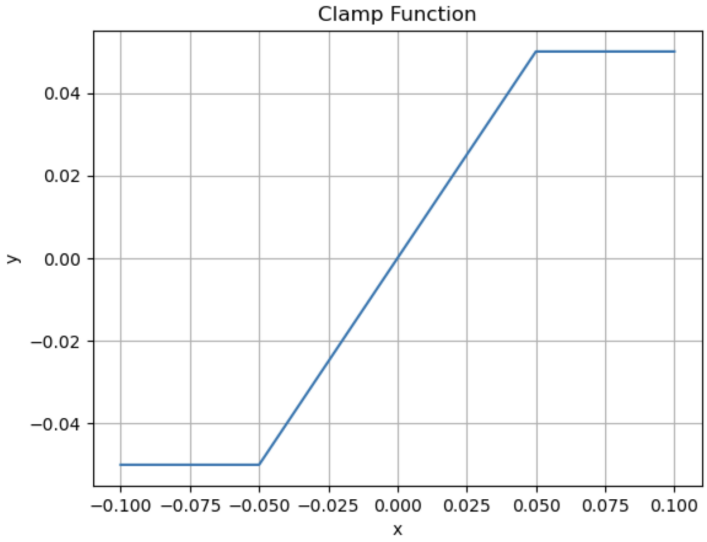

Figure 5: The clamp function C(.) plotted in Python

fee deducted every 8 hours. This all whilst the spot Bitcoin or Ethereum is trading cheaper and does not have this fee included. The perceived benefit of speculating with leverage is creating additional demand for these perpetual futures, and speculators are willing to pay for that. As a result, it is reasoned here that the funding rate is a well suited and quantify able metric to measure market sentiment. In the next section additional arguments will be given to support this claim. A visual representation shown in Figure 31 shows that high values of the funding rate coincide with rising prices, and vise versa.

3.2 Sentiment and Leveraged Speculation in Cryptocurrency Futures

The previous section introduced quarterly and perpetual futures. This section will illustrate the high leverage ratio that is possible on these futures, and what connection futures have to perceived investor sentiment.

3.2.1 Leverage in Crypto

Both quarterly and perpetual futures on crypto-native exchanges offer extremely high leverage ratios compared to traditional futures platforms. To compare the high amount of leverage that crypto exchanges offer, a comparison between the CME Bitcoin futures and Binance futures is made.

The CME Bitcoin futures have a contract size of 5 Bitcoin per contract and have an expiration date. This means that the minimum position size at any time is the dollar value of 5 Bitcoin according to a Bitcoin time-weighted average price metric determined by the CME itself. In comparison, Binance has significantly lower requirements for a minimum position size, a quantity of 0.001 Bitcoin for USD-M futures, and the multiplier size as discussed (37), which is often 10 or 100 USD. The lower requirements offered by Binance therefore attract more retail traders than CME. At the time of writing, one CME Bitcoin futures contract costs over $140,000, causing most retail traders to be priced out of CME futures.

In order to achieve a large position size with a small amount of capital, cryptocurrency exchanges

such as Binance offer extremely high *leverage ratios*[16] on their futures platforms. The maximum leverage ratio on Binance is 125x, which means that for a deposit of $1, a trader can achieve a position size of $125, essentially borrowing $124 from Binance. This maximum leverage ratio, however, is capped by a certain maximum position size in dollars. It is not possible to deposit $1M dollars and use leverage to get a position size of $125M. Binance determines the maximum leverage ratio in tiers. The maximum leverage ratio per tier for USD-M quarterly and perpetual futures can be found in Figures 27 and 28 in the Appendix. For Coin-M futures the leverage ratios are comparable, and therefore omitted.

To properly compare the high leverage offered by crypto-native platforms such as Binance to the CME, we will compare a similar position size taken on both platforms. The CME has a contract size of 5 BTC per contract. This is a value of approximately $140,000 at current prices. Considering Figures 27 and 28 in the Appendix again, we see that for quarterly futures this falls in the first tier (25x max leverage), and for perpetual futures this falls in the second tier (100x max leverage). Table 16 clearly shows the lower maintenance margin requirements and higher leverage potential for Binance futures compared to the CME.

Platform	Type	Settlement	Position Size	Max Leverage	Min. Maintenance Margin
CME	Delivery	USD	5 BTC	2x	25%
Binance	Delivery	USD	$140,000	25x	2%
Binance	Delivery	BTC	5 BTC	50x	1%
Binance	Perpetual	USD	$140,000	100x	0.5%
Binance	Perpetual	BTC	5 BTC	100x	0.5%

Table 16: Showing the differences in the leverage ratios and maintenance margins between CME and Binance. It is assumed here that 1 BTC = $28,000 such that 5 BTC = $140,000.

To explain the determination of the 'Max Leverage' column of table 16, the max leverage is $\frac{1}{IM}$, which is 1 divided by the initial margin. This means that for CME Bitcoin futures, an initial margin of 50% has to be held, and for Binance futures with a leverage ratio of 100x, an initial margin of only 1% has to be held. This means that to open a $140,000 position size on the CME, at least $70,000 has to be posted on collateral initially, and a minimum of $35,000 when the position is open. For Binance futures, the initial collateral can be as low as $1,400 to open and $700 to maintain. Traders on Binance futures thus have the potential to greatly lever up their capital, both for quarterly and perpetual futures. The benefit of this is that small capitalized traders are able to enjoy larger trading capital, but there is also significant risk associated with this. At 100x leverage, a move greater than 0.5% of the underlying in the wrong direction would already liquidate the position. High leverage ratios are therefore a double-edged sword, where high returns but also high losses can be made. As a result of this availability of high leverage, it is expected that users on crypto-native exchanges such as Binance use a considerably higher leverage ratio than in other markets and platforms, such as the CME.

Schmeling et al. (2022) confirm this hypothesis in their analysis in the cryptocurrency futures market. It is found that the futures basis for crypto-native exchanges is more volatile than for CME futures, possibly by the higher leverage that crypto-exchanges offer. This is also visible through the *open interest* [17] for perpetual and quarterly Coin-M futures. Specifically, we will look at the increases and decreases of open interest and how this relates to leverage being used on crypto-exchanges. Figure 29 shows the total open interest for Bitcoin Coin-M futures (both perpetual and quarterly) throughout 2021. From January 1st 2021 up until the peak of the market at April 13th, the price of Bitcoin increased 113.97% ($29,700 to $63,552), whilst the total open interest increased 216.19% ($4.2B to $13.28B). This shows that a large amount of positions were

[16]The leverage ratio is the amount of money that can be borrowed from the platform, given a deposit size. This allows traders to achieve a higher total position size than the money they deposited, essentially borrowing capital.
[17]Open interest is the total Dollar value of all margin positions currently open

opened in bullish market regimes as demand for leveraged speculation increased. To show why this is leveraged demand, consider Figure 29 again, now looking at April 14th 2021- June 1st 2021. The price of Bitcoin decreased 45.50% ($63,552 to $34,640) whilst the Coin-M open interest decreased 67.16% ($13.28B to $4.36B). This enormous drop in open interest is due to a large amount of liquidations as a result of negative convexity of Coin-M futures as shown in Figure 4. In fact, over $1.74B in liquidations happened on May 19th 2021 alone (Coinalyze [18]). For USD-M futures in the same time period, this increase and decrease is found to be less extreme than for Coin-M futures. Figure 30 shows a total increase of open interest on the way up of 139.5% ($1.966B to $4.71B) and a subsequent decrease in open interest of 54.5% ($4.71B to $2.14B). The amount of liquidations on May 19th 2021 were 1.16B. Schmeling et al. (2022) describe that a large portion of speculators in the cryptocurrency market are 'trend-chasing' retail investors with a high demand for high leveraged exposure through futures. The open interest data supports this argument. It is also verified that due to negative convexity of Coin-M futures that the amount of leverage in these type of contracts is much higher than on USD-M futures.

3.2.2 Sentiment in the Cryptocurrency Market

In section 3.2.1 it has been shown that futures in the cryptocurrency market offer high leverage ratios and this is seen through the behavior of open interest. Later on in this thesis, the role of sentiment, modeled through perpetual futures funding rate, will be used to analyze the quarterly futures basis. This section quantifies sentiment in the cryptocurrency market, and shows that the perpetual futures funding rate is a suitable proxy for modeling sentiment.

The effect of sentiment on price behavior in the cryptocurrency market is well-studied and documented in the literature. Bouteska et al. (2022) use Principal Component Analysis (PCA) to study the effect of sentiment in Reddit and StockTwits messages on the returns of Bitcoin. It is found that highly positive sentiment observed through these platforms is a significant predictor of Bitcoin returns. Burggraf et al. (2020) use the transfer entropy model to classify investor sentiment, which is found to have strong predictive power on Bitcoin returns. It is also widely known that the cryptocurrency market is notorious for its bubble-like behavior. Cheah and Fry (2015) find that cryptocurrency markets have the stylized fact of being venerable to bubbles. This strong influence of investor sentiment on returns, and the observed bubble-like behavior can be explained by the great presence of retail investors in the cryptocurrency market. In addition, it is found that the type of investors in cryptocurrencies are risk-seeking. Lammer et al. (2019) report that investors in cryptocurrencies are more likely to invest in other risky assets such as emerging markets, and are more likely to trade penny stocks. In addition, retail participants in the cryptocurrency market are more active than in other markets, and log in to their brokerage account approximately 9 times per month, compared to the average retail investor in other markets who does this 2 times per month. Grobys and Junttila (2020) investigate the 'lottery-like demand' in the cryptocurrency market, which is the interest in cryptocurrencies due to its possible high returns, whilst the probability of this happening is quite slim. It is found that this lottery-like demand is present in the cryptocurrency market due to its volatile nature. The tendency of investors in the cryptocurrency market to be more active and speculative also translates itself into the area of research of this thesis, the futures market.

The example of open interest in section 3.2.1 has shown the leveraged speculation of market participants in the cryptocurrency market. It is a direct result of sentiment, where an increase in prices lead to a higher level of perceived sentiment, and demand for leveraged speculation increases as a result. However, sentiment itself can be difficult to quantify as it is not some known quantity. He et al. (2023) use the *Crypto Fear and Greed Index (CFNGI)* provided by *Alternative* [19] to quantify market sentiment. This is the crypto-counterpart of the well-known Fear and Greed Index (FNGI) used in the traditional market, which is constructed by *CNN Business*. The exact

[18] Retrieved from https://coinalyze.net/ on March 2nd, 2023
[19] https://www.alternative.me

components of the FNG can be found in Table 26. The CFNGI is a similar index as the FNGI, but specified for the cryptocurrency market. The CFNGI is compiled using multiple components on a daily basis by *Alternative*, and aims to quantify the current market sentiment on a scale from 0 to 100. The labels classified to each range of values can be found in Table 27 in the Appendix.

The CFNGI consist of multiple components and weights. It is worth noting that the exact determination of the weights is not made public by the issuer of the index, only the components, weights and description of the estimation. In terms of transparency, this limits the applicability of analysis of the CFNGI. Despite this, the CFNGI is widely-used as a sentiment indicator in the cryptocurrency market, and its use in this thesis will only be to illustrate the dynamics between sentiment and futures prices. The exact components can be found in Table 28 in the Appendix. An overlay of the CFNGI and Bitcoin prices can be found in Figure 32 in the Appendix.

The CFNGI is a well-known measure of market sentiment, but has its drawbacks. It is a proprietary metric that does not show its exact calculation. It may also be up to debate what the exact relationship between this sentiment indicator and the futures basis may be. We now refer back to section 3.1.2, where introduced perpetual futures were introduced and the associated funding rate. Since perpetual futures are a similar contract to the quarterly futures that are being analyzed here, using the funding rate associated with these perpetual futures seems a more natural candidate to model sentiment. It is tested here if the perpetual futures funding rate is a suitable proxy for investor sentiment. To do so, we will consider the CFNGI, the perpetual futures funding rate and returns of Bitcoin and Ethereum.

To show the dynamics between prices, funding rates and the CFNGI, plots are shown in Figures 33 , 34 and 35 in the Appendix. From this simple visual analysis, we can deduce that high values of the funding rate and the CFNGI coincide with rising prices, and vice versa low values of funding rates and the CFNGI coincide with decreasing prices. To make this more concrete, we follow He et al. (2023) and create a correlation matrix.

	$R_{B,7}$	$R_{E,7}$	FR_7	$CFNGI_7$
$R_{B,7}$	-	-	-	
$R_{E,7}$	0.918	-	-	-
FR_7	0.791	0.794	-	-
$CFNGI_7$	0.774	0.688	0.675	-

Table 17: Correlation matrix between weekly Bitcoin and Ethereum spot returns, weekly funding rates, and weekly Crypto Fear and Greed index (CFNGI).

Table 17 shows a strong correlation between returns, funding rates, and the CFNGI. Note that for the funding rates and CFNGI the weekly mean of daily values were used. This is to filter out noise and give a more long-term overview of the correlation between the indicators (funding rates, CFNGI) and the weekly returns. Note that $R_{B,7}$,$R_{E,7}$ denote the weekly Bitcoin and Ethereum returns. FR_7 and $CFNGI_7$ are the weekly values of the weekly funding rates and weekly crypto fear and greed index, respectively. This strong positive correlation shows first of all how correlated Bitcoin and Ethereum are. Secondly, it seems that funding rates and the CFNGI are good predictors of Bitcoin and Ethereum returns. It is not the goal here to predict returns, the purpose of Table 17 is to show that funding rates are an equivalent, if not better indicator of market sentiment than the CFNGI as used by He et al. (2023). Therefore, later on in this thesis funding rates will be used as a measure of investor sentiment in the analysis of quarterly futures prices.

3.3 Cost-of-Carry Parameters in the Cryptocurrency Market

In section 2.2.5 we have discussed several cost of carry models for different asset classes. The goal of this thesis is to test these models against market data of Bitcoin and Ethereum, and to see how well these models fit. In order to do so, we have to first define certain parameters. The first parameter which is involved in all of the models is the risk-free rate $r_{t,T}$. The most natural choice for the risk-free rate, and most common in the literature is to use US treasury bills as a proxy of the risk-free rate. This will be the starting choice of the risk-free rate parameter to test the models against. The specifics of the choice of the risk-free rate proxies are given in the section which will test the models.

The next parameter which has to be tailed to the cryptocurrency market is the parameter k_t. This is the storage cost parameter found in the cost of carry models for commodities. The question if cryptocurrencies have storage costs associated with them is up for debate. In principle, anyone can create a wallet on a blockchain and hold cryptocurrencies without incurring any costs. The only costs associated with this would be the transaction fees for making a transaction. In practice, the storage costs of holding cryptocurrencies may be higher than only transaction costs of moving the cryptocurrencies. Since cryptocurrencies operate on a blockchain and are peer-to-peer, a wallet getting compromised, or losing the credentials of a wallet means losing all of the cryptocurrencies stored in that wallet. There is no third-party that can access the wallet, or restore a password. This property of full self-custody of funds, which may be beneficial since it eliminates counter party risk, does add extra cost of security. It is common practice to use a hardware wallet, a device that is used to access a cryptocurrency wallet. These hardware wallets have a cost of around $100 associated to them. It is worth noting that this is not a per-unit cost of holding a cryptocurrency. Hardware wallets allow for storage of $1 or $1 million worth of cryptocurrencies, and no per-unit cost is incurred. The value of k_t is therefore reasoned to be low for cryptocurrencies, and its effect on the futures basis limited.

The next parameter which is present in the cost-of-carry model for commodities is the convenience yield Ψ_t. As briefly stated earlier, the convenience yield is the additional benefit of holding the underlying asset instead of its derivative. Reflecting this towards the market of cryptocurrencies requires us to answer the question in which scenario investors would prefer to hold the actual underlying asset instead of a futures position on the underlying asset. Hilliard and Ngo (2022) state that the benefit of holding cryptocurrencies is not analogous to holding an actual commodity, but owning the actual cryptocurrency instead of a derivative does have benefits. The most obvious benefit of holding the underlying cryptocurrency is that transactions can be made with the cryptocurrency, which is not possible with a derivative. Investors who value the benefit of making transactions with cryptocurrencies may pay prefer to hold the actual cryptocurrency instead of a derivative. Another important factor which may influence the convenience yield is counterparty risk. As briefly stated earlier when discussing the storage cost parameter k_t, holding cryptocurrencies in a wallet means full self-custody of funds and eliminates counterparty risk. The sudden bankrupcy of one of the largest cryptocurrency exchanges FTX illustrates the large counterparty risk in the cryptocurrency market. Hilliard and Ngo (2022) also describe a form of negative convenience yield. Self-custody of funds means that a lost password without a backup means a total loss of funds. Holding a derivative on a centralized party does not have this risk, and a lost password can be restored. It is therefore plausible that technically sophisticated investors with priority on security prefer holding the actual cryptocurrency, whilst less sophisticated investors may prefer a derivative held on a centralized party. Schmeling et al. (2022) hypothesize that a form of convenience yield may even be demand for leveraged speculation through futures contracts. This claim will be investigated in more detail in a later section.

3.4 Bitcoin (BTC) and Ethereum (ETH) (bi-)Quarterly Futures Basis

This section shows the observed futures basis for Bitcoin and Ethereum. It may be wise to gain a broad understanding of how spot and futures prices behave relative to each other, before applying more rigorous models. It can be deduced if the market is, on average, in contango or backwardation, and to what extent the spot and quarterly futures prices differ. From here on, the difference between the quarterly futures and spot prices will be referred to as the *basis*. The basis is simply the difference between the futures price at time t, and the spot price at time t. Mathematically, $B(t,T) = F(t,T) - S_t$. In other words, the futures basis of Bitcoin and Ethereum at time t, $B(t,T)$ is the level of contango or backwardation at time t.

We will look at the basis for Bitcoin and Ethereum quarterly futures for both Coin-M and USD-M quarterly futures. In section 3.1.1, the properties of Coin-M and USD-M quarterly futures were given, as well as their differences. Recall that Coin-M futures allow traders to hold their respective assets as collateral to open futures position. This likely means that there is more leverage involved in Coin-M futures than in USD-M futures. This could be something we see in the basis of Coin-M and USD-M futures.

3.4.1 Price Data

Price data of Bitcoin (BTC) and Ethereum (ETH) quarterly futures, perpetual futures and the spot market will be used in this thesis. The price data will consist of hourly OHLC (open, high, low, close) data from the exchange *Binance*. The testing period ranges from 2020-07-01 up until 2022-09-30. The method for gathering data is from the open-source library *Binance Vision* [20], which is provided by Binance itself. Through Python all data is pulled from the website and extracted into a large data set. There are 10 futures contracts which have matured in this time period which will be used.

3.4.2 Bitcoin (BTC) (bi-)Quarterly Futures Basis

Table 18 shows the summary statistics of the futures basis of BTC bi-quarterly Coin-M futures and USD-M quarterly futures. Coin-M futures have a maturity of 6-months, and therefore are called bi-quarterly futures. USD-M futures have a maturity of 3-months and therefore are referred to as quarterly futures. Taking a closer look at Table 18, it is observed that for both futures types and every interval analyzed, there has been a positive basis, expressing a contango structure. The level of the basis observed is quite substantial, especially given the short duration of the futures. Coin-M Bitcoin futures reached a maximum basis greater than 18% , with a maturity of 6 months. USD-M futures reached a maximum level of 11.45%, with a maturity of 3 months. These are extremely high levels, and it means that investors in 2021 were willing to pay an 18% premium for a futures contract that expired a maximum of 6 months later. The more extreme level of basis for Coin-M futures compared to USD-M futures could be the additional leverage that is present in the Coin-M futures.

In addition to a high mean, the variance in the level of the basis is observed to be substantial as well. The range between the minimum and maximum observation is wide, especially throughout 2021. For Coin-M futures, the interval *2021-03-26 - 2021-09-24* experienced a minimum basis of -5.647% and a maximum of 18.899%, all in the same 6 months. For USD-M futures, the interval *2021-03-16 - 2021-06-25* had a minimum level of -1.437% basis, and a maximum of 11.450%, in a time period of only three months. Figures 6 and 36 visualize the futures basis over time.

[20] https://data.binance.vision/

Bitcoin Coin-M futures							
Start Date	End Date	N	Mean(%)	Median (%)	Std. (%)	Min (%)	Max (%)
2020-06-30	2020-09-25	2008	1.265	1.152	0.935	-0.395	3.49
2020-07-01	2020-12-25	3949	2.200	1.813	1.358	-0.406	6.219
2020-09-25	2021-03-26	4062	3.502	3.780	1.370	-1.424	6.972
2020-12-25	2021-06-25	4178	5.472	6.547	3.295	-2.700	11.389
2021-03-26	2021-09-24	4176	4.011	1.036	4.933	-8.212	18.349
2021-06-25	2021-12-31	4340	2.279	2.715	1.154	-0.086	4.379
2021-09-24	2022-03-25	4183	2.255	2.356	2.223	-0.087	7.440
2021-12-31	2022-06-24	4024	1.131	0.890	1.157	-2.203	4.426
2022-03-25	2022-09-30	4395	0.738	0.423	0.825	-1.220	3.164
Bitcoin USD-M futures							
Start Date	End Date	N	Mean(%)	Median (%)	Std. (%)	Min (%)	Max (%)
2021-02-03	2021-03-26	1169	3.046	2.437	2.071	-0.582	7.875
2021-03-16	2021-06-25	2318	3.747	3.494	3.216	-1.437	11.450
2021-06-18	2021-09-24	2259	0.783	0.867	0.371	-2.22	2.386
2021-09-22	2021-12-31	2302	1.925	1.954	1.276	-0.363	4.775
2021-12-24	2022-03-25	2097	0.795	0.501	0.822	-0.117	2.992
2022-03-22	2022-06-24	2166	0.432	0.284	0.457	-0.431	2.363
2022-06-20	2022-09-30	2403	0.302	0.329	0.299	-0.560	1.135

Table 18: Summary statistics of Bitcoin (BTC) Coin-M and USD-M futures basis ($F(t,T) - S_t$). Each row represents a different contract maturity. Note that each column is given in '(%)', which represents $\frac{F(t,T)-S_t}{S_t} * 100$.

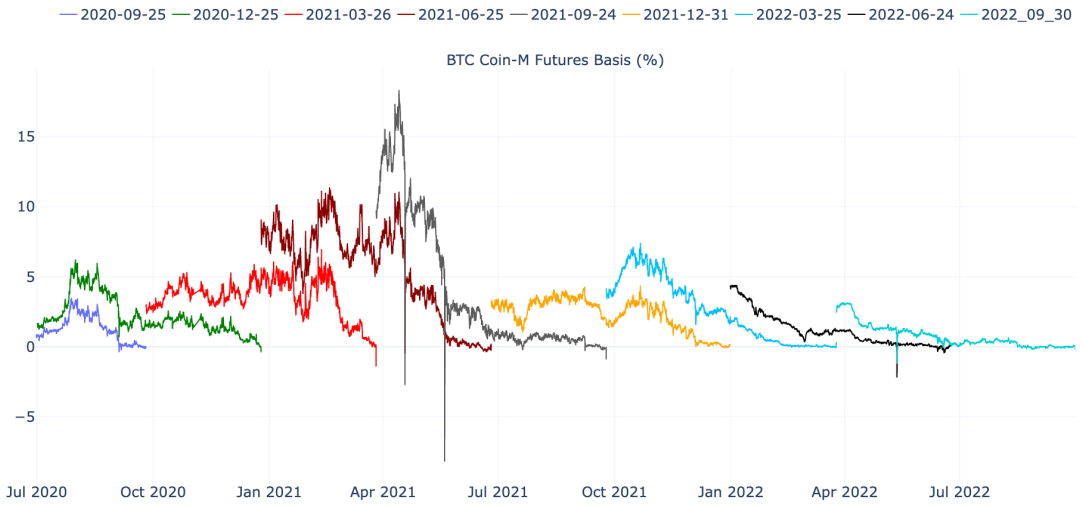

Figure 6: BTC Coin-M bi-quarterly futures basis

3.4.3 Ethereum (ETH) (bi-)quarterly futures basis

In this section, a similar analysis will be performed on Ethereum futures as in section 3.4.2. Table 19 shows the summary statistics for Ethereum Coin-M and USD-M (bi-) quarterly futures.

ETH Coin-M futures							
Start Date	End Date	N	Mean(%)	Median (%)	Std. (%)	Min (%)	Max (%)
2020-07-24	2020-09-25	1449	1.572	1.260	1.384	-0.777	6.022
2020-08-05	2020-12-25	1950	2.236	1.442	1.864	-1.408	7.170
2020-09-25	2021-03-26	3349	3.272	3.464	1.489	-3.789	6.534
2020-12-25	2021-06-25	4178	5.481	6.448	3.292	-5.647	11.436
2021-03-26	2021-09-24	4177	4.140	1.059	5.021	-5.078	18.899
2021-06-25	2021-12-31	4340	2.243	2.756	1.249	-0.094	5.330
2021-09-24	2022-03-25	4183	2.718	2.524	2.431	-0.183	7.822
2021-12-31	2022-06-24	4009	1.055	0.812	1.145	-2.501	4.622
2022-03-25	2022-09-30	4395	0.361	0.173	1.129	-1.692	3.351
ETH USD-M futures							
Start Date	End Date	N	Mean(%)	Median (%)	Std. (%)	Min (%)	Max (%)
2021-02-03	2021-03-26	1147	3.501	2.168	2.732	-0.113	9.530
2021-03-16	2021-06-25	2318	3.980	3.476	3.598	-3.737	12.31
2021-06-18	2021-09-24	2259	0.906	0.967	0.390	-0.650	2.415
2021-09-22	2021-12-31	2302	2.039	2.150	1.317	-0.722	5.396
2021-12-24	2022-03-25	2097	0.752	0.317	0.884	-0.185	3.085
2022-03-22	2022-06-24	2166	0.457	0.278	0.497	-0.288	2.321
2022-06-20	2022-09-30	2403	-0.382	-0.098	0.623	-1.610	0.791

Table 19: Summary statistics of Ethereum (ETH) Coin-M and USD-M (bi-) quarterly futures basis $F(t,T) - S_t$. Each row represents a different contract maturity. Note that each column is given in '(%)', which represents $\frac{F(t,T)-S_t}{S_t} * 100$.

The results for Ethereum Coin-M bi-quarterly and USD-M quarterly futures are very similar to those of Bitcoin in table 18. The Ethereum futures market experiences an average stage of contango, including a high variance. The maximum observed value of the basis is approximately 18% similar to that of Bitcoin. Notice that for the Ethereum USD-M futures, the last interval: *2022-06-20 - 2022-09-30* shows backwardation. This is also visible in Figure 8, where we see a negative basis for a significant amount of time. The observed negative basis during interval could be explained as an anomaly, and will be discussed in greater detail in the next section when the notion of convenience yield is introduced.

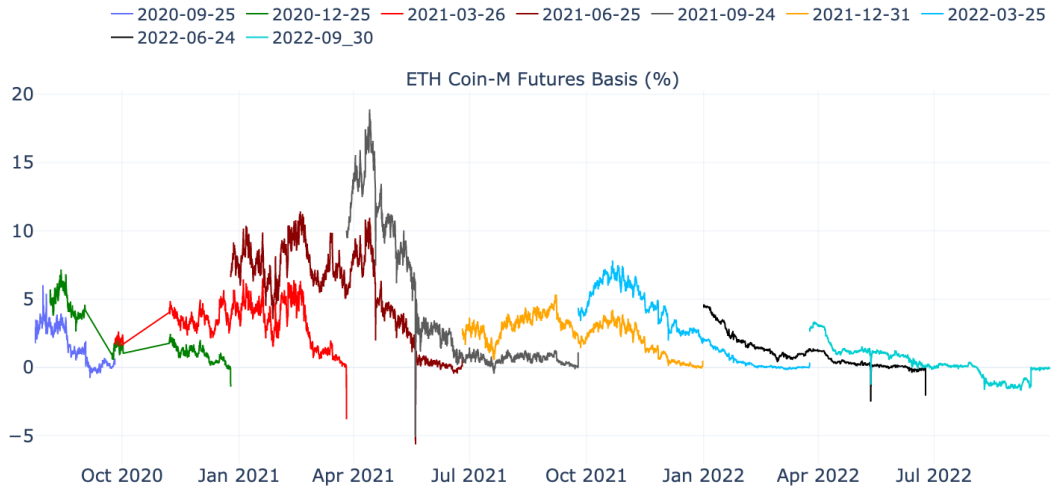

Figure 7: ETH Coin-M bi-quarterly futures basis

Figure 8: ETH USD-M quarterly futures basis

4 Time Series Analysis

Throughout this section notation of Neusser (2016) will be used.

4.1 Random Walk and Order of Integrataion

4.1.1 Random Walk

Prices of financial assets followed over time are classified as time series data. Specifically, financial assets are often modeled as a *random walk* process. Granger and Newbold (1974) decribe a random walk process to represent speculative assets particularly well. Neusser (2016) defines a random walk process with drift as:

$$X_t = \mu + X_{t-1} + Z_t \tag{40}$$

μ is the drift term, X_t is the stochastic process of asset prices, and $Z_t \sim N(0, \sigma^2)$. Modeling asset prices as in (40) is done under the random walk theory. As the name suggests, the random walk theory states that prices of financial assets are random to some extent. The asset price at time t is its its own value at time $t-1$ with some random movement Z_t and a constant drift term μ. The randomness in Z_t results in the asset prices being unpredictable according to the random walk theory. Modeling a stock price as a random walk is the discrete version of the geometric Brownian motion, which is often used to model asset prices in the continuous time. Fama (1965) links the random walk theory of asset prices to the *Efficient Market Hypothesis (EMH)*, although they are not identical [21]. Specifically, Fama (1965) states that the theory of random walk begins under the assumption of efficient markets, where it is assumed that prices of assets trade around their intrinsic value. However, there may be uncertainty or discussion regarding what exactly this intrinsic value may be. This results in prices moving randomly around the intrinsic value and gives rise to the random walk theory. A plot of a random walk can be found in Figure 9.

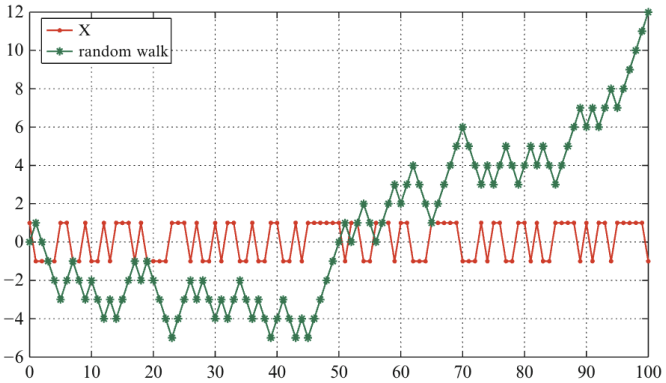

Figure 9: Stationary time series as shown by Neusser (2016) (page 17).

4.1.2 Stationarity and Unit Roots in Time Series

In next chapter, time series analysis will be performed on data of the cryptocurrency market. The property of stationarity will often be discussed. Therefore this subsections aims to give a

[21] The Efficient Market Hypothesis states that markets are efficient and all information that is publicly available is reflected in market prices.

description of stationarity in time series, and what it means when a time series has a unit root. Stationarity is often necessary in order to gain correct statistical interference of time series data, such as a correct asymptotic distribution. Neusser (2016) denotes the following conditions for a time series to be (weakly) stationary:

- $\mathbb{E}[X_t] = \mu$
- $Var[X_t]$ is finite
- $Cov[t, s] = Cov[t + r, s + r]$

The conditions above imply that a stationary time series has a constant mean and a (finite) covariance that does not change over time. This does not imply that the covariance is the same between each two time periods, but it should be the same for any two time periods which are equally far apart, i.e. $Cov(X_1, X_2) = Cov(X_{11}, X_{12})$ and $Cov(X_4, X_7) = Cov(X_{11}, X_{14})$. Figure 10 shows what a stationary time series might look like.

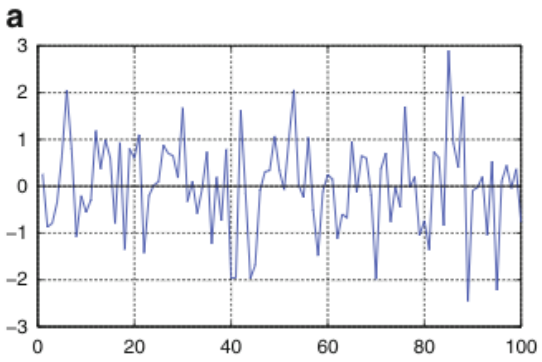

Figure 10: Stationary time series as shown by Neusser (2016) (page 17).

Stationarity is required in many time series models. To show why a random-walk may not be stationary, consider the following $AR(1)$ model:

$$X_t = \mu + \phi X_{t-1} + Z_t \tag{41}$$

, where $Z_t \sim N(0, \sigma^2)$ again, similar to (40). We can recursively express X_t as an Moving Average (MA) model:

$$\begin{aligned} X_t &= \mu + \phi X_{t-1} + Z_t = \mu + \phi(\mu + \phi X_{t-2} + Z_{t-1}) + Z_t && (42)\\ &= \mu + \phi\mu + \phi^2(X_{t-2}) + \phi Z_{t-1} + Z_t && (43)\\ &= ... && (44)\\ &= \phi^t X_0 + \mu \sum_{i=0}^{t} \phi^i + \sum_{i=0}^{t} \phi^i Z_{t-i} && (45) \end{aligned}$$

Using the expression in (45), the expectation and variance can be computed as follows:

$$\mathbb{E}[X_t] = \mathbb{E}[\phi^t X_0 + \mu \sum_{i=0}^{t} \phi^i + \sum_{i=0}^{t} \phi^i Z_{t-i}] = \phi^t X_0 + \mu \sum_{i=0}^{t} \phi^i + \sum_{i=0}^{i} \mathbb{E}[\phi^i Z_{t-i}] = \phi^t X_0 + \mu \sum_{i=0}^{t} \phi^i \tag{46}$$

$$Var[X_t] = Var[\phi^t X_0 + \mu \sum_{i=0}^{t} \phi^i + \sum_{i=0}^{t} \phi^i Z_{t-i}] = Var[\sum_{i=0}^{t} \phi^i Z_{t-i}] = \sum_{i=0}^{t} \phi^{2i} Var[Z_{t-i}] = \sum_{i=0}^{t} \phi^{2i} \sigma^2 \tag{47}$$

To get to the variance expression in (47), it is assumed that white noise $Z_t, Z_{t-1}, Z_{t-2}, ...$ are independent, therefore $Cov(Z_j, Z_k) = 0 \quad \forall j \neq k$. As a result, $Var[\sum_{i=0}^{t} X_i] = \sum_{i=0}^{t} Var[X_i]$. Now consider the first case, $|\phi| < 1$. Notice that we have two geometric series in (46) and (47) with a common ratio $r = -1 < \phi < 1$ and $r = \phi^2 < 1$, respectively. If $t \to \infty$, these geometric series converge to $\frac{1}{1-\phi}$ and $\frac{1}{1-\phi^2}$, respectively. Therefore, if $|\phi| < 1$, $\mathbb{E}[X_t] = \frac{\mu}{1-\phi}$, and $Var[X_t] = \frac{\sigma^2}{(1-\phi^2)}$. Both the expectation and variance are not dependent on t. For $t < s$, $Cov(X_t, X_s) = Cov(X_t, \phi^{s-t} X_t) = \phi^{s-t} Var[X_t] = \phi^{(s+r)-(t+r)} Var[X_t] = Cov(X_{t+r}, X_{s+r})$, and therefore the time series is weakly stationary for $|\phi| < 1$. In the case when $|\phi| > 1$, we clearly see that when $t \to \infty$, the two geometric series in (46) and (47) diverge to infinity, and the time series is non stationary.

In the last case where ϕ =1, which is the random walk process as discussed earlier, it follows from (46) that $\mathbb{E}[X_t] = X_0 + \mu t$, which is dependent on t. The first property of stationarity is thus violated with a drifting mean that increases or decreases over time. From (47), it follows that for $\phi = 1$, $Var[X_t] = \sum_{i=1}^{t} 1^{2i} \sigma^2 = t\sigma^2$, which also has dependence on t. Finally, for two time periods equally far apart, $Cov(X_1, X_3) = \phi^2 Var[X_1] = Var[X_1] = \sigma^2$, and $Cov(X_{11}, X_{13}) = Var(X_{11}) = 11\sigma^2$. Covariance stationarity does therefore not hold. The AR(1) process X_t is said to have a *unit root* in this last case, where $\phi = 1$.

The term unit root arises from the fact that 1 is the root of the characteristic equation derived from (40). The expression in (40) can be written in terms of a lag operator L (where $X_t L = X_{t-1}$) as $X_t = \mu + \phi X_t L + Z_t \iff Z_t - \mu = X_t(1 - \phi L)$. If we now consider the characteristic equation, we obtain $1 - \phi L = 1 - L = 0 \iff L = 1$. This shows that a unit root is present, since 1 is a solution of the characteristic equation. A random walk process without drift ($X_t = X_{t-1} + Z_t$), is also non stationary. This is since $Var[X_t] = Var[Z_0 + ... + Z_t] = t\sigma^2$, which is dependent on t. Therefore the random walk process with or without drift is non stationary. Intuitively, this is not a surprising result. It is well known that financial assets have a long-term trend and they are considered to be non-stationary. Figure 37 in the Appendix from Neusser (2016) showing the Swiss stock index also shows that prices of financial assets (stocks in this case) are clearly not stationary and have a long term trend.

4.1.3 Order of Integration

The concept of unit roots was defined in section 4.1.2, and it was shown that a process with a unit root is non stationary. Throughout this thesis non stationary data will often be considered. To classify for what type of non stationary data we are working with, the *order of integration* of time series is introduced. Engle and Granger (1987) define a time series to be integrated of order d, if first differencing a non stationary time series d times makes the time series weakly stationary. A time series integrated of order d is denoted by $I(d)$. Neusser (2016) gives an equivalent but definition of an integrated time series in mathematical notation, where a time series is $I(d)$ if $(1 - L)^d X_t$ is weakly stationary. If $X_t \sim I(1)$, then $\Delta X_t = X_t - X_{t-1} \sim I(0)$ according to Engle and Granger (1987). To prove this result, consider again the random walk time series with drift from (40). It was shown in section 4.1.2 that the random walk with drift has one unit root, which means that (4.1.2) is an $I(1)$ process. In order to make the time series stationary, consider $\Delta X_t = X_t - X_{t-1}$. This results in:

$$\begin{aligned}\Delta X_t &= X_t - X_{t-1} && (48)\\ &= \mu + \phi X_{t-1} + Z_t - X_{t-1} && (49)\\ &= \mu + (\phi - 1)X_{t-1} + Z_t = \mu + (1-1)X_{t-1} + Z_t && (50)\\ &= \mu + Z_t && (51)\end{aligned}$$

From (51) it follows that $\mathbb{E}[\Delta X_t] = \mathbb{E}[\mu + Z_t] = \mu$ and $Var[\Delta X_t] = Var[\mu + Z_t] = \sigma^2$. The random walk process with drift as in (40) has a unit root (i.e. $\phi = 1$) and is non stationary, but ΔX_t is weakly stationary. Therefore, X_t is an $I(1)$ process.

The motivation behind explicitly showing the dynamics of $I(1)$ processes is that economic variables are often $I(1)$. Prices of financial asset or GDP growth express a long-term trend and therefore are not stationary by themselves. Using the example of the Swiss stock index as in Figure 37 it was shown that financial assets have a long-term trend and therefore a unit root and possibly a drift term. Relating this to the topic of this thesis, where spot and futures price time series will be analyzed, Dolatabadi et al. (2015) state that it is generally accepted that a unit root in both spot and futures prices is present similar to the random walk in (40).

4.1.4 Spurious Regressions

In the next chapter the relationship between spot and futures prices will be analyzed. As Dolatabadi et al. (2015) pointed out, these are both $I(1)$ processes. Performing regression analysis on non stationary data may cause a *spurious regression*, which describes a strong relationship between two time series that does not exist. To illustrate the phenomenon of a spurious regression, the findings of Hendry (1980) are discussed. Hendry (1980) tested the fit between the UK M3 money supply and another time series, obtaining a R^2 of 0.999, indicating an almost perfect fit. This time series was later showed to be the cumulative rainfall in the UK, which should not be able to perfectly explain the money supply. The reason for this high fit is that both time series are non stationary and move up over time, incorrectly expressing a non-existent relationship, therefore being spurious. Granger and Newbold (1974) show the same phenomenon by generating two independent random walk processes, X_t and Y_t of length 50. Both random walks have unit roots, $X_t = X_{t-1} + Z_t$ and $Y_t = Y_{t-1} + \tilde{Z}_t$, where $Z_t \sim N(0, \sigma^2)$ and $\tilde{Z}_t \sim N(0, \sigma^2)$. Granger and Newbold (1974) specified the regression equation as $Y_t = \beta_0 + \beta_1 X_t + \epsilon_t$. Since the random walks are generated completely independent, there is no actual relationship between the two time series ($\beta_1 = 0$). Despite this, Granger and Newbold (1974) find that in three-quarters of their observations the null hypothesis $\beta_1 = 0$ is rejected, which means that β_1 is significantly different from zero despite the random walks being independent, and no causal relationship exists. Spurious regressions occur in $I(1)$ processes because of the existence of a long-term trend. Over the long run, two $I(1)$ processes may start drifting in the same direction. This drifting process may cause linear regressions to give non-existent relationships. To see how the OLS estimator may become significant, consider two random walks with drift, $X_t = \alpha_1 + X_{t-1} + \epsilon_{1,t}$, $Y_t = \alpha_2 + Y_{t-1} + \epsilon_{2,t}$. Recall that this can be written as $X_t = \alpha_1 t + X_0 + \sum_{t=1}^{T} \epsilon_{1,t}$ and $Y_t = \alpha_2 t + X_0 + \sum_{t=1}^{T} \epsilon_{2,t}$. For

the regression $Y_t = \beta_0 + \beta_1 X_t + u_t$, Whelan (2011) shows:

$$\hat{\beta} = \frac{\sum_{t=1}^{T} X_t Y_t}{\sum_{t=1}^{T} X_t^2} \tag{52}$$

$$= \frac{\sum_{t=1}^{T} (\alpha_1 + X_{t-1} + \epsilon_{1,t})(\alpha_2 + Y_{t-1} + \epsilon_{2,t})}{\sum_{t=1}^{T} (\alpha_1 + X_{t-1} + \epsilon_{1,t})^2} \tag{53}$$

$$= \frac{\sum_{t=1}^{T} (\alpha_1 t + X_0 + \sum_{t=1}^{T} \epsilon_{1,t})(\alpha_2 t + Y_0 \sum_{t=1}^{T} \epsilon_{2,t})}{\sum_{t=1}^{T} (\alpha_1 t + X_0 + \sum_{t=1}^{T} \epsilon_{1,t})^2} \tag{54}$$

$$\to \frac{\alpha_1 \alpha_2}{\alpha_1^2} = \frac{\alpha_2}{\alpha_1} \quad \text{if} \quad T \to \infty \tag{55}$$

Where in (54), in the numerator there is a term $\sum_{t=1}^{T} \alpha_1 \alpha_2 t^2 = \alpha_1 \alpha_2 \frac{2T^3+3T^2+T}{6}$ and in the denominator $\sum_{t=1}^{T} \alpha_1 t^2 = \alpha_1^2 \frac{2T^3+3T^2+T}{6}$. These are the only terms with a T^3 factor. For $T \to \infty$, these terms dominate all other terms according to Whelan (2011). As such, $\hat{\beta} \to \frac{\alpha_2}{\alpha_1}$. The OLS estimate $\hat{\beta}$ will therefore indicate a relationship between two independent time series as shown above based on the ratio of the drift terms. Phillips (1987) shows that for two random walks without drift the OLS estimator $\hat{\beta}$ converges to the ratio of two Wiener Processes $\frac{\int_0^1 W_r dW(r)}{\int_0^1 W(r)^2 dr}$. A spurious regression tends to have a high unjustified R^2. Granger and Newbold (1974) describe a spurious regression as a regression with a high degree of fit in terms of R^2, but a low value of the Durbin-Watson statistic. In fact, Phillips (1987) shows that the Durbin-Watson statistic converges to zero as $T \to \infty$ for a spurious regression . The Durbin-Watson (DW) test in the regression $Y_t = \beta_0 + \beta_1 X_t + \epsilon_t$, is checking whether $\rho \neq 0$ in $\epsilon_t = \rho \epsilon_{t-1} + u_t$. Stationarity in the error term therefore implies $\rho = 0$. Durbin and Watson (1951) propose the following test statistic $DW = \frac{\sum_{t=2}^{T} (\epsilon_t - \epsilon_{t-1})^2}{\sum_{t=1}^{T} \epsilon_t^2} \to 2(1-\rho)$. Granger and Newbold (1974) developed the rule of thumb, where a regression is said to be spurious if the $R^2 > DW$.

4.1.5 Unit Root Tests

As seen in section 4.1.4, the existence of unit roots in time series data may cause spurious regressions. A formal testing procedure for unit roots is therefore essential. Considering the $AR(1)$ model again given by $X_t = \mu + \phi X_t + Z_t$, it was shown that a unit root exists when $\phi = 1$, which causes an expectation and variance dependent on t as shown in (46) and (47). It was also shown that for a random walk $\Delta X_t \sim I(0)$, therefore $X_t \sim I(1)$. In order to formally test whether a time series has a unit root and is an $I(1)$ process, the *Dickey-Fuller Test*, proposed by Dickey and Fuller (1979) is often used. Dickey and Fuller (1979) use three versions of an $AR(1)$ model in their paper, and the test will work for all three versions. The different versions are an AR(1) process without drift and linear term ($X_t = \phi X_{t-1} + Z_t$), an AR (1) process with drift and no linear term ($X_t = \mu + \phi X_{t-1} + Z_t$), and an AR(1) process with drift and linear term ($X_t = \mu + \beta t + \phi X_{t-1} + Z_t$). We will stick to the $AR(1)$ process with drift which we have used so far in this chapter. The Dickey-Fuller Test takes the first difference to obtain the following regression equation:

$$\Delta X_t = \mu + (\phi - 1) X_{t-1} + Z_t \tag{56}$$

$$= \mu + \delta X_{t-1} + Z_t \tag{57}$$

Under the null hypothesis, (57) has a unit root present, ($\phi = 1 \Rightarrow \delta = 0$). Under the alternative hypothesis, no unit root is present ($\phi < 1 \Rightarrow \delta < 0$). To get the intuition behind the testing

procedure, consider Figure 9. Realizations of X_t are truly random, and a positive (negative) value of X_{t-1} does not lead to a higher probability of a negative (positive) value of X_t. Therefore we would not expect the lagged value X_{t-1} in (57) to have any relationship or predictive power on X_t. As a result, under the null hypothesis, $\delta = 0$. Under the alternative hypothesis, where it is assumed that X_t is stationary, consider Figure 10 for intuition. The time series seems to be mean-reverting. That is, a spike far away from the mean seems to be pulled back to the mean. It is therefore hypothesized under the alternative hypothesis that a positive (negative) value of X_{t-1} has a negative (positive) effect on X_t due to its mean-reverting nature. Therefore, X_{t-1} is a predictor of X_t and we have under the alternative hypothesis $\delta < 0$. The negative sign stems from its mean reverting nature.

The parameter δ in (57) estimated through OLS. Since $\delta = (\phi - 1)$, we have that $\hat{\delta} = (\hat{\phi} - 1) \iff \hat{\phi} = \hat{\delta} + 1$. The T-statistic of the OLS regression is given by $t_{\hat{\delta}} = \frac{\hat{\phi}-1}{\sigma_{\hat{\phi}}}$. The result in the denominator is the standard error of $\hat{\phi}$, which arises from $Var[\hat{\delta}] = Var[\hat{\phi} + 1] = Var[\hat{\phi}]$. First of all, notice that under the **alternative** hypothesis ($|\phi| < 1$) that $t_{\hat{\delta}}$ converges to a normal distribution, because of (46) and (47), which we have seen for $|\phi| < 1$ results in $E[X_t] = \frac{\mu}{1-\phi}$ and $Var[X_t] = \frac{\sigma^2}{(1-\phi^2)}$. Using these results, Central Limit Theorem and the Yule-Walker estimator, we find similar to Neusser (2016):

$$\sqrt{T}\left(\hat{\phi} - \phi\right) \xrightarrow[d]{} N(\mu, 1 - \phi^2) \tag{58}$$

Figure 11 shows the distribution of the OLS estimator $\hat{\phi}$ for different values of ϕ. We see that the higher the value of ϕ, the more left-skewed the distribution of the OLS estimator becomes. If ϕ approaches 1, $\hat{\phi}$ approaches a degenerate distribution. This degenerate distribution arises from (58), where the variance approaches zero as ϕ approaches 1. Under the null hypothesis, there is a downward bias of the OLS estimator, and no asymptotic normality.

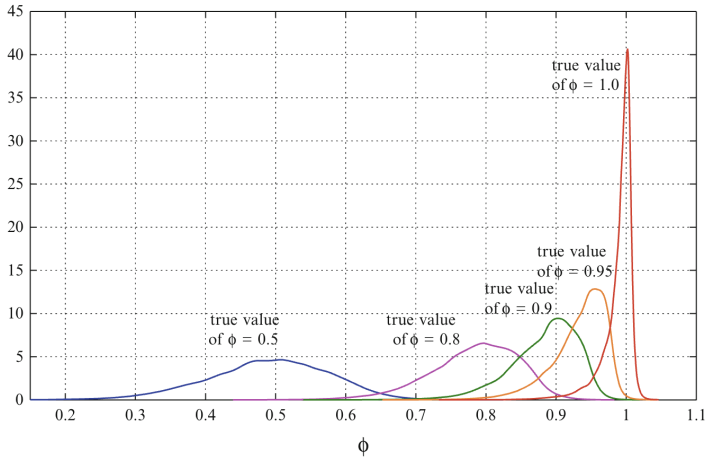

Figure 11: Distributions of the OLS estimator for different values of ϕ in the AR(1) model. Retrieved from Neusser (2016) (page 142)

Dickey and Fuller (1979) overcome this degenerate distribution by scaling with T, instead of $\sqrt{T}$ as in (58). We obtain the limiting distribution $T\left(\hat{\phi} - \phi\right) \to DF$, where DF is the *Dickey-Fuller Distribution*. Notice that by scaling by T instead of $\sqrt{T}$ implies a faster rate of convergence to the true parameter value ϕ. Neusser (2016) then shows using this procedure, we get a T-statistic value of $t_{\hat{\delta}} = \frac{\hat{\phi}-1}{\sqrt{\frac{S_T^2}{\sum_{i=1}^{T} X_{T-1}^2}}}$, where $S_T^2 = \frac{1}{T-2}\sum_{i=1}^{T}\left(X_t - \hat{\phi}X_{t-1}\right)^2$ follows the Dickey-Fuller distribution.

Figure 12 shows Monte Carlo simulations of the t-statistic under the null hypothesis (where the t statistic follows a Dickey-Fuller distribution):

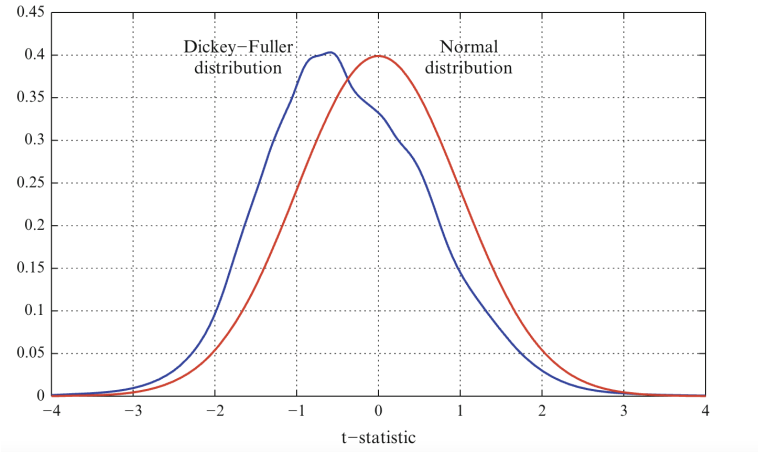

Figure 12: 10,000 Monte Carlo simulations of the Dickey-Fuller distribution and the normal distribution. Retrieved from Neusser (2016) (page 144)

Figure 12 shows that the Dickey-Fuller distribution has lower T-values compared to the normal distribution. If compared to the normal distribution, it thus has a left skewness similar to the empirical results seen in (11). It is therefore appropriate to use the Dickey-Fuller critical values in the Dickey-Fuller test instead of critical values of the normal distribution under the null hypothesis. The critical values of the Dickey Fuller distributions were determined using Monte Carlo simulations in Dickey and Fuller (1979). A table of critical values of the Dickey-Fuller distribution can be found in the appendix in Figure 38 retrieved from Fuller (1994). Notice that for each case of the model, for instance a drift, no drift, or a linear trend, the critical values are different. The correct specification of the model is therefore important and will be discussed in more detail in the next chapter.

In addition to the Dickey-Fuller test, we can also use the *Augmented Dickey-Fuller (ADF)* test to test for a unit root in time series. The ADF test is an extension of the Dickey-Fuller test, and uses higher order autoregressive terms in the regression equation. The null hypothesis of the ADF test is $\phi = 1$, and the alternative is $\phi < 1$, similar to the Dickey-Fuller test. Another similarity to the Dickey-Fuller test is that we have to specify the model specifications beforehand, choosing a model with drift term ($\mu \neq 0$), a linear trend ($\beta \neq 0$), or neither. In addition, we need to specify a value of p, which is the number of lags in the regression equation. If we suspect a high degree of serial correlation, we may need to use a large number of lags and vise versa if we suspect a low degree of serial correlation in our model. The regression equation in the Augmented Dickey-Fuller (ADF) test is given by:

$$\Delta X_t = \mu + \beta t + \phi X_{t-1} + \sum_{i=1}^{p} \rho_i \Delta X_{t-i} + Z_t \tag{59}$$

The regression equation of the ADF test is similar to that of the Dickey-Fuller test, with the addition of additional autoregressive terms. In the next chapter the ADF test will be performed on the data. In terms of selecting the optimal numbers p, two widely used criteon for model slection are the *Akaike Information Criterion (AIC)* and *Bayesian Information Criterion (BIC)*. The AIC is developed by Akaike (1973), and used to select the best model out of a variety of different models. The application in the case of this thesis is that a different number of lags p are possible. The AIC is used to choose the optimal number of lags p used in the ADF test. If the

number of lags in the ADF test is given by p, then the AIC is given by

$$AIC = 2p - 2ln(\hat{L_p}) \tag{60}$$

, where $\hat{L_p}$ is the Maximum Likelihood Function of the ADF model with p parameters, as defined in (59). The p that minimizes the AIC will be the best model according to Akaike (1973). There is a trade-off between the best log likelihood function and the number of parameters. In general, adding extra parameters p will improve the model fit, but is vulnerable to over fitting. Therefore the term $2p$ is a penalty term, penalizing extra lags added. The BIC is given by:

$$BIC = p\ln(N) - 2ln(\hat{L_p}) \tag{61}$$

The BIC is similar to the AIC in adding a penalty term. The difference between the two lies in the determination of the penalty term. $ln(N)$ is the natural logarithm of the number of observations in the sample. The penalty of the BIC will be stricter than for the AIC if $p\ln(N) > 2p \iff ln(N) > 2 \iff N > e^2 \iff N > 7.389$. Since N is an integer, for samples with 8 or more observations the BIC will be stricter. In this thesis, samples greater than 1000 observations will be tested, resulting in the BIC being stricter than the AIC.

Once the optimal number of lags is chosen using the AIC or BIC, the testing procedure is similar to that of the Dickey-Fuller test, and the same critical values as in (38) are used.

This section has introduced two statistical tests, the (Augmented) Dickey-Fuller tests. These tests are often used to test for unit roots in time series data, which is often a problem when performing time series analysis on economic data. Performing the (Augmented) Dickey-Fuller test will clarify whether our time series has a unit root present. The choice between the 'standard' and augmented Dickey-Fuller test depends on the a priori expectation of the data. If the processes analyzed are suspected to have serial correlation, it may be more convenient to choose the augmented version of the test with a large number of lags. If a more simple model is considered, the default Dickey-Fuller test may be more suitable.

4.2 Cointegration

4.2.1 Introduction to Cointegration

So far in this chapter, $I(1)$ processes and its problems in statistical analysis have been discussed. The presence of unit roots in $I(1)$ result in difficulty interpreting OLS estimates, as the regression may be spurious, indicating a non existent relationship. However, there is a special case under which it is possible to interpret the OLS estimates and test for a long-run relationship between two non stationary time series. If the time series are *cointegrated*, then this long-run relationship of two integrated time series can be determined, and statistical interference can be drawn. The concept of cointegration is relatively new in econometrics, introduced by Engle and Granger (1987).

Consider K time series. Let $X \in \mathbb{R}^{TxK}$, where all components of X are $I(d)$. According to Engle and Granger (1987), these K time series are cointegrated of order b if there exists at most $K-1$ linearly independent vectors $v \neq 0 \in \mathbb{R}^{Tx1}$, such that $\epsilon = v^T X \sim I(d-b)$. This means that if a linear combination between the K time series exists such that the residuals ϵ are $I(d-b)$, then the K time series are cointegrated of order b. In the application within this thesis, only $I(1)$ time series are considered. Therefore, K time series are cointegrated of order 1 if $\epsilon = Y - v^T X \sim I(0)$ with mean zero. The vectors v that satisfy this condition are called the *cointegrating vectors*. It is possible that a maximum of $K-1$ cointegrating vectors exist. Suppose that $r \leq K-1$ cointegrating vectors exist, then $v \in \mathbb{R}^{TxR}$. Engle and Granger (1987) call the rank of this matrix the *cointegrating rank*.

Similar research as in this thesis, such as Heany (2001) test for cointegration between several spot and future pairs, therefore allowing for the existence of multiple cointegrating vectors. Given the lack of research of cointegration between Bitcoin and Ethereum spot prices, the main area of research in this thesis will be whether the futures price of each asset is cointegrated with its own spot price. It will not be tested whether the Bitcoin futures price is cointegrated with Ethereum spot prices, and vice versa. This is perhaps an interesting area for future research, but the goal of this thesis is to establish the cointegrating relationship between the pairs themselves. As a result, we will consider two time series for both assets, the spot and futures time series. The maximum number of cointegrating vectors is therefore 1. For two time series X and Y, which are both $I(1)$, cointegration is achieved if, $Y - \alpha - \beta X \sim I(0)$, where α and β are now scalars. Equivalent notation used, for instance by Mackinnon (2010) is to use vector notation:

$$U = \begin{bmatrix} Y & 1 & X \end{bmatrix} \begin{bmatrix} 1 \\ -\alpha \\ -\beta \end{bmatrix} = Y - \alpha - \beta X \sim I(0) \text{ with mean zero.}$$

Maslyuk and Smyth (2009) describe two time series to be cointegrated if the time series express a long-run relationship. To get an intuition as to what this means, Figure 13 show two cointegrated time series. Despite the two time series moving together in the long run, short-term deviations may occur. The bottom green line shows the difference between the two time series, where deviations from zero are frequently observed. The condition that needs to be satisfied is that the residuals, i.e. the green line is $I(0)$. In Figure 13 this does seem to be the case, with a mean around zero and deviations from the mean being reverted back to the mean over time. This implies stationarity of the residuals and therefore cointegrated time series.

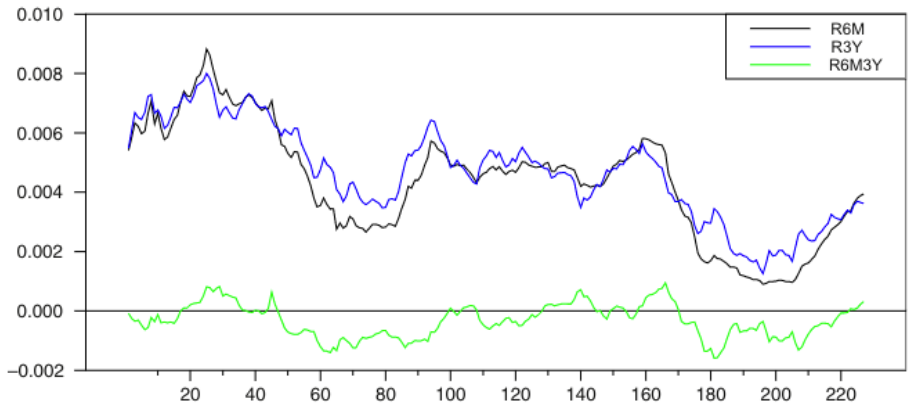

Figure 13: Two cointegrated time series. Graph retrieved from Johansen (2015).

To illustrate how cointegration filters out possible spurious regression, consider Figure 14, which shows two random walks which both move up. If a linear regression were to be performed, a positive coefficient between the two random walks is likely to occur, as over the entire period the two random walks move up. This would indicate any relationship between the two random walks. The green line in figure 14 highlights the difference between the two random walks. This difference between the random walks seems non stationary. For the first 200 observations this difference is negative and becomes positive afterwards. It is therefore unlikely that we can find a single value β for which the residuals of the regression $Y = \alpha + \beta X + \epsilon$ are stationary. A linear regression may indicate a relationship between the two random walks, whilst for cointegration this would not be the case. Therefore cointegration may filter out two time series that may not have any long-run relationship.

Cointegration fits well in the application of this thesis. The goal in the next chapter is to fit the cost-of-carry models to the observed market prices. Suppose that f is the time series of futures

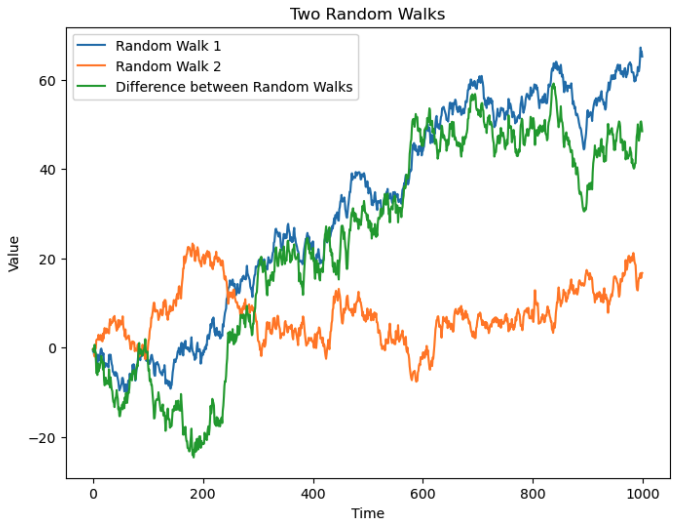

Figure 14: Two independent random walks with normal increments created in Python with T=1000.

prices, s the spot price time series, and r the time series of the risk-free rate. Suppose that $f - s = r$ is the equilibrium in the cost-of-carry model. Under the no-arbitrage condition in which the cost-of-carry models operate, any deviation from the long-run equilibrium between $f - s$ and r would imply an arbitrage opportunity, as shown in Table 10. In an efficient market, the existence of an arbitrage opportunity ($f - s > r$ or $f - s < r$) would cause arbitrageurs to take the possible arbitrage opportunities which would then restore equilibrium. Randomness in the market will cause $f - s \neq r$ to deviate in the short-term, but the importance lies in this arbitraging force that would restore equilibrium. Cointegration therefore seems a natural way of testing whether the cost-of-carry models hold in the market. There are two $I(1)$ time series of prices, and it is to be established whether a linear combination of the two results in an equilibrium around zero. The residuals $I(0)$ and mean-reverting with a mean of zero due to arbitrage opportunities.

4.2.2 Properties OLS under Cointegration

Under cointegration, there is consistency of the OLS estimates, and are thus interpretable. Consider the two $I(1)$ random walks with drift again, as in (53). Let $X = \sum_{i=1}^{T} X_t$, $Y = \sum_{i=1}^{T} Y_t$ and $U = \sum_{i=1}^{T} u_t$. Whelan (2011) shows that under under cointegration of X and Y, i.e. $U = Y - \beta X \sim I(0)$ with mean zero. Consistency of the OLS estimator $\hat{\beta}$ then follows from:

$$\hat{\beta} = \frac{\sum_{t=1}^{T} X_t Y_t}{\sum_{t=1}^{T} X_t^2} = \beta + \frac{\sum_{t=1}^{T} X_t u_t}{\sum_{t=1}^{T} X_t^2} \tag{62}$$

$$= \beta + \frac{\sum_{t=1}^{T} (\alpha_1 + X_{t-1} + \epsilon_{1,t}) u_t}{\sum_{t=1}^{T} (\alpha_1 + X_{t-1} + \epsilon_{1,t})^2} = \beta + \frac{\sum_{t=1}^{T} (\alpha_1 t + X_0 + \sum_{t=1}^{T} \epsilon_{1,t}) u_t}{\sum_{t=1}^{T} (\alpha_1 t + X_0 + \sum_{t=1}^{T} \epsilon_{1,t})^2} \tag{63}$$

$$= \beta + \frac{\sum_{t=1}^{T} u_t}{\sum_{t=1}^{T} (\alpha_1 t + X_0 + \sum_{t=1}^{T} \epsilon_{1,t})} = \beta + \frac{\sum_{t=1}^{T} u_t}{\sum_{t=1}^{T} (\alpha_1^2 t + ...)} \to \beta \tag{64}$$

$$\tag{65}$$

The convergence $\hat{\beta} \to \beta$ occurs due to $u_t \sim I(0)$ under cointegration, which does not increase with t. The denominator has a term which includes a t and will therefore grow faster, implying $\hat{\beta} \to \beta$.

It is thus shown by using derivations from Whelan (2011) that the OLS estimator is consistent when X and Y are cointegrated. Another fact is that the OLS estimator is in fact more than consistent, since the rate of convergence is faster than the traditional $\sqrt{(T)}$ of the OLS estimator. Whelan (2011) shows:

$$T(\hat{\beta}-\beta) = \frac{T\sum_{t=1}^{T}(\alpha_1 t + X_0 + \sum_{t=1}^{T}\epsilon_{1,t})u_t}{\sum_{t=1}^{T}(\alpha_1 t + X_0 + \sum_{t=1}^{T}\epsilon_{1,t})^2} \tag{66}$$

$$= \frac{\frac{1}{T^3}T\sum_{t=1}^{T}(\alpha_1 t + X_0 + \sum_{t=1}^{T}\epsilon_{1,t})u_t}{\frac{1}{T^3}\sum_{t=1}^{T}(\alpha_1 t + X_0 + \sum_{t=1}^{T}\epsilon_{1,t})^2} = \frac{\frac{1}{T^2}\sum_{t=1}^{T}(\alpha_1 t + X_0 + \sum_{t=1}^{T}\epsilon_{1,t})u_t}{\frac{1}{T^3}\sum_{t=1}^{T}(\alpha_1 t + X_0 + \sum_{t=1}^{T}\epsilon_{1,t})^2} \tag{67}$$

$$= \frac{\frac{1}{T^2}\left(\alpha_1\frac{T(T+1)}{2} + ...\right)u_t}{\frac{1}{T^3}\left(\alpha_1\frac{2T^3+3T^2+T}{6} + ...\right)} = \frac{\frac{\alpha_1}{2}u_t + ...}{\frac{\alpha_1^2}{3} + ...} \to 0 \tag{68}$$

Despite the numerator in (68) being divided by T^2 instead of T^3, the multiplication by u_t which is zero mean results in the numerator converting to 0 as $T \to \infty$. Thus under cointegration, we have $T(\hat{\beta}-\beta) \underset{p}{\to} 0$. We have convergence at rate T instead of $\sqrt{T}$ and this is super-consistency of the OLS estimator. Under cointegration, the OLS estimates thus can be interpreted and converge faster to the true parameter values.

Testing for cointegration can be done using the *Engle-Granger* test, proposed in Engle and Granger (1987). It is a two-step procedure, where two $I(1)$ time series can be tested for cointegration. Before the testing procedure the order of integration of the time series has to be verified. The Engle-Granger test works soley for $I(1)$ processes, therefore the time series tested for cointegration need to be tested for a unit root beforehand, using the Augmented-Dickey Fuller test, for instance. The first step of the Engle-Granger test is setting up the regression equation:

$$Y = \alpha + \beta X + \epsilon \tag{69}$$

Notice that an intercept is included here, but the cointegrating parameter remains β. One of the properties of cointegration is $Y - \beta X \sim I(0) \Rightarrow \alpha + (Y - \beta X) \sim I(0)$. This arises due to adding a constant to a stationary process does not change the stationarity. Including an intercept in the regression is standard practice in the Engle-Granger test, and it will be explained in the next chapter that in the case of this thesis it is expected that α is close to zero. It was established earlier in this section that under cointegration, $\hat{\beta}$ estimated from (69) is is super-consistent and it can therefore be estimated through OLS. In order to establish this, it needs to be verified whether $\hat{\epsilon} = Y - \hat{\alpha} - \hat{\beta}X \sim I(0)$ with mean zero. If this holds, Y and X are cointegrated with cointegration parameter β. A unit root test, the Augmented Dickey-Fuller test with the regression equation (59) will be performed on the residuals to test for stationarity. If the null hypothesis of the second step is rejected, there is stationarity in the residuals. Therefore the null hypothesis of the Engle-Granger test is no cointegration, and the alternative hypothesis is cointegration.

Engle and Granger (1987) state that cointegration implies the existence of an Error Correction Model (ECM). A simple error correcting model of

$$\Delta Y_t = \alpha_1 + \sum_{i=1}^{p}\phi_i \Delta X_{t-i} + \theta(Y_{t-1} - \beta X_{t-1}) + \epsilon_t \tag{70}$$

The interesting aspect of the ECM as defined in (70) is that all variables are now $I(0)$. It was assumed $Y_t \sim I(1)$, therefore $\Delta Y_t \sim I(0)$, and if Y_t and X_t are cointegrated, then $(Y_{t-1} - \beta X_{t-1}) \sim I(0)$. All time series being stationary implies OLS to give correct statistical interference. The first parameters ϕ_i incorporate the short-term dynamics of ΔY_t and ΔX_t, and θ captures the long-run

relationship using the cointegration between Y_t and X_t. Notice that the coefficient θ should be negative, since $Y_t > \beta X_t$ implies a value of Y_t above its long-run equilibrium. As a result, it is more likely that $\Delta Y_t < 0$ and vice versa for $Y_t < \beta X_t$.

5 Cointegration Analysis of Cost-of-Carry Models

This section will perform the cointegration tests on the cost-of-carry models specified in section 2.2.5. In addition, a new model will be proposed and tested.

5.1 Risk-free Rate Proxy

Since all of the models given in section 2.2.5 contain the risk free rate $r_{t,T}$, a good proxy for $r_{t,T}$ has to be chosen. The risk-free rate is considered to be, as the name suggests, the return on a risk-free investment. In practice, an investment is never fully risk-free, but we can choose an asset that is perceived to be the most safe among all assets. Typically, government bonds are considered to be the safest investments possible, but even these investments have *default-risk*, which is the risk that the government will not be able to pay back its debt when the bond matures. Government bonds of third-world countries with a less-developed economy will have higher default risk than those of a developed economy. It is common practice to use US government bonds (often referred to as US *treasuries*) as a proxy of the risk-free rate, since the creditworthiness of the US is considered high and US treasuries are the most liquid government bonds in the world. This is also why almost every country in the world holds some US government bonds (US treasuries) on its balance sheet. These arguments lead to US treasuries being a natural choice for the risk-free rate to test the spot-future parities against. Last, US treasuries are a natural choice because almost all liquid cryptocurrency markets are settled in dollars.

Damodaran (2008) states that in addition to the asset chosen for the risk-free rate, duration is also important. US treasuries are all zero-coupon bonds, of which the duration is simply the maturity of the bond. In this thesis quarterly futures with a maturity of 3 or 6 months are considered. To match the duration, the corresponding risk-free rate proxy of 3 or 6 months *US Treasury Bills*[22] will be used. Specifically, we look at the *3 or 6-Month Treasury Bill Secondary Market Rate, Discount Basis (DTB3)* provided by the St. Louis FED [23]. The term *Discount Basis* arises due to the property of US treasuries being zero-coupon, so the risk-free rate is the *yield* of the 3-month US treasury, which is the discount[24] of the bond relative to face value and maturity of the bond. The *Yield to Maturity (YTM)* of a bond is: $\frac{\text{FV}}{P(t,T)}^{\frac{1}{T-t}} - 1$, where FV is the face-value of a bond (dollar amount the bond gets paid back at time T), $P(t,T)$ is the current bond price at time t with maturity at time T, and $T-t$ is the duration in years the bond has left. Note that the only term that is non-constant is $P(t,T)$, which is the market price of the bond. Thus the current discount (premium) of the bond determines the yield of the bond. Suppose a bond with 3 years to maturity and a face value of \$1000 trades at \$800. The yield to maturity is: $(\frac{1000}{800})^{\frac{1}{3}} - 1 = 0.077$ (7.7%). If the bond were to have 2 years maturity instead of 3 and trades at the same price, we would have a yield of: $(\frac{1000}{800})^{\frac{1}{2}} - 1 = 0.118(11.8\%)$.

Given the examples above, it makes sense to match the duration of the risk-free rate proxy to the duration of the contract we want to investigate, as Damodaran (2008) states. Suppose we want to model the cost-of-carry of a Bitcoin futures contract with 6 months to maturity, and a 6-month and 30-year treasury have an annual yield of 2% and 4%, respectively. Using the 30-year bond will give a higher risk-free rate, but matures more than 29 years after our Bitcoin contract expires. Using the 4% as a risk-free rate is thus not accurate as the duration of the 30-year treasury is much longer.

A problem that we run into quickly is the fact that US treasuries do not trade during the weekend, whilst the market for cryptocurrencies trades 24/7. Therefore a proxy during the weekend for the risk-free rate has to be chosen. Similar research on the topic of this research such as Lian et al.

[22] A treasury bill is US government debt with a maturity shorter than 1 year.

[23] https://fred.stlouisfed.org/series/TB3MS

[24] In extreme cases of negative interest rates, we can have the situation where bond prices are higher than their face value, but in general zero-coupon bonds trade at a discount to face value.

(2019), Kapar and Olmo (2019) and Hu et al. (2020) do not run into this problem as only CME and CBOE futures are discussed, which only trade during the weekdays. Since the futures traded on Binance do trade over the weekend, we will include weekend prices in this thesis. During the weekend, market participants also do not have information on the risk-free rate at that given time since the bond market is closed. We will therefore use the risk-free rate at the close of Friday for modeling the cost of carry for Saturday and Sunday.

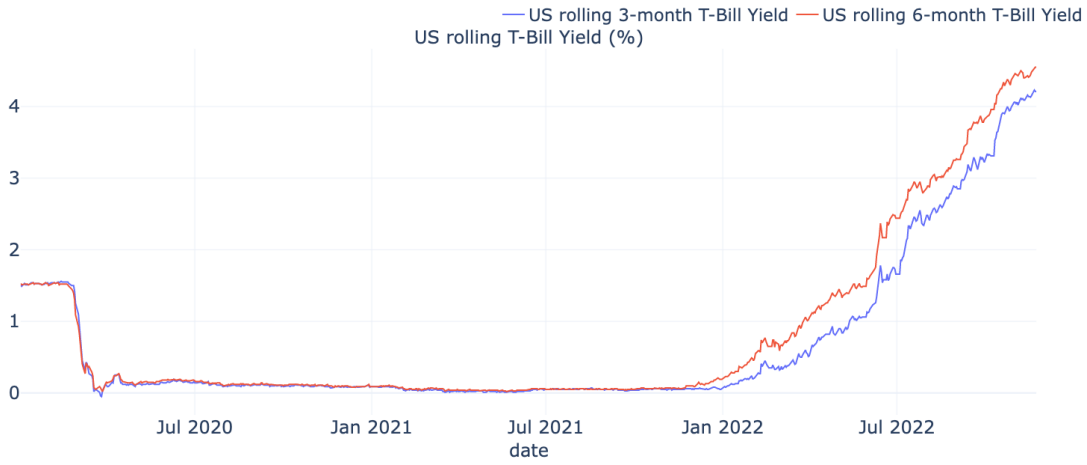

Figure 15: US 3 and 6 month treasury bill yield plotted.

Figure 15 shows that for the majority of the testing period, the risk-free rate was very close to zero. Only from 2022 onwards the yield of US treasuries started to go up rapidly. This long period of near zero rates results in the cost of carry purely from an interest rate alone being very low. Especially since the maturities of futures considered here are a maximum of 6 months, the yield on US treasuries throughout 2020 and 2021 for short maturities is very low. Early 2022, interest rates surged as rising inflation caused central banks to increase rates.

5.2 Cointegration Test of Futures and Spot Prices

In the following sections the cost-of-carry models will be tested on market data. The goal is to test whether the cost-of-carry models can explain the observed basis in (bi-) quarterly futures given the spot prices and carry variables. Under the no-arbitrage assumption in which the cost-of-carry models operate, there should be a long-run relationship between the futures prices and the spot price adjusted by carry variables. Any deviation from equilibrium would be reverted back by arbitrageurs. In section 4.1 it was established that this long-run relationship can be tested for by cointegration analysis. From here on, methodology of Wu et al. (2021) will be followed, and a log transformation applied. Let $log(F(t,T)) = f_{t,T}$ and $log(S_t) = s_t$. In addition, vector notation will be used to transform from a time t setting to considering the entire time series. f is the vector of all log futures prices from time 0 to time T, and s the vector of log spot prices.

5.2.1 Data Generating Process $f_{t,T}$ and s_t

In section 4.1, it was discussed that the Augmented Dickey-Fuller test has multiple possibilities for the regression equation. This includes the following three possibilities for the data generating processes (DGP) of X_t:

$$X_t = \mu + \gamma t + \phi X_{t-1} + Z_t \tag{71}$$
$$X_t = \mu + \phi X_{t-1} + Z_t \tag{72}$$
$$X_t = \phi X_{t-1} + Z_t \tag{73}$$

The correct model which best represents the actual underlying data generating process (DGP) has to be chosen to give correct results of the ADF test. This is since the critical values for (71,72 and 73) are all different. Figure 39 shows the Bitcoin hourly prices for the entire testing period. In order to establish a valid regression equation and remove the carry variables from the exponent, log prices will be considered. Figure 16 shows the Bitcoin log prices over the entire interval.

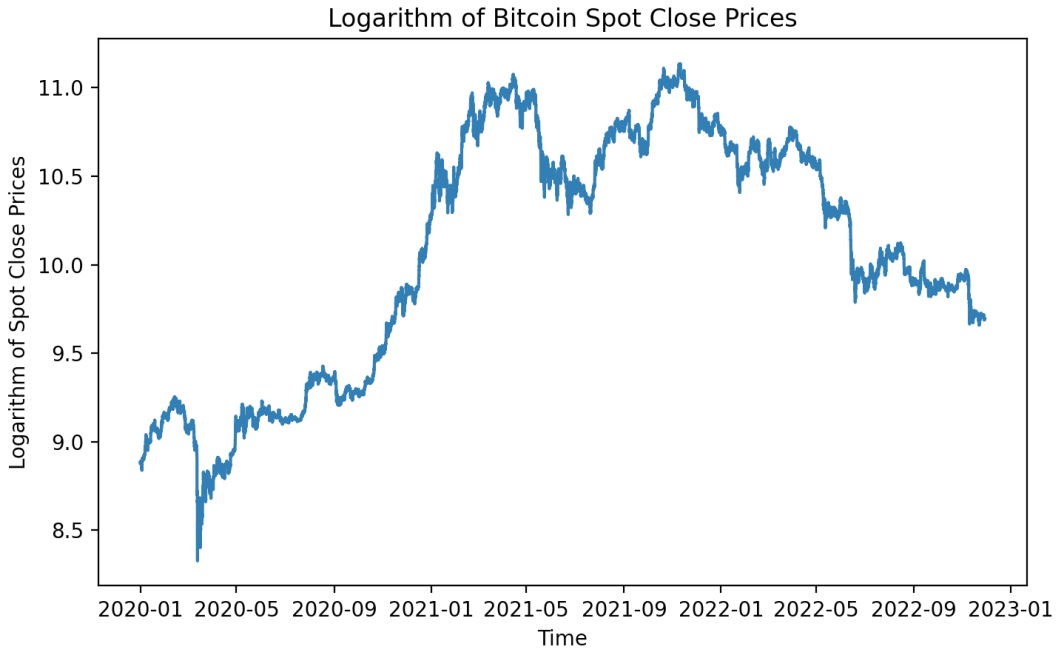

Figure 16: Bitcoin hourly log closing prices over our entire testing period

Over the entire sample period, the Bitcoin log prices have increased, on average. Purely modeling the DGP of Bitcoin log prices as a random walk, i.e. using (73), would imply $\mathbb{E}[X_t] = X_0$. Historical data does not back the claim $\mathbb{E}[X_t] = X_0$, as the price of Bitcoin has risen in a decade from a few dollars to tens of thousands, indicating a growth rate. It therefore makes sense to include a drift term or trend in the DGP of Bitcoin log prices. The choice of DGP now comes down to distinguishing between a drift term μ or the existence of a linear trend γt. Visually from Figure 16, a purely linear (deterministic) trend does not seem to be present. There is volatility both on the upside and downside. Therefore the trend in Bitcoin (log) prices seems stochastic. In addition to visual inspection, Stadnytska (2010) describe an approach originally proposed by Elder and Kennedy (2001). This procedure is starting off under the DGP (72), the simpler one without a linear trend. A unit root test on is then performed on this DGP. If the null hypothesis of a unit root is rejected,($\phi \neq 1$), then it is very likely that the true DGP is given by (71) , and X_t is *trend stationary*. Stadnytska (2010) state that a unit root and a deterministic trend together is very unrealistic, and therefore this approach is viable. Either the growth rate is due to a unit root, or a deterministic trend. We therefore start off with (72) as the DGP for Bitcoin prices. The DGP (72) in the unit root test is also used for Bitcoin prices by Corelli (2018) and Wu et al. (2021).

Ethereum (log) prices can be found in Figures 40 and 41 in the Appendix. The behavior of the (log) prices is very similar to that of Bitcoin, except a total higher return over the testing period. We will therefore also use the $AR(1)$ model with drift (72) to test for a unit root.

5.2.2 Checking For $I(1)$ Processes

In order for cointegration between f and s to hold, it needs to be verified that both series are $I(1)$. Dolatabadi et al. (2015) state that it is widely accepted that both spot and futures time series are $I(1)$ processes. Therefore, it will be tested in this subsection whether f and s are $I(1)$, such that cointegration can exist. If time series are $I(1)$, there is a unit root present. The Augmented Dickey-Fuller (ADF) test specified in (59) will be performed on f and s. The test will be performed under the opimal number of lags established by the AIC and BIC. The maximum number of lags out of which the AIC and BIC can choose is the criterion developed by Schwert and Simon (1989), which is often used and given by $p_{max} = 12(\frac{N}{100})^{\frac{1}{4}}$.

It will first be tested whether s for both Bitcoin and Ethereum is $I(1)$. Recall that the null hypothesis of the ADF test is a unit root present, where the alternative hypothesis is no unit root present. Note that the ADF test with underlying DGP $X_t = \mu + \phi X_{t-1} + Z_t$ will be used, such that $\Delta X_t = \mu + (\phi - 1)X_{t-1} + Z_t$, as established in section 5.2.1. Table 20 shows large p-values, both using the AIC and BIC criterion. These p-values are well above any rejection region. The null hypothesis of a unit root is therefore not rejected. It follows that s has a unit root present for both Bitcoin and Ethereum, and $s \sim I(1) \Rightarrow \Delta s \sim I(0)$. Figure 42 in the Appendix shows that first differencing Bitcoin log prices results in a stationary time series. For Ethereum the plot looks similar and can be found in the Appendix in (43).

Bitcoin log spot price s_t								
Start Date	End Date	N	γ_{AIC}	$\hat{t}_{AIC}$	p_{AIC}	γ_{BIC}	$\hat{t}_{BIC}$	p_{BIC}
2020-01-01	2022-09-30	24061	35	-1.677	0.443	1	-1.662	0.451
Ethereum log spot price s_t								
Start Date	End Date	N	γ_{AIC}	$\hat{t}_{AIC}$	p_{AIC}	γ_{BIC}	$\hat{t}_{BIC}$	p_{BIC}
2020-01-01	2022-09-30	24015	45	-1.971	0.299	0	-1.959	0.305

Table 20: Augmented Dickey-Fuller test for BTC and ETH log transformed spot prices for the entire sample period. The test is used to assess whether a unit root is present in the log spot price vector s. The null hypothesis (H0) is a unit root present, where the alternative (H1), is that no unit root is present.

Now for the futures log prices f, it will also be tested to see if the time series are $I(1)$. This will be done this for every interval, for both Coin-M and USD-M quarterly futures. The results of the ADF test can be found in Table 29 in the Appendix. Only 4 out of 32 intervals tested have a test statistic that is is significant at the 10 or 5% level. None of the intervals tested have a significant test statistic at the 1% level. Based on the data in Table 29 we can thus not reject the null hypothesis of a unit root being present in log futures prices. It is therefore concluded that $f \sim I(1)$.

The results in Tables 20 and 29 have shown that both s and f are $I(1)$ and therefore integrated of the same order. It is now possible to test for cointegration.

5.2.3 Cointegration Test of Futures and Spot Prices

This section will test for cointegration between log spot and futures prices, f, and s, where f denotes the vector of log futures prices $f_{0,T}, ..., f_{T,T}$, and s the vector of log spot prices $s_0, ..., s_T$. The goal is to test whether a long-run equilibrium between spot and futures exist. It is widely accepted in the literature that spot and futures prices are cointegrated. Hu et al. (2020) state that there is in general a strong expectation that futures and spot prices have a strong cointegrated relationship. Despite this, it has been noted in Figures 18 and 19 that a significant basis can exist between spot and futures prices in the cryptocurrency market. In order to establish if a long-run relationship between spot and futures prices exists, without the addition of cost-of-carry, the Engle-Granger test will be performed on f and s in this section. Recall that the Engle-Granger test consists of two steps. The first step involves an OLS regression on the regression equation $f = \alpha + \beta s + \epsilon$. In the second step we test if $\hat{\epsilon} = f - \hat{\alpha} - \hat{\beta}s \sim I(0)$. This is done using the Augmented Dickey-Fuller (ADF) test on the residuals to test for stationarity.

Enle-Granger Test Bitcoin Coin-M futures											
$\hat{\alpha}$	$\hat{\beta}$	$\sigma_{\hat{\beta}}$	t_β	p_β	R^2	γ_{AIC}	$\hat{t}_{AIC}$	p_{AIC}	γ_{BIC}	$\hat{t}_{BIC}$	p_{BIC}
2020-06-30 - 2020-09-25 ($N = 2008$)											
-0.304	1.034	0.002	522.398	0.000***	0.993	12	-0.591	0.458	1	-1.225	0.203
2020-08-05 - 2020-12-25 ($N = 3949$)											
0.230	0.978	0.001	1376.404	0.000***	0.998	14	-2.100	0.034**	1	-2.323	0.019**
2020-09-25 - 2021-03-26 ($N = 4062$)											
0.103	0.993	0.000	2803.696	0.000***	0.999	18	-1.617	0.062*	1	-2.792	0.005***
2020-12-25 - 2021-06-25 ($N = 4178$)											
-0.354	1.038	0.002	529.571	0.000***	0.985	21	-1.333	0.169	2	-1.887	0.056**
2021-03-26 - 2021-09-24 ($N = 4176$)											
-1.715	1.164	0.002	494.196	0.000***	0.983	9	-0.931	0.316	4	-1.304	0.178
2021-06-25 - 2021-12-31 ($N = 4340$)											
0.077	0.995	0.002	1201.650	0.000***	0.997	8	-1.396	0.151	3	-1.638	0.096
2021-09-24 - 2022-03-25 ($N = 4183$)											
-1.127	1.1069	0.001	1290.925	0.000***	0.997	2	-2.818	0.005***	2	-2.818	0.005***
2021-12-31 - 2022-06-24 ($N = 4024$)											
-0.322	1.032	0.001	1445.955	0.000***	0.998	29	-2.400	0.016**	7	-2.326	0.019**
2022-03-25 - 2022-09-30 ($N = 4395$)											
-0.258	1.026	0.000	6459.561	0.000***	1.000	15	-3.186	0.001***	7	-3.265	0.001***

Table 21: Results of performing the Engle-Granger test on each interval of BTC log Coin-M futures prices and BTC log prices. The left hand side of the table $\hat{\beta}$,$\sigma_{\hat{\beta}}$, t_β and R^2 are parameters corresponding to the OLS regression $f = \alpha + \beta_1 s + \epsilon$, and the parameters γ_{AIC}, $\hat{t}_{AIC}$, p_{AIC}, γ_{BIC}, $\hat{t}_{BIC}$ and p_{BIC} are parameters corresponding to the Augmented Dickey Fuller (ADF) test. Notice that *, ** and *** imply significant t-statistics at the 10,5, and 1% level, respectively.

Table 21 shows the results of the Engle-Granger test for Bitcoin Coin-M futures and spot log prices. In order for the cointegrating parameter to be interpretable, there must be stationarity of the residuals in the second stage. For the majority of the intervals tested, the null hypothesis

of a unit root in the residuals is not rejected, both for the AIC and BIC. It can therefore not be concluded that f and s are cointegrated. This implies there is no equilibrium between f and s itself for Bitcoin Coin-M futures. To illustrate how this might arise, consider Figure 44 in the Appendix. It shows how the difference between the (log) prices may not always move in the same direction, as there is more (less) demand for the futures contract than on the spot Bitcoin, therefore causing the prices to diverge.

Table 30 in the Appendix shows the results for the Engle-Granger between on Coin-M Ethereum futures log prices and log spot price. The results are similar to those of Bitcoin Coin-M futures, although we accept the reject hypothesis of no cointegration for one more interval for Ethereum Coin-M futures. It seems as if Ethereum spot and futures prices are slightly more cointegrated, but we are can not say this with certainty as the null hypothesis is not rejected for every interval. A plot of the first interval of which the null hypothesis is not rejected can be found in Figure 45 in the Appendix.

USD-M futures have a shorter maturity and lower basis than Coin-M futures. Tables 31 and 32 in the Appendix show the results of the Engle-Granger test on Bitcoin and Ethereum USD-M futures. The results are in line with those of Coin-M futures, where the null hypothesis of f and s not being cointegrated is not rejected in every interval. Therefore, it is can not be concluded with certainty that Bitcoin USD-M log futures prices and log spot prices are cointegrated.

In this subsection, it has been tested whether the (log) futures and spot time series are cointegrated. If cointegration would hold, then there would be a long-run relationship between f and s. The results of the Engle-Granger test do not imply cointegration for every interval tested. In order to explain the observed deviation between futures and spot prices as seen in (6,36, 7, and 8) there is additional work to do. The next section will introduce cost-of-carry variables to find an equilibrium between futures and spot prices.

5.3 Testing Cost-of-Carry Models

This section will attempt to find a stronger cointegrating relationship than between the prices alone by applying the cost of carry models explained and derived in section 2.2.5. In doing so, a predicted fair futures price at any time given the spot price and cost-of-carry variables is determined. This predicted fair price is then tested for cointegration against the observed market prices.

5.3.1 Cost-of-Carry Model Investment Assets

In section 2.2, the most simple cost-of-carry model, that for investment assets has been defined as $F(t,T) = S_t e^{r_{t,T}(T-t)}$. The intuition behind this model, is that the futures contract does not have a payment due until time T, whilst buying the spot asset has a payment due at time t; a deferred payment. Therefore, carrying the spot asset from time t to time T has an opportunity cost, which is the risk-free rate. In Table 10, the arbitrage opportunities for a violation of this model have been outlined. A deviation from the theoretical price gives rise to an arbitrage opportunity. To empirically test this model, the methodology as used by Wu et al. (2021) is applied, which is a log transformation to get a more desirable form:

$$F(t,T) = S_t e^{r(T-t)} \tag{74}$$
$$\iff log(F(t,T) = log(S_t) + r_t(T-t) \tag{75}$$
$$\iff log(F(t,T) - log(S_t) = r_t(T-t) \tag{76}$$
$$\tag{77}$$

We now move from a time t perspective to a whole time series. Let $\tilde{r}$ denote the vector:

$$\begin{bmatrix} r_0 T \\ r_1(T-1) \\ \vdots \\ r_{T-1} \end{bmatrix}$$

, where each component is the risk free rate at that particular entry multiplied by the time to maturity in years. We then obtain the regression equation:

$$f - s = \alpha + \beta\tilde{r} + \epsilon \tag{78}$$

The intuition behind (78) is that that the futures basis (left-hand side) can be explained by the cost-of-carry term $\tilde{r}$. In the previous section it was concluded that f and s alone are not cointegrated. The cost-of-carry model explains that an interest rate carry has to be included, to overcome opportunity costs (cost of capital) for arbitrageurs. The Engle-Granger test will now be performed on (78). A cointegrating relationship between the futures basis and the cost-of-carry under the simple model is found, if the the residuals of (78) ,$\hat{\epsilon} = f - s - \hat{\alpha} - \hat{\beta}\tilde{r} \sim I(0)$. In addition, the restriction is imposed that the cost-of-carry model for investment assets holds if $\hat{\alpha} = 0$ and $\hat{\beta} = 1$. To prove this, let $r_t, f_{t,T}$ and s_t denote the t-th element of the vectors $\tilde{r}$,f and s, respectively. Then at some time $t < T$ under the cost of carry model for investment assets, we have: $f_{t,T} - s_t = log(F(t,T)) - log(S_t) = log(\frac{F(t,T)}{S_t}) = \tilde{r_t} \iff e^{\left(log(\frac{F(t,T)}{S_t})\right)} = e^{r_t} \iff F(t,T) = S_t e^{r_{t,T}(T-t)}$. For any deviation from this theoretical futures price $S_t e^{r_{t,T}(T-t)}$, Table 10 shows the arbitrage opportunities that would arise. Suppose a deviation from the cost of carry model occurs, where (78) no longer holds. Arbitrageurs could in turn make a riskless profit and restore equilibrium. As a result, the errors themselves are mean-reverting and correcting. This is why testing for stationarity of the residuals in (78) is an elegant application for testing the cost-of-carry models. Stationarity in the residuals implies a mean-reverting time series, and this is what we also expect to happen in the market due to arbitrageurs as described above.

Before performing the Engle-Granger test, it has to be ensured that both $f - s$ and $\tilde{r} \sim I(1)$. Table 33 in the Appendix shows the results of the ADF test on each interval for $f - s$, under Coin-M and USD-M futures. The null hypothesis of a unit root is rejected both using the AIC and BIC for the interval: *2021-12-31 - 2022-06-24* for Bitcoin Coin-M futures. For Ethereum Coin-M futures these are the intervals: *2020-09-25 - 2021-03-26* and *2021-12-31- 2022-06-25*. For Ethereum USD-M futures this is the interval: *2021-12-24 - 2022-03-25*. In these intervals, cointegration tests do not give interpretable results due to $f - s$ not being $I(1)$. Table 34 in the Appendix shows that $\tilde{r} \sim I(1)$ for every testing period.

Table 22 shows the results of the Engle-Granger test between $f - s$ and $\tilde{r}$ for Bitcoin Coin-M futures. First of all, note that the interval *2021-12-31 - 2022-06-24* is not discussed as $f - s$ is $I(1)$ on this interval. Compared to Table 21, the p-values of the ADF test of the residuals for the simple cost-of-carry model all decreased in Table 22, implying stronger stationarity of the residuals. Instead of 3 intervals not being cointegrated, it is reduced to 2 by adding $\tilde{r}$. For the intervals where stationarity of the residuals is ensured, the OLS estimates of the first-stage regression in the left-hand side of the table can be interpreted, and $\hat{\alpha}$ and $\hat{\beta}$ are super-consistent. The intercept $\hat{\alpha}$ is close to zero, as expected. However, the estimate of the cointegration parameter $\hat{\beta}$ is extremely high. On three separate intervals a value of $\hat{\beta} > 100$ is observed, while the hypothesis of the cost-of-carry model was $\beta = 1$. The implications of this will be discussed at the end of this section.

Engle Granger test Bitcoin Coin-M futures using cost-of-carry for investment assets											
$\hat{\alpha}$	$\hat{\beta}$	$\sigma_{\hat{\beta}}$	t_β	p_β	R^2	γ_{AIC}	$\hat{t}_{AIC}$	p_{AIC}	γ_{BIC}	$\hat{t}_{BIC}$	p_{BIC}
2020-06-30 - 2020-09-25 ($N = 2008$)											
0.009	23.754	1.780	13.343	0.000***	0.082	12	-1.44	0.140	1	-1.805	0.068*
2020-08-05 - 2020-12-25 ($N = 3949$)											
0.012	32.717	0.875	37.400	0.000***	0.262	19	-2.302	0.020**	1	-2.503	0.012**
2020-09-25 - 2021-03-26 ($N = 4062$)											
0.029	23.616	1.130	20.899	0.000***	0.097	18	-1.827	0.064*	1	-2.796	0.005***
2020-12-25 - 2021-06-25 ($N = 4178$)											
0.0323	125.897	2.655	47.415	0.000***	0.350	24	-1.630	0.097*	2	-2.203	0.0265***
2021-03-26 - 2021-09-24 ($N = 4176$)											
-0.029	635.06	8.939	71.048	0.000***	0.547	9	-2.172	0.029**	4	-2.516	0.011**
2021-06-25 - 2021-12-31 ($N = 4340$)											
0.006	106.407	1.766	60.245	0.000***	0.456	8	-3.0595	0.002***	2	-3.342	0.0008***
2021-09-24 - 2022-03-25 ($N = 4183$)											
0.052	-67.77	1.557	-43.552	0.000***	0.312	7	0.156	0.734	1	-0.191	0.617
2021-12-31 - 2022-06-24 ($N = 4024$)											
0.011	0.1525	0.282	0.540	0.589	0.000	16	-2.938	0.003***	7	-2.809	0.005***
2022-03-25 - 2022-09-30 ($N = 4395$)											
-0.003	2.1694	0.066	32.686	0.000***	0.196	15	-2.765	0.001***	7	-2.256	0.01**

Table 22: Results of performing the Engle-Granger test on BTC Coin-M futures using the cost of carry model for investment assets. The left hand side of the table $\hat{\beta}$,$\sigma_{\hat{\beta}}$, t_β and R^2 are parameters corresponding to the OLS regression $f - s = \alpha + \beta\tilde{r} + \epsilon$, and the parameters γ_{AIC}, $\hat{t}_{AIC}$, p_{AIC}, γ_{BIC}, $\hat{t}_{BIC}$ and p_{BIC} are parameters corresponding to the Augmented Dickey Fuller (ADF) test. Notice that *, ** and *** imply significant t-statistics at the 10,5, and 1% level, respectively.

Table 35 in the Appendix shows the results for Ethereum Coin-M futures, where the intervals *2020-09-25 - 2021-03-26* and *2021-12-31- 2022-06-25* are not considered due $f - s$ not being $I(1)$. For all intervals considered, stationarity of the residuals is concluded. The estimate for the cointegrating parameter $\hat{\beta}$ for Ethereum Coin-M futures is also far off the value of 1 hypothesized. Tables 36 and 37 in the Appendix for USD-M futures show analogous results.

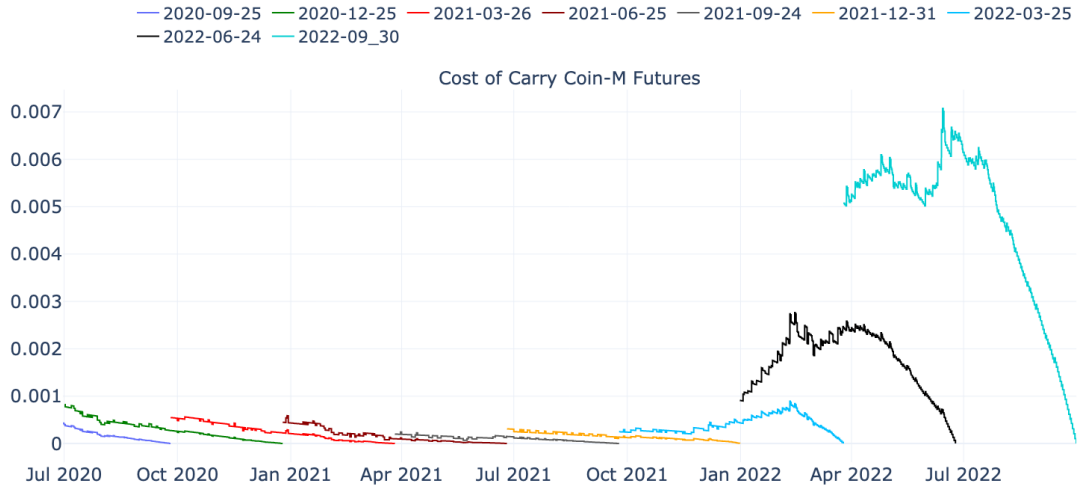

Figure 17: Cost of Carry ($r_{t,T}(T-t)$) per interval of Coin-M futures. The declining cost of carry throughout the interval can be explained by $(T-t)$ getting smaller as t increases.

In general, under the cost-of-carry model for investment assets, the regression equation $f - s = \alpha + \beta\tilde{r} + \epsilon$ is an improvement in terms of cointegration compared to $f - s$ alone. However, for the model to hold, $\beta = 1$ is required. This is not what is observed in the data, and large values of $\hat{\beta} > 100$ are estimated. This means that the cost of carry model for investment assets, which only consists of the risk-free rate, is unable to explain the observed (log) basis between Bitcoin and Ethereum Coin-M futures. In some intervals, the cost-of-carry of the risk-free rate needs to be scaled by a factor of 100 to explain the variation in the futures basis. This result may seem surprising, given that the cost of carry model for investment assets is widely used throughout large markets such as for stocks and bonds. To analyze this further, Figure 17 shows the cost-of-carry $\tilde{r}$ across all 9 intervals for Coin-M futures. For the majority of the intervals, this cost-of-carry was close to zero. This can be explained due to zero interest rates which can be seen in Figure 15. The negligible cost-of-carry start to disappear from the beginning of 2022, when interest rates moved from zero to higher rates. In the latter intervals, all Tables show declining values of $\hat{\beta}$ as the cost-of-carry becomes meaningful. For the majority of intervals, the cost-of-carry model for investment assets is unable to explain the high value of the basis observed in figures 6, 36, 7 and 8. At face value, the results of this section conclude that the futures market for Bitcoin and Ethereum is not efficient. It has been demonstrated before that for values $\hat{\beta} \neq 1$ arbitrage opportunities are possible through Table 10. Performing a 'cash-carry'[25] trade by arbitrageurs would have been profitable on almost every interval tested. The lack of arbitrage opportunities restoring parity between the futures and spot prices could be because of an omitted parameter in the regression equation 78. In the next section we will build upon this analysis to find this omitted parameter.

[25]Reminder that a cash-and-carry trade implies taking a short position in the futures contract at time t, buying the spot asset at time t and closing the trade at time T profiting $F(t,T) - S_t$.

5.4 Cost-of-Carry Model for Commodities

In section 5.3.1, it was concluded that using the cost-of-carry model for investment assets does not explain all observed futures basis in the market. In order to further explain the observed gap, we consider the cost-of-carry models for commodities, given by $F(t,T) = S_t e^{(r_t+\delta_t)}$, where $\delta_t = (k_t - \Psi_t)$, which we will refer to as the net convenience yield as explained in section 2.2.5. Since the parameter δ_t originates from the commodities market, it is necessary to provide an interpretation in relation to the cryptocurrency market. In section 3.3, it has been attempted to rationalize what δ_t might be. It was concluded that storage costs (if any) were relatively low and fixed costs instead of per unit. In fact, Schmeling et al. (2022) even omit storage costs completely from cryptocurrencies. The pure convenience yield Ψ_t could be the utility of the physical Bitcoin or Ethereum as a means of transaction, or for Ethereum specific the usage of smart contracts. Another possible interpretation for Ψ_t is the self-custody benefit, in wake of bankruptcies of some prominent cryptocurrency exchanges. Schmeling et al. (2022) even argue that Ψ_t may originate from demand in leveraged speculation, which will be discussed in greater detail later.

Recall that δ_t is an intangible parameter found through market prices. Under the cost-of-carry model for commodities, all unobserved futures bases from section 5.3.1 can be explained by δ_t. Again moving from a time t scenario to vector notation, let δ note the vector of convenience yield over time, i.e.

$$\delta = \begin{bmatrix} \delta_0 \\ \delta_1 \\ \vdots \\ \delta_{T-1} \end{bmatrix}$$

We then obtain, using (34), $\delta = f - s - \tilde{r}$. The right hand side of this equation is already known due to the previous section. To illustrate the value of δ over time, Figures 18, 19, 47 and 48 show the net convenience yield δ over time. All figures show that, on average, we observe a positive value of δ. This implies that the market implies either high storage costs k, or a highly negative convenience yield Ψ. The plots show a value of δ exceeding 0.1 ($\approx 10\%$) for some time periods. This level is simply too high to attribute to storage costs, which we argued to be negligible. Assuming a low k leads to the cost-of-carry model directing the high observed futures basis to a negative value of Ψ, since $\delta = (k - \Psi)$. This implies that market participants prefer to hold a futures contract instead of the physical Bitcoin or Ethereum. The high observed futures basis thus stems from a highly time variant Ψ which is negative most of the time. This is also what Schmeling et al. (2022) conclude. Their analysis concludes with the observation that the convenience yield on Bitcoin futures is highly time variant. Possible reasons for this were absence of arbitrageurs that restore parity, and small speculators that have high demand for leveraged speculation through futures.

The claim of δ being high (as a result of a negative Ψ) leads to contradictory arguments. To illustrate why, consider Figure 19, which shows the net convenience yield of Ethereum USD-Margined futures over time. The last interval shows a negative sustained value of δ. In September 2022, the Ethereum merge took place. This resulted in holders of Ethereum gaining an additional token called *ETHPOW*. This additional token is similar to a dividend payment, and futures contracts did not get this token. Therefore the value of Ψ rose sharply during this time, causing $\delta < 0$ and the future to go in backwardation. The backwardation immediately reverted after the merge took place. This shows that the parameter Ψ is present in its natural form as in the commodities market. Taking this evidence into account, theorizing δ for all other intervals to be high means that Ψ is both positive and negative at the same time. Concluding the analysis as is leads to too many question marks about the value and interpretation of δ as a result of a strong time-varying Ψ. It is hypothesized here that it is not δ alone that is this volatile, but perhaps the proxy of the risk-free rate as chosen is too simplistic.

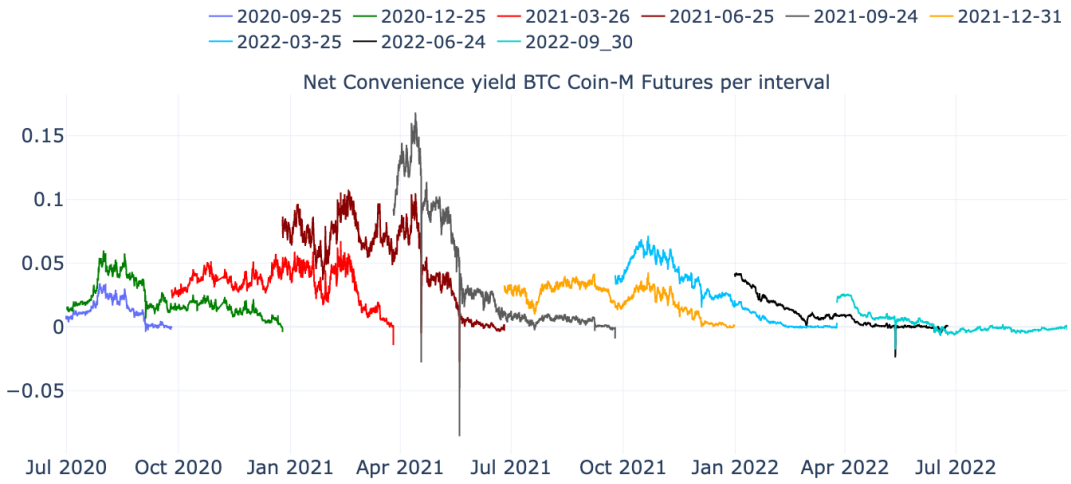

Figure 18: Plot of the net convenience yield for Bitcoin Coin-M futures

Figure 19: Plot of the net convenience yield for Ethereum USD-M futures

5.5 Funding Rate Cost-of-Carry Model

Schmeling et al. (2022) perform similar research to this thesis, and concluded their analysis with stating that δ is highly time variant due to a lack of arbitrageurs, and high demand for leveraged speculation by small traders. The previous section in this thesis found similar results. The highly time-varying δ could be market irrationality of small speculators as Schmeling et al. (2022) hypothesized, but could also be to incorrect risk-free proxies being used to price quarterly futures. In Figure 17, it was shown that the cost-of-carry during 2020 and 2021 was negligible, despite the quarterly futures expressing contango greater than 10% at times. In this section, through the scope of opportunity costs and sentiment, a new proxy to model the risk-free rate in the cryptocurrency market will be proposed. It will be investigated whether a new model, using this new proxy for the risk-free rate, will lead to δ becoming less time-variant and constant over time.

5.5.1 Opportunity Costs and the Effect of Perpetual Futures on Quarterly Futures

Empirical results from the data in this thesis have shown in Figures 18, 19, 47 and 48 that large values of δ are present in the quarterly futures market for Bitcoin and Ethereum. Schmeling et al. (2022) hypothesized that a possible explanation of this phenomenon is a lack of arbitrageurs to put capital into the cash-and-carry trade to restore the high observed futures basis back in lower territory. In this section, this claim will be analyzed, and it will be shown that opportunity costs exist for arbitrageurs due to other opportunities in the market yielding higher returns. If the amount of possible opportunities is greater than the total amount of capital willing to restore the quarterly futures basis, it could explain the sustained high basis on Bitcoin and Ethereum quarterly futures. Specifically, the more frequently traded perpetual futures is one of such opportunities. Arbitrageurs have to choose between deploying capital in the cash-and-carry trade for perpetual or quarterly futures. Recall that if the perpetual futures price is, on average, greater than the spot price ($F_p(t) > S_t$) during an 8-hour period, the funding rate would be positive. Arbitrageurs could take a short position in the perpetual futures contract and receive the funding rate. Notice that this is a very similar trade to the cash-and-carry described in Table 10, where for $F(t,T) > S_t e^{r_{t,T}(T-t)}$ an arbitrageur would carry the spot asset from time t to T, and take a short position in the futures contract (perform a cash-and-carry trade).

Let $\Gamma_1(0,T)$ denote the trading strategy of cash-and-carry of perpetual futures. This is the strategy of buying the underlying spot Bitcoin or Ethereum S_0 at time 0, and taking a short position on the perpetual future $F_p(0)$, receiving the funding rate $FR(\cdot)$ every 8 hours. For simplicity and fair comparison, the start and end dates of the strategy will be matched with the maturity dates of the quarterly futures contracts, so from time 0 to time T for every interval. Let $\Theta(\cdot,0,T)$ denote profit function at time T of this strategy, which started at time 0. Then, $\Theta(\Gamma_1,0,T) = (F_p(0) - F_p(T)) + (S_T - S_0) + \sum_{i=1}^{3\widetilde{(T)}} FR(i)$, where the first two terms are the profit or loss due to price changes, and the latter is the sum of all funding rate payments received from time 0 to time T. Notice that the summation has an upper limit of $3\widetilde{(T)}$. So far in this thesis, $(T-t)$ has been expressed in years, to scale the annual risk-free rate with. However, for the funding rate, 3 daily payments from time 0 to T are incurred, therefore measuring in days is appropriate, and $\widetilde{(T)} = 365(T)$. Figures 20 and 50 show $\Theta(\Gamma_1,0,T)$ for every interval of Coin-M perpetual futures. The results for USD-M perpetual futures are similar and therefore plots are omitted. It is clearly visible from the figures that $\Gamma_1(0,T)$ has been a profitable trading strategy with $\Theta(\Gamma_1,0,T)$ exceeding 10% in two occasions with a total duration of 6 months. $\Gamma_1(0,T)$ also experiences little drawdown.

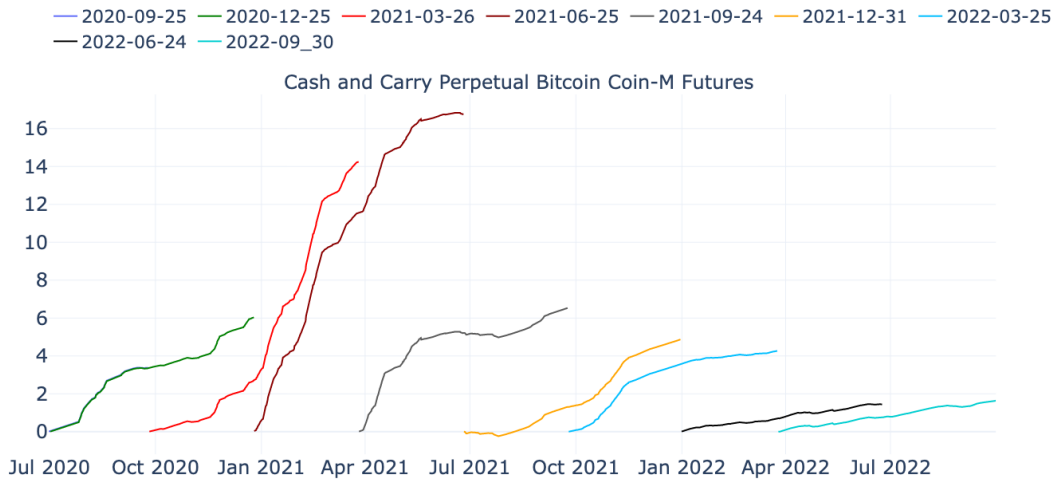

Figure 20: Returns in percentage of the cash and carry strategy for Bitcoin Coin-M perpetual futures

Next, let $\Gamma_2(0,T)$ denote the cash-and-carry strategy of quarterly futures. This strategy is buying the underlying Bitcoin or Ethereum at time 0, taking a short position in the quarterly futures at time 0, and closing out the positions at time T, where we have $F(T,T) = S_T$. As a result, $\Theta(\Gamma_2, 0, T) = (F(0,T) - F(T,T) + S_T - S_0) = (F(0,T) - S_T + S_T - S_0) = F(0,T) - S_0$. Figure 21 shows the returns for the cash-and-carry strategy for Bitcoin Coin-M quarterly futures per interval. It is worth noting that the returns of $\Gamma_2(0,T)$ are not realized until time T, therefore the equity curve of the strategy is the profit (loss) if the position would be closed out before time T. In Figure 21 it can be seen that $\Theta(\Gamma_2, 0, T) > 0$ for all intervals, similar to the case of perpetual futures. However, there is a lot more drawdown observed than for $\Gamma_1(0,T)$. Drawdown is defined as an unrealized loss at time $t \in \{0, ..., T-1\}$ due to unfavorable price changes. This high observed drawdown could be a problem for arbitrageurs performing $\Gamma_2(0,T)$, if not enough margin is posted. If too little margin is posted and large drawdowns occur, an arbitrageur could be forced to unwind the position at an unfavorable point in time causing a huge loss, similar what happened to Long Term Capital Management in 1998. This risk could limit the amount of capital willing to take the other side of such a trade, since arbitrageurs try to mitigate risks as much as possible. For Ethereum Coin-M futures we observe similar results as can be seen in Figure 49. The plots for USD-M futures look similar to those of Coin-M futures and are therefore omitted.

Tables 38 and 39 in the Appendix show more rigorous comparisons between $\Gamma_1(0,T)$ and $\Gamma_2(0,T)$. The majority of intervals show that $\Theta(\Gamma_1(0,T))$ was higher, and experienced lower drawdown than $\Theta(\Gamma_2(0,T))$. It is worth noting that only the final return and max drawdown are computed, since a cash-and-carry trade for quarterly futures is taken with the target in mind to hold it until time T. It could be argued that the perpetual futures funding rate is a more interesting trade for arbitrageurs, emphasized by the significantly lower drawdown observed in (20) in comparison to (21). Arbitrageurs take on less price risk and the returns are comparable, making the perpetual futures carry trade more attractive on paper. It is worth noting, however, that the return of a cash-and-carry trade for quarterly futures $\mathbb{E}[\Theta(\Gamma_2, 0, T)] = \mathbb{E}[F(0,T) - S_0] = F(0,T) - S_0$ is deterministic at time 0, since the profit is locked in at time 0, assuming that the boundary condition $F(T,T) = S_T$ holds. For perpetual futures, we have $\mathbb{E}[\Theta(\Gamma_2, 0, T)] = \mathbb{E}[(F_p(0) - F_p(T) + (S_T - S_0) + \sum_{i=1}^{\widetilde{3(T)}} FR(i)] = (F_p(0) - S_0) + \mathbb{E}[S_T - F_p(T) + \sum_{i=1}^{\widetilde{3(T)}} FR(i)]$. This is not deterministic because no boundary condition exists, and because the funding rate is stochastic. This gives the perpetual futures cash and carry trade less certainty. However, empirical data suggests that the drawdown of the perpetual futures cash-and-carry strategy $\Gamma_1(0,T)$ is low.

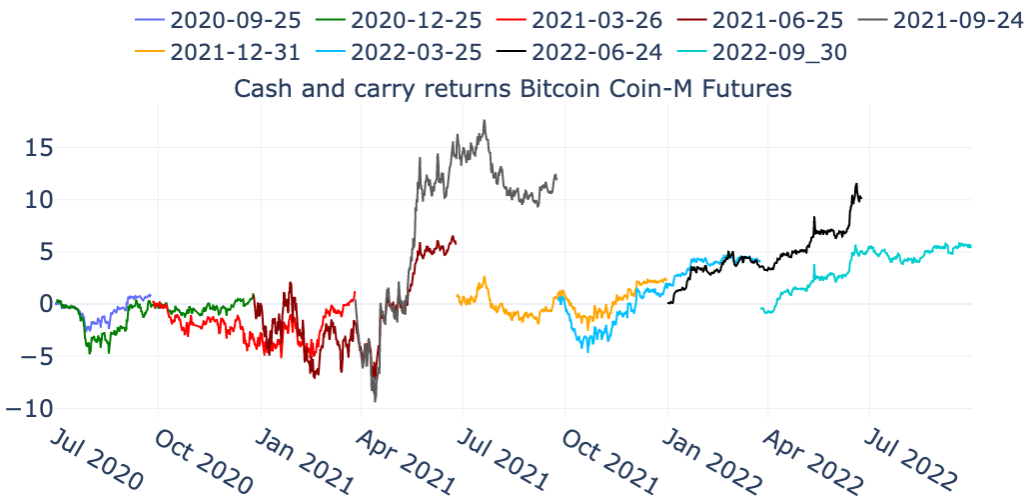

Figure 21: Returns in percentage of the cash and carry strategy for Bitcoin Coin-M futures

The arguments given above analyze the claim of Schmeling et al. (2022) of absence of arbitrageurs in quarterly futures markets. Empirical data in this section has shown that perpetual futures cash-and-carry opportunities compared to quarterly futures are as good, if not better, from a risk/return perspective for arbitrageurs. The cash-and-carry trades of quarterly futures incurred high drawdown between time 0 and T, which may result in arbitrageurs staying away. The perpetual futures market is also magnitudes larger than quarterly futures, therefore more capital can be deployed in perpetual futures than quarterly futures. It is therefore argued here that perpetual futures affect the basis of quarterly futures. This follows purely from the profit-maximizing mindset of arbitrageurs, who can achieve higher returns and lower risk in perpetual futures, therefore the amount of capital in the cash and carry trades of quarterly futures is limited. Arbitrageurs will require at least the return of the cash-and-carry trade of perpetual futures in order to take the cash-and-carry trade on quarterly futures. This implies high opportunity costs, or equivalently a high cost of capital for taking the cash-and-carry trade on quarterly futures and locking up capital for a longer time. It may therefore be necessary to add this cost of capital in the cost-of-carry model for Bitcoin and Ethereum quarterly futures.

In addition to the opportunity cost expressed in cost of capital, it can also be shown that through excess demand for leveraged speculation driven by market sentiment, that the perpetual futures funding rate directly influences the quarterly futures basis. Suppose a speculator wants to take a leveraged futures position on Bitcoin or Ethereum. To do this, there is a choice between quarterly and perpetual futures contracts. If both $F(t,T)$ and $F_p(t)$ are higher than their theoretical fair value by the cost-of-carry model, then a rational investor would simply buy S_t at time t. However, it has been argued in section 3.2.1 that euphoric sentiment results in high demand for leveraged speculation, resulting in speculators willing to pay extra for the opportunity to borrow capital to speculate on price increases. Suppose the speculator is indifferent between the two and wants to maximize his return at time T. For the speculator at time t, choosing between the two options results in $\min_t \left(B(t,T), \mathbb{E}_t^{\mathbb{Q}}[\sum_{i=1}^{\widetilde{3(T-t)}} FR(i)] \right)$. Recall that $B(t,T) = F(t,T) - S_t$, and $\mathbb{E}_t^{\mathbb{Q}}[\sum_{i=1}^{\widetilde{3(T-t)}} FR(i)]$ is the time t expected value of all perpetual futures funding rate payments. If at time t, $B(t,T) < \mathbb{E}_t^{\mathbb{Q}}[\sum_{i=1}^{\widetilde{3(T-t)}} FR(i)]$, then the speculator may choose to buy the quarterly futures contract $F(t,T)$, even if $F(t,T) > S_t e^{r_{t,T}(T-t)}$. Similarly, if $B(t,T) > \mathbb{E}_t^{\mathbb{Q}}[\sum_{i=1}^{\widetilde{3(T-t)}} FR(i)]$, then any rational investor would pick the perpetual futures contract as it maximizes the return at time T.

Another example can be given from the point of view of an arbitrageur. Suppose again that $B(t,T) < \mathbb{E}_t[\sum_{i=1}^{\widetilde{3(T-t)}} FR(i)]$. The arbitrageur could simply take a short position in the perpetual futures contract at time t, and a long position in the quarterly futures position. At time T, the perpetual futures position is closed, and the arbitrageur receives $[\sum_{i=1}^{\widetilde{3(T-t)}} FR(i)] - B(t,T)$. A note on why an arbitrageur may take a long position in the quarterly futures contract instead of buying S_t is that this can be done extremely capital efficient, as the two positions offset most of the price movement. If the actual spot asset is bought, more capital is required.

An additional point worth mentioning here, is that it is assumed $F_p(T) = S_T$, such that the arbitrageur does not lose money on the negative price difference between the perpetual futures and spot price. For quarterly futures, we have the boundary condition $F(T,T) = S_T$. However, perpetual futures do not have an expiration date. As He et al. (2023) points out, convergence of the perpetual futures price to the spot price is therefore not guaranteed. Empirically, however, we see that this difference is very small. Figure 51 in the Appendix shows that this difference historically has been a maximum of -0.2% except some very short term deviations. This is much smaller than the quarterly futures basis observed in (6,36,7 and 8).

The arguments and examples given above show that the funding rate will have an influence on the basis of quarterly futures. If the (risk-neutral) expected value of funding rate payments from time t to T is greater than the futures basis, then an arbitrage / profitable trading strategy is possible. This means that if the quarterly futures price were to trade exactly at fair value as computed by (23), this arbitrage/profitable trading strategy would therefore cause $F(t,T)$ to rise above its fair value.

The hypothesized relationship is therefore as follows. As a result of high perceived investor sentiment, market participants are willing to pay heavily for the ability to speculate on leverage. This translates itself into high funding rates on the perpetual futures contract. If the quarterly basis does not rise accordingly, i.e. $B(t,T) < \mathbb{E}^{\mathbb{Q}_t}[\sum_{i=1}^{\widetilde{3(T-t)}} FR(i)]$, it is shown that a profitable cash-and-carry strategy exists, which would cause $B(t,T)$ to rise. It is reasoned that perpetual futures influence quarterly futures, instead of the other way. This is due to the size differential, where perpetual futures have almost 100x more volume than quarterly futures (14).

5.5.2 Funding Rate Cost-of-Carry Model

In the previous section, the direct effect of perpetual futures funding rate on the basis of quarterly futures was hypothesized, both using arguments about opportunity costs, and excess demand for speculation driving the funding rate and quarterly futures basis higher. This hypothesis will be formally tested in this section. To measure the direct effect of the funding rate on the quarterly futures basis, the funding rate $r_{t,T}^{p_f}$ will be used as a proxy for the crypto-native risk-free rate. The model proposed here has the following form:

$$F(t,T) = S_t e^{\left(r_{t,T}^{p_f} - (r_{t,T} + \delta_t)(T-t)\right)} \tag{79}$$

, where $r_{t,T}^{p_f} = \mathbb{E}_t^{\mathbb{Q}}[\sum_{i=1}^{\widetilde{3(T-t)}} FR(i)]$ and $\delta_t = (k_t - \Psi_t)$. Notice that the $(T-t)$ vanishes in $r_{t,T}^{p_f}$ since it sums over all future funding rate payments from time t to T. The model formulated in (79) will be called the *funding rate cost-of-carry model*. The model falls under the category of cost-of-carry model for foreign currencies, described in (33). The intuition behind this model stems from arguments in the previous section about opportunity costs regarding perpetual futures. If the expected return on the cash-and-carry trade on perpetual futures from time t to time T is $y\%$, then the quarterly futures basis $B(t,T)$ should be at least $y\%$ to make the arbitrage opportunity attractive. The risk-free rate is subtracted here as the opportunity cost to abstain from making any trade at all. If $r_{t,T} > r^{f_p}{}_{t,T}$, then arbitrageurs are better off investing in the risk-free rate.

Notice that (79) is still in a time t setting with parameters in the exponent. Using vector notation and applying a log transformation to extract the parameters from the exponent results in:

$$f = s + (r^{p_f} - \tilde{r}) + \delta \tag{80}$$

In (80), f and s again represent the log futures and spot prices, and r^{p_f} is given by:

$$\begin{bmatrix} \mathbb{E}_0^{\mathbb{Q}}[\sum_{i=1}^{3\widetilde{T}} FR(i)] \\ \mathbb{E}_1^{\mathbb{Q}}[\sum_{i=1}^{3\widetilde{(T-1)}} FR(i)] \\ \vdots \\ \mathbb{E}_{T-1}^{\mathbb{Q}}[\sum_{i=1}^{3} FR(i)] \end{bmatrix}$$

$\tilde{r}$ is the vector with the risk-free rate, and δ the vector of convenience yields across time. The challenge in (79) and hence in (80) lies in finding a suitable estimation for r^{p_f}, since it is stochastic. At some time $t < T$, we have $r_{t,T}^{p_f} = \mathbb{E}_t^{\mathbb{Q}}[\sum_{i=1}^{3\widetilde{(T-t)}} FR(i)]$, which means that the upcoming funding rates from time t to time T have to be estimated at time t. In order to choose a suitable model, we start with a visual inspection of Figure 31 in the Appendix. It is visible that periods with an elevated funding rate periods seem to stay elevated for some time. It appears as if the funding rate time series is non stationary, and that previous realizations of the funding rate impact future realizations. It will therefore be attempted to model the perpetual futures funding rate using an Autoregressive Integrated Moving Average ($ARIMA(p,d,q)$) model, which allows for forecasting non stationary time series, and allows for previous realizations to affect future realizations. The model where $d = 0$ is called the $ARMA(p,q)$ model, which requires stationary data to have proper forecasts. Since it is suspected that funding rates may be non stationary, the $ARMA(p,q)$ model is not feasible. Therefore an $ARIMA(p,d,q)$ model is considered to determine r^{f_p}. An $ARIMA(p,d,q)$ model is simplistic and suffices for the application within this thesis. The goal of this section is to test whether including the funding rate in the cost of carry model leads to a higher explanation of the Bitcoin and Ethereum futures basis. Developing an extensive model to forecast the behavior of funding rates would be a thesis on its own. Therefore, due to time and length constraints, the goal of these simple ARIMA models in this thesis is to test the hypothesis that the perpetual futures funding rate impact the pricing of quarterly futures. It is acknowledged that modeling the funding rate is done in a simplistic way and more precise and extensive estimation methods are possible.

Adhikari and Agrawal (2013) define a process X_t to follow an $ARIMA(p,d,q)$ if X_t satisfies:

$$\left(1 - \sum_{i=1}^{p} \phi_i L^i\right)(1-L)^d X_t = \left(1 + \sum_{j=1}^{q} \theta_j L^j\right)\epsilon_t \tag{81}$$

, where ϕ represents the coefficients of the p autoregressive terms, and θ the coefficients of the q moving average terms. In order to select the corresponding parameters p, d, q, a two-step procedure will be used. The first step is to identify the correct model out of a class of general $ARIMA(p,d,q)$ models. In order to do this, the Auto Correlation Function (ACF) is considered. Figure 22 shows that for both Bitcoin and Ethereum Coin-M funding rate, the ACF is decaying slowly, and in fact does not converge to zero.

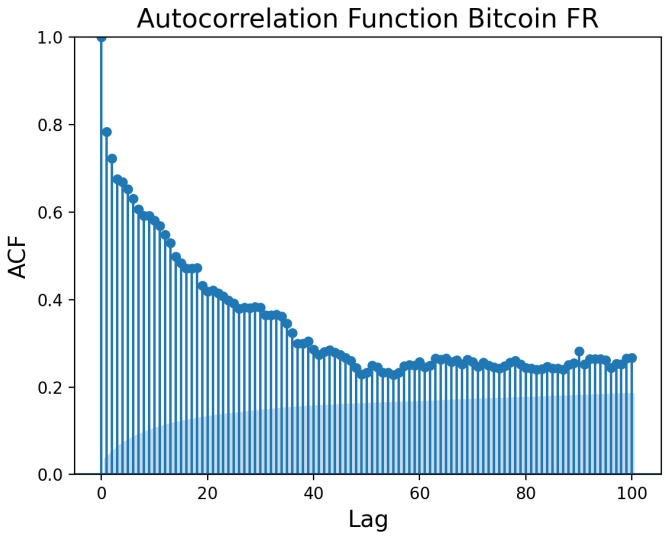

(a) Autocorrelation Function (ACF) for the Bitcoin Coin-M funding rate

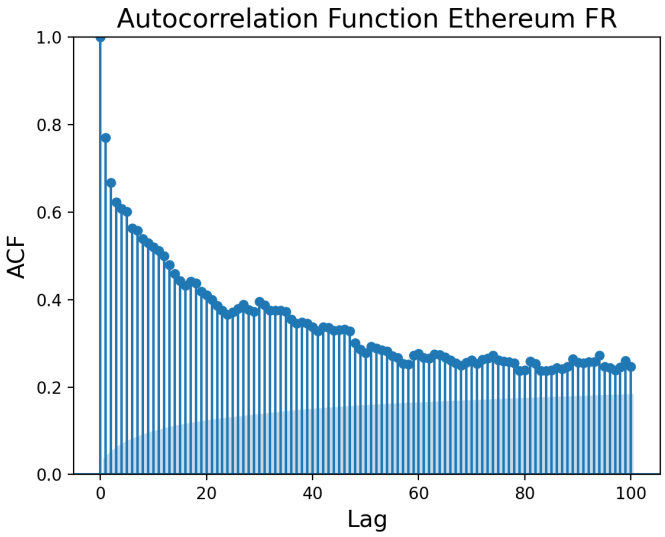

(b) Autocorrelation Function (ACF) for the Ethereum Coin-M funding rate

Figure 22: Autocorrelation Function (ACF) for the Bitcoin and Ethereum Coin-M funding rate

Adhikari and Agrawal (2013) argue that an ACF that does not decay towards zero violates the stationarity assumption that $ARMA(p, q)$ models require. This follows from stationary time series being mean-reverting; a value of X_t above its mean implies a higher probability of X_{t-1} being a lower value and thus reverting to its mean. The ACF plot shows that this is not true for the funding rate time series, and a high degree of autocorrelation is present. This is also what was found in the visual analysis of Figure 31, where certain market regimes experienced sustained high funding rates. In order to remove this autocorrelation, the first-differene of the time series r^{p_f} is taken. To formally test whether stationarity is guaranteed under the first-differenced time series, Table 40 in the Appendix shows the results of the ADF test of Δr^{p_f}. The test statistic is highly significant, both using the AIC and BIC. Therefore Δr^{p_f} is stationary, and $d = 1$ in the ARIMA model. For USD-M futures the same results are found and therefore omitted.

After $d = 1$ is chosen, the first step of specifying the correct $ARIMA(p, 1, q)$ models is selecting a class of suitable models through a visual inspection of the ACF and Partial Autocorrelation Function (PACF) of Δr^{p_f}. This is similar to the first step of the Box-Jenkins method. Figures 52 and 53 in the Appendix show the ACF and PACF for Δr^{p_f}. Starting with USD-M futures, it could be argued that both for Bitcoin and Ethereum the PACFs are decaying in a geometric way towards zero. A geometric decay of the PACF is a characteristic of an $ARIMA(0, 1, q)$ according to Neusser (2016). For the ACF, it is visible that after a maximum of 3 lags, the ACF is well in the significance region, indicating an $ARIMA(0, 1, 1)$, $ARIMA(0, 1, 2)$ or $ARIMA(0, 1, 3)$ model. However, it could also be argued that the decay of the PACF is not geometric, and in fact is only significant after 10 lags. It will therefore also be tested if an $ARIMA(10, 1, 1)$, $ARIMA(10, 1, 2)$ or $ARIMA(10, 1, 3)$ is appropriate. For Bitcoin and Ethereum Coin-M futures a similar visual inspection is performed, and the $ARIMA(0, 1, 6)$, $ARIMA(0, 1, 7)$, $ARIMA(0, 1, 8)$, $ARIMA(6, 1, 6)$, $ARIMA(6, 1, 7)$ and $ARIMA(6, 1, 8)$ are picked using the same procedure. Table 23 shows the AIC values for all six models chosen. It follows that that the best model for the Bitcoin USD-M funding rate is the $ARIMA(0, 1, 2)$ model, and for Ethereum USD-M this is an $ARIMA(0, 1, 1)$ model. For Coin-M Bitcoin and Ethereum futures the AIC is minimized for an $ARIMA(0, 1, 6)$ model and thus chosen.

AIC for different $ARIMA(p,1,q)$ models for USD-M futures						
Asset	$ARIMA(0,1,1)$	$ARIMA(0,1,2)$	$ARIMA(0,1,3)$	$ARIMA(10,1,1)$	$ARIMA(10,1,2)$	$ARIMA(10,1,3)$
BTC	-39830	-42921	-39826	-39810	-39808	-41404
ETH	-40680	-38134	-38132	-38116	-38114	-39439
AIC for different $ARIMA(p,1,q)$ models for Coin-M futures						
Asset	$ARIMA(0,1,6)$	$ARIMA(0,1,7)$	$ARIMA(0,1,8)$	$ARIMA(6,1,6)$	$ARIMA(6,1,7)$	$ARIMA(6,1,8)$
Bitcoin	-16240	-16239	-16238	-15984	-15982	-15980
Ethereum	-15106	-15104	-15103	-15096	-15099	-14942

Table 23: AIC values ARIMA models

Now that the models are chosen, a quick explanation of the forecasting method is given. Recall that r^{p_f} is given by:

$$\begin{bmatrix} \mathbb{E}_0^{\mathbb{Q}}[\sum_{i=1}^{3\widetilde{T}} FR(i)] \\ \mathbb{E}_1^{\mathbb{Q}}[\sum_{i=1}^{\widetilde{3(T-1)}} FR(i)] \\ \vdots \\ \mathbb{E}_{T-1}^{\mathbb{Q}}[\sum_{i=1}^{3} FR(i)] \end{bmatrix}$$

The first step is fitting the $ARIMA(p,1,q)$ models on the entire testing period to obtain the corresponding coefficients. Then at each time $t \in \{0,..,T-1\}$ we use the previous funding rate values and the $ARIMA(p,1,q)$ model to forecast from time t to T. All forecasted funding rates are then summed and $\mathbb{E}_t^{\mathbb{Q}}[\sum_{i=1}^{\widetilde{3(T-t)}} FR(i)]$ is obtained. We now have an estimate for r^{p_f}, and the Engle-Granger test for is performed again to check for improvement in terms of cointegration. The regression in the first step of the Engle-Granger test is now given by:

$$f - s = \alpha + \beta(r^{p_f} - \tilde{r}) + \epsilon \tag{82}$$

In order for cointegration to be valid, it must be checked whether $(r^{p_f} - \tilde{r}) \sim I(1)$. Table 41 shows that for Coin-M futures the intervals *2020-09-25 - 2021-03-26* and *2021-12-31 - 2022-06-24* are $I(0)$ at the 5% significance and thus can not be interpreted. For USD-M futures this is the interval *2022-03-22 - 2022-06-24*. For $f - s$, Table 33 in the Appendix has shown that for Bitcoin Coin-M this is the case for *2021-12-31 - 2022-06-24*.

Table 24 shows the results of performing the Engle-Granger test on the funding rate cost-of-carry model for Bitcoin Coin-M futures. First drawing our attention to the right hand of the table, it is clear that under the AIC and BIC, for all intervals tested the residuals are stationary, with the caveat that the two intervals highlighted above cannot be considered, due to $(r^{p_f} - \tilde{r}) \sim I(1)$. For all other intervals it is therefore possible to interpret the OLS estimate (cointegration parameter) $\hat{\beta}$, and $\hat{\alpha}$. In comparison to the model for the investment asset where the cointegration parameter for some intervals was greater than 100, we now observe the cointegration parameter $\hat{\beta}$ much closer to 1, and $\hat{\alpha}$ close to zero. This implies that the funding rate cost-of-carry model explains more of the observed quarterly futures basis, as was hypothesized, and in the long-run $f - s \approx (r^{p_f} - \tilde{r})$.

Bitcoin Coin-M futures funding rate model											
$\hat{\alpha}$	$\hat{\beta}$	$\sigma_{\hat{\beta}}$	t_β	p_β	R^2	γ_{AIC}	$\hat{t}_{AIC}$	p_{AIC}	γ_{BIC}	$\hat{t}_{BIC}$	p_{BIC}
2020-06-30 - 2020-09-25 ($N = 2008$)											
0.005	0.827	0.015	54.427	0.000***	0.599	15	-3.694	0.001***	0	-4.623	5.557e-6***
2020-08-05 - 2020-12-25 ($N = 3949$)											
0.011	0.869	0.015	58.339	0.000***	0.464	1	-3.839	0.001***	1	-3.839	0.001***
2020-09-25 - 2021-03-26 ($N = 4062$)											
0.027	0.379	0.01	40.284	0.000***	0.287	23	-2.659	0.007***	1	-4.067	5.613e-5***
2020-12-25 - 2021-06-25 ($N = 4178$)											
0.034	0.718	0.012	61.705	0.000***	0.478	24	-3.102	0.002***	1	-3.971	8.198e-5**
2021-03-26 - 2021-09-24 ($N = 4176$)											
0.017	0.790	0.008	98.108	0.000***	0.699	29	-4.770	2.945e-6***	2	-4.687	4.25e-6***
2021-06-25 - 2021-12-31 ($N = 4340$)											
0.019	0.417	0.016	26.476	0.000***	0.140	3	-2.440	0.014**	2	-2.562	0.011**
2021-09-24 - 2022-03-25 ($N = 4183$)											
0.009	0.889	0.008	107.7	0.000***	0.751	1	-4.312	2.073e-5***	0	-4.532	8.225e-6***
2021-12-31 - 2022-06-24 ($N = 4024$)											
0.008	1.074	0.02	53.152	0.000***	0.414	15	-4.157	3.909e-5**	0	-4.939	1.392e-6***
2022-03-25 - 2022-09-30 ($N = 4395$)											
0.007	0.040	0.018	2.156	0.031**	0.001	26	-2.474	0.013**	7	-2.471	0.013**

Table 24: Results of performing the Engle-Granger test on each interval of BTC Coin-M futures using the funding rate cost of carry model. The left hand side of the table $\hat{\beta}$,$\sigma_{\hat{\beta}}$, t_β and R^2 are parameters corresponding to the OLS regression $f - s = \beta(r^{p_f} - \tilde{r}) + \epsilon$, and the parameters γ_{AIC}, $\hat{t}_{AIC}$, p_{AIC}, γ_{BIC}, $\hat{t}_{BIC}$ and p_{BIC} are parameters corresponding to the Augmented Dickey Fuller (ADF) test. Notice that *, ** and *** imply significant t-statistics at the 10,5, and 1% level, respectively.

For Ethereum Coin-M futures, similar results can be deduced from Table 42 in the Appendix. Each interval contains $I(0)$ residuals from the first-stage regression, and the OLS estimate of the cointegrating parameter $\hat{\beta}$ improved dramatically. In Table 35, the first six intervals reported cointegrating parameters of approximately 186,99,23,124,627 and 96, respectively. This has now been improved to 0.827, 0.869, 0.379, 0.718, 0.789 and 0.417, respectively. The cointegration parameters are closer to 1, indicating a better explanation of the futures basis.

To get more intuition about the remaining unexplained futures basis under the funding rate cost-of-carry model, Figure 23 plots the net convenience yield δ for Bitcoin Coin-M futures. Under this model, $f - s - r^{p_f} + \tilde{r} = \delta$. Figure 23 shows that using $(r^{f_p} - \tilde{r})$ as the interest-rate carry term has flattened the value of δ in general, being more centered around zero. The highest observed value of δ is slightly above 0.1, whilst using $\tilde{r}$ alone resulted in a maximum $\delta > 0.15$ (as seen in (18)). The cointegration parameter $\hat{\beta}$ being closer to 1 thus also seen visibly. It is also visible in Figure 23 that δ is more volatile under the funding rate model than under the investment asset model. This is due to the fact that r^{p_f} itself is volatile, as it is estimated based on previous observations using an $ARIMA(0, 1, 2)$ model. This model uses relatively short-term lags which can explain the observed volatility, since the funding rate computed every 8 hours can deviate significantly.

In addition, under the funding rate model, r^{p_f} is vulnerable to outliers, where multiple deviation from the mean are seen, but revert back quickly. It is worth noting that the two largest outliers (in grey) are also seen in Figure 18. An explanation for this model to be more vulnerably is the choice of model. As stated earlier, it is acknowledged that the choice of model is simplistic and could be modeled to higher precision in future research. Relatively few lagged terms are used here, perhaps more extensive models could mitigate this volatility. In general, the unexplained futures basis δ is much more flat than for the earlier model, confirming the findings in Table 24 about drastically improving the fit using the $(r^{f_p} - \tilde{r})$ carry term. A similar plot regarding Ethereum Coin-M futures can be found in Figure 54.

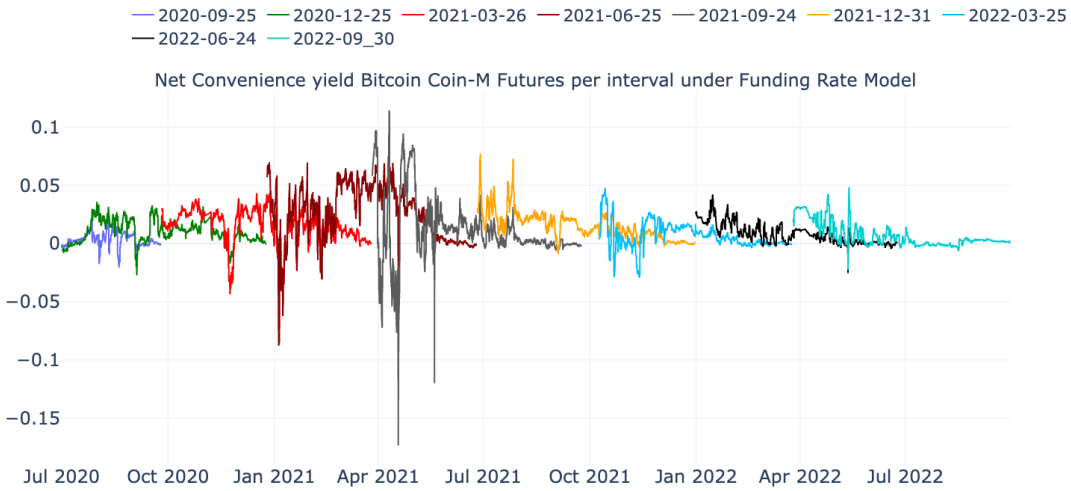

Figure 23: Net convenience yield δ Bitcoin Coin-M futures under the funding rate cost of carry model.

The same procedure is now performed on USD-M futures. Table 43 and 44 in the Appendix show the results of the Engle-Granger test on Bitcoin and Ethereum Coin-Futures under the funding rate cost-of-carry model. The residuals of the first-stage OLS regression are all $I(1)$ except for the second-to-last interval, which could not be considered due to Table 41 concluding $(r^{p_f} - \tilde{r}) \sim I(1)$. The cointegration parameters found on almost all intervals are close to 1, greatly improving the fit of the models compared to the cost-of-carry model for investment assets. Figure 24 shows the net convenience yield δ under the cost-of-carry model. Notice the relatively flat structure compared to Figure 24 with in general lower values for δ under the funding rate model.

This section has shown that using the funding rate cost-of-carry-model with the carry term $(r^{p_f} - \tilde{r})$ has greatly improved the explanation of the observed futures basis, leading to smaller values of δ. For all intervals tested, the residuals of the cointegrating regression expressed $I(0)$ residuals, and the estimate of the cointegration parameter $\hat{\beta}$ close to 1, improving by a factor of 100x compared to the cost-of-carry models for investment assets.

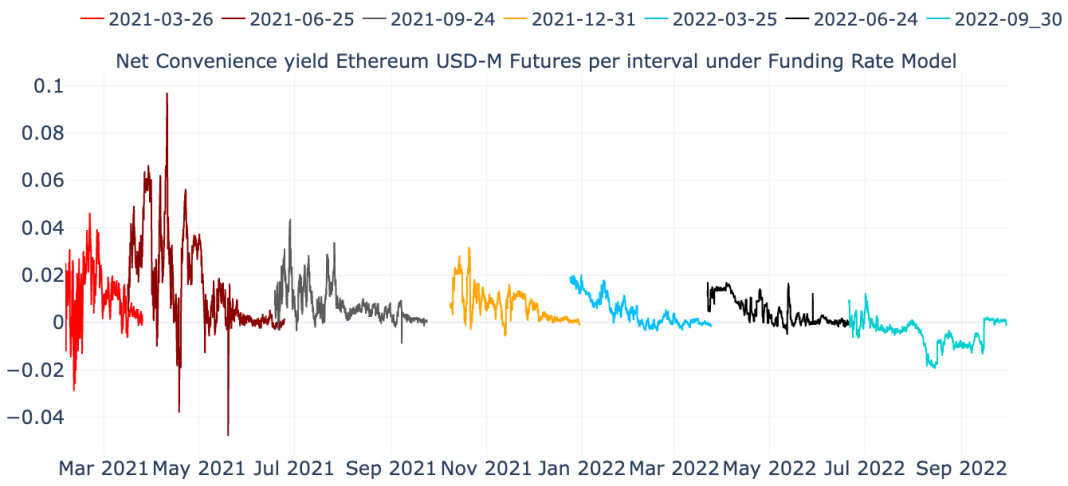

Figure 24: Net convenience yield δ Ethereum USD-M futures under the funding rate cost of carry model.

6 Summary and Conclusions

6.1 Summary and Discussion of Results

This thesis attempted to explain the futures basis of Bitcoin and Ethereum using several cost-of-carry models. The motivation behind the research in this thesis is a highly volatile futures basis. For USD-M futures, a basis as high as 10% with a maturity of 3 months was observed. For Coin-M futures with a higher underlying leverage, the futures basis was even higher at 18% with a maturity of only 6 months. This high futures basis is unprecedented compared to other asset classes, and consequently an explanation was sought after.

In an efficient market, a no-arbitrage futures price should exist, where arbitrageurs restore equilibrium for any deviation from this no-arbitrage price. The literature was investigated, where well-researched and tested models from different asset classes were gathered. These models, the so-called cost-of-carry models, explain that the no-arbitrage price of futures consists of the underlying spot asset, and a set of carry variables arising from the deferred payment property of futures contracts.

The benchmark model chosen is the cost-of-carry model for investment assets, which is given by $F(t,T) = S_t e^{r_{t,T}(T-t)}$. This benchmark model uses the yield of US-treasuries as a proxy for the risk-free rate. In the commodity markets, it is often observed $F(t,T) \neq S_t e^{r_{t,T}(T-t)}$. The reasoning behind the benchmark model not holding in the commodity markets is the storage costs k_t associated with storing a commodity, higher barriers of arbitrage, and the existence of a convenience yield Ψ_t. The latter stems from commodities being a consumption asset, and therefore, the physical commodity may be preferred over a derivative. The cost-of-carry model in the commodities market is given by: $F(t,T) = S_t e^{(r_t + k_t - \Psi_t)(T-t)}$ in a time t setting. Often, k_t and Ψ_t are bundled together, leading to $\delta_t = (k_t - \Psi_t)$ and $F(t,T) = S_t e^{(r_{t,T}+\delta_t)(T-t)}$. For foreign currencies, the cost-of-carry model is given by $F(t,T) = S_t e^{(r_{t,T} - r^f_{t,T})(T-t)}$, the carry term being the difference between local and foreign currency.

Testing of cost-of-carry models in related literature such as Quan (1992), Heany (2001), Asche and Guttormsen (2002) and Wu et al. (2021) is done using a cointegration approach. The motivation behind cointegration is the non-stationarity of time series and the interest in a long-run mean reverting relationship, which is to be expected in efficient markets. Under the cost-of-carry models, any deviation from the equilibrium between the two would result in an arbitrage opportunity, which should restore equilibrium again. The cointegration test in this thesis is the two-step Engle-Granger test, which performs a linear regression in the first step, and a test for stationarity of the residuals in the second step. If the null hypothesis of the Engle-Granger test is rejected, cointegration is concluded.

It was established in Section 5 that Bitcoin and Ethereum log spot and log futures prices are not cointegrated, contrary to what is found in other markets. A reasoning for this is the large futures basis that is observed in the cryptocurrency market. The results of testing the cost-of-carry model for investment assets using the first-stage regression $f - s = \alpha + \beta\tilde{r} + \epsilon$ established cointegration in most intervals, explaining more of the futures basis than without the carry term $\tilde{r}$. However, the estimate of the cointegrating parameter $\hat{\beta}$ was reported to be greater than 100 for a large proportion of the intervals tested. This implies that the observed futures basis is, on average, 100 times greater than the cost-of-carry term. It follows from this observation that the model $F(t,T) = S_t e^{r_{t,T}(T-t)}$ is not sufficient to explain the futures basis observed. This result on its own is not surprising, as the testing period (2020-2022) had a large period of zero interest rates and futures with short maturities. It can therefore not be expected that such a simple carry term can explain the large variation observed in future basis. Essentially, this finding implies that the futures market for Bitcoin and Ethereum is not efficient. If $F(t,T) \neq S_t e^{r_{t,T}(T-t)}$, then arbitrage opportunities are possible.

Attention was then turned to the cost-of-carry model with net convenience yield parameter δ. Plotting the unexplained futures basis led to a highly time-variant δ, reaching a value as high as 0.15 for some intervals. Schmeling et al. (2022) found similar results and concluded that the cryptocurrency market has a highly time-variant δ. This is a result of a combination of two factors, the shortage of capital performing cash-and-carry trades, and the excess demand for leveraged speculation. At face value, the cryptocurrency futures market is inefficient, and too little capital takes trades to restore equilibrium between futures and spot prices. It was argued in Section 5 that the opportunity costs for cash-and-carry trades in the cryptocurrency market are substantial, and can be quantified as the return on a similar strategy involving perpetual futures. This high opportunity cost may limit the amount of capital that performs the cash-and-carry trade on quarterly futures. Another argument was given, outlining the influence that excess demand for speculation on perpetual futures has on the quarterly futures basis. These arguments led to the proposition of the hypothesis that the perpetual futures funding rate is a well-suited proxy to model the risk-free return in the cryptocurrency market.

This native risk-free rate in the cryptocurrency market consisting of perpetual futures funding rate, is given by $r_{t,T}^{p_f} = \mathbb{E}_t^{\mathbb{Q}}[\sum_{i=1}^{\widetilde{3(T-t)}} FR(i)]$, the time t expectation of all future funding rate payments. Since this is a stochastic quantity, it was attempted to simplistically model this from the perspective of an investor at time t using an $ARIMA(p,d,q)$ model. It was observed visually that the time-series of funding rates has a non-decaying Autocorrelation Function. As such, models that require stationarity of data therefore cannot be applied. It was found that the time series Δr^{f_p} was stationary and therefore an $ARIMA(p,1,q)$ model was found to be suitable to model $\mathbb{E}_t^{\mathbb{Q}}[\sum_{i=1}^{\widetilde{3(T-t)}} FR(i)]$. The parameters p and q, which minimize the AIC, were chosen to construct the model. After the choice of $ARIMA(p,d,q)$ models, the *funding rate cost-of-carry model* was proposed as $F(t,T) = S_t e^{\left(r_{t,T}^{p_f} - (r_{t,T} + \delta_t)(T-t)\right)}$. The Engle-Granger test concluded stationary residuals for every interval of the regression equation $f - s = \alpha + \beta(r^{p_f} - \tilde{r}) + \epsilon$. The cointegrating parameters $\hat{\beta}$ were thus all super-consistent, and substantially closer to 1. For the new model, all cointegrating parameters ranged between 0 and 1.885, and for the benchmark model this was a range of -75 to 1269. This indicates a substantial improvement in terms of the fit of the model, hypothesized by a cointegrating parameter $\hat{\beta}$ close to 1. As such, the arguments that the funding rates directly impact quarterly futures prices does seem to have merit. Visually, the value of δ was seen to be lower resulting in a flatter futures basis.

Despite the large improvement in the cointegrating parameter, the model can be improved on. For instance, the last interval suggested a parameter $\hat{\beta}$ close to 0, which is odd, and may need extra investigation. A visual representation of the remaining unexplained futures basis δ was shown to be highly volatile, and regardless of the large improvement, a sustained futures basis was still observed. The high volatility of δ can be explained by the volatility of the underlying funding rate data, and the short and simple $ARIMA(p,1,q)$ model. It is acknowledged that this model is likely too simple to truly estimate the future funding rates, and more complex and extensive models will lead to a better estimation of $r_{t,T}^{p_f}$ and hence the futures basis.

6.2 Academic and Practical Takeaways

The results of this thesis provide several interesting academic and practical takeaways. As for the academic takeaways, the gap between the existing literature of no-arbitrage futures pricing and the cryptocurrency market is bridged, applying cost-of-carry models from all asset classes on cryptocurrencies. In addition, a new model was proposed. This model explains substantially more futures basis in the cryptocurrency market, through establishing the link between perpetual and quarterly futures. This creates a deeper understanding of the behavior of the new and unknown cryptocurrencies futures market, which opens possibilities for future research in the field of futures pricing in the cryptocurrency market. As for practical takeaways, the empirical analysis of the behavior of futures prices insist that uneducated investors trading in Bitcoin or Ethereum futures

should exercise caution when trading these futures contracts. It has been shown that Bitcoin and Ethereum futures trade well outside of the bands of traditional no-arbitrage models. An investor should realize that the high futures basis on Bitcoin and Ethereum impose additional downside risk, as convergence of the futures price to the spot price is guaranteed. Lastly, this thesis has been extensive in describing all relevant mechanics of the futures market of cryptocurrencies market such as the collateralization types, leverage and irrationality due to sentiment. This may contribute to a greater understanding of the products, and lead to a more efficient and transparent market. This benefits multiple stakeholders, such as researchers, investors, or arbitrageurs.

6.3 Limitations and Future Research

The methodology used to model the expected funding rate has its limitations. Estimation was done through an $ARIMA(p, 1, q)$ model, with p and q different for each futures type and asset, consisting of relatively few lags. The funding rate data itself is volatile, leading to the $ARIMA(p, 1, q)$ models expressing a high degree of volatility in estimating the funding rate. This model is likely too simplistic to precisely forecast all future funding rate payments. Future research could extend on this thesis by making a more elaborate model of forecasting funding rates. Another limitation of this research is the relatively short testing period. The time frame of the analysis in this thesis is from 2020 to 2022, since the cryptocurrency futures market is still in its infancy. As a result, the high observed futures basis observed in 2021 may prove to be an anomaly, and as the market matures, this inefficiency decays. Subsequently, it may be that traditional cost-of-carry models hold better in the future as the market becomes more efficient. An opportunity for future research is to conduct the same analysis as in this thesis at a later time period, and compare the results to test if this efficiency does arise.

In terms of future research, the methodology could be extended. In this thesis, the cointegrating parameter was estimated to test the fit of the cost-of-carry models. This was done in a univariate case, with one carry parameter at the time. The analysis performed in this research could be extended to the multivariate case, by proposing a VAR model that allows for cointegration between different assets, for instance. The Johansen test could be applied in that case. Since cointegration implies the existence of Error Correction Models, several Error Correction Models could be developed given the results of this thesis, to model the short and long-run dynamics between futures and spot prices in the cryptocurrency market. Furthermore, this research has limited itself to the largest two cryptocurrencies, Bitcoin and Ethereum. Future research could perform similar analysis as performed here on smaller cryptocurrencies to see if similar behavior is found. Lastly, this thesis has focused on the cost-of-carry approach to price futures contracts. Other theories, such as adding risk premiums to futures prices could be applied on the futures market of cryptocurrencies to explain the futures basis.

References

Adhikari, R., & Agrawal, R. K. (2013). *An introductory study on time series modeling and forecasting*.

Aïd, R., Campi, L., & Lautier, D. (2015). On the spot-futures no-arbitrage relations in commodity markets. http://arxiv.org/abs/1501.00273

Akaike, H. (1973). Information theory and an extension of the maximum likelihood principle. *Second International Symposium on Information Theory*, *1*, 267–281.

Antonopoulos, A. M. (2014). *Mastering bitcoin : Unlocking digital crypto-currencies* (M. Loukides & A. MacDonald, Eds.; Vol. 1). O'Reilly Media.

Asche, F., & Guttormsen, A. G. (2002). Lead lag relationships between futures and spot prices.

Bentov, I., Gabizon, A., & Mizrahi, A. (2014). Cryptocurrencies without proof of work. http://arxiv.org/abs/1406.5694

Black, F., & Scholes, M. (1973). The pricing of options and corporate liabilities. *Source: The Journal of Political Economy*, *81*, 637–654.

Bouteska, A., Mefteh-Wali, S., & Dang, T. (2022). Predictive power of investor sentiment for bitcoin returns: Evidence from covid-19 pandemic. *Technological Forecasting and Social Change*, *184*. https://doi.org/10.1016/j.techfore.2022.121999

Burggraf, T., Huynh, T. L. D., Rudolf, M., & Wang, M. (2020). Do fears drive bitcoin? *Review of Behavioral Finance*, *13*, 229–258. https://doi.org/10.1108/RBF-11-2019-0161

Carmona, R., & Ludkovski, M. (2004). Spot convenience yield models for the energy markets. *Contemporary Mathematics*, *351*, 65–80.

Cheah, E. T., & Fry, J. (2015). Speculative bubbles in bitcoin markets? an empirical investigation into the fundamental value of bitcoin. *Economics Letters*, *130*, 32–36. https://doi.org/10.1016/j.econlet.2015.02.029

Ciner, C. (2006). Hedging or speculation in derivative markets: The case of energy futures contracts. *Applied Financial Economics Letters*, *2*, 189–192. https://doi.org/10.1080/17446540500461729

Corelli, A. (2018). Cryptocurrencies and exchange rates: A relationship and causality analysis. *Risks*, *6*. https://doi.org/10.3390/risks6040111

Cornell, B., & French, K. R. (1983). Taxes and the pricing of stock index futures. *Source: The Journal of Finance*, *38*, 675–694.

Cornell, B., & Reinganum, M. R. (1981). Forward and futures prices: Evidence from the foreign exchange markets. *Source: The Journal of Finance*, *36*, 1035–1045.

Corradin, S., & Rodriguez-Moreno, M. (2016). Violating the law of one price: The role of non-conventional monetary policy.

Cox, J., Ingersoll, J., & Ross, S. (1981). The relation between forward prices and futures prices*. *Journal of Financial Economics*, *9*, 321–346.

Damodaran, A. (2004). *Investment fables: Exposing the myths of "can't miss" investments strategies*.

Damodaran, A. (2008). *What is the riskfree rate? a search for the basic building block*. www.damodaran.com

Detzel, A., Liu, H., Strauss, J., Zhou, G., & Zhu, Y. (2021). Learning and predictability via technical analysis: Evidence from bitcoin and stocks with hard-to-value fundamentals. *Financial Management*, *50*, 107–137. https://doi.org/10.1111/fima.12310

Dickey, D. A., & Fuller, W. A. (1979). Distribution of the estimators for autoregressive time series with a unit root. *Journal of the American Statistical Association*, *74*, 427. https://doi.org/10.2307/2286348

Dolatabadi, S., Nielsen, M. Ã., Xu, K., & Nielsen, M. Ø. (2015). *A fractionally cointegrated var model with deterministic trends and application to commodity futures markets a fractionally cointegrated var model with deterministic trends and application to commodity futures markets **.

Durbin, J., & Watson, G. S. (1951). *Testing for serial correlation in least squares regression. ii* (1). https://www.jstor.org/stable/2332325?seq=1&cid=pdf-

Elder, J., & Kennedy, P. E. (2001). Testing for unit roots: What should students be taught? *The Journal of Economic Education*, *32*(2), 137–146. https://doi.org/10.1080/00220480109595179
Enders, W. (2004). *Applied econometric time series* (2nd ed.). John Wiley; Sons.
Engle, R. F., & Granger, ; C. W. J. (1987). Co-integration and error correction: Representation, estimation, and testing. *Econometrica*, *55*, 251–276.
Enoksen, F. A., Landsnes, C. J., Lučivjanská, K., & Molnár, P. (2020). Understanding risk of bubbles in cryptocurrencies. *Journal of Economic Behavior and Organization*, *176*, 129–144. https://doi.org/10.1016/j.jebo.2020.05.005
Fahim, A. (2019). *Introduction to financial mathematics*. Florida State University Libraries. https://doi.org/10.33009/financialmath1
Fama, E. F. (1965). Random walks in stock-market prices. *Financial Analysts Journal*, *21*, 55–59.
Fattah, J., Ezzine, L., Aman, Z., Moussami, H. E., & Lachhab, A. (2018). Forecasting of demand using arima model. *International Journal of Engineering Business Management*, *10*. https://doi.org/10.1177/1847979018808673
Franchi, M. (2007). The integration order of vector autoregressive processes. *Econometric Theory*, *23*, 546–553. https://doi.org/10.1017/S0266466607070259
French, K. R. (1983). A comparison of futures and forward prices*. *Journal of Financial Economics*, *12*, 311–342.
Fuller, W. (1994). *Introduction to statistical time series* (2nd ed.). Wiley.
Gibson, R., & Schwartz, E. S. (1990). American finance association stochastic convenience yield and the pricing of oil contingent claims. *Source: The Journal of Finance*, *45*, 959–976.
Girard, E. (2010). *Cost of carry on steroids: Application to oil futures pricing* (2). http://ssrn.com/abstract=1667134
Granger, C. W. J., & Newbold, P. (1974). *Spurious regressions in econometrics* (6). North-Holland Publishing Company.
Grobys, K., & Junttila, J.-P. (2020). Speculation and lottery-like demand in cryptocurrency markets. *SSRN Electronic Journal*. https://doi.org/10.2139/ssrn.3551948
Hamilton, J. D. (D. (1994). *Time series analysis*. Princeton University Press.
He, S., Manela, A., Ross, O., & von Wachter, V. (2023). Fundamentals of perpetual futures. http://arxiv.org/abs/2212.06888
Heany, R. (2001). *Does knowledge of the cost of carry model improve commodity futures price forecasting ability? a case study using the london metal exchange lead contract*. www.elsevier.com/locate/ijforecast
Hendry, D. F. (1980). *Econometrics-alchemy or science?* (188).
Herbst, A., McCormack, J., & West, E. (1987). Investigation of a lead-lag relationship between spot stock indices and their futures contracts. *Journal of Futures Markets*, *7*, 373–381.
Hilliard, J. E., & Ngo, J. T. (2022). Bitcoin: Jumps, convenience yields, and option prices. *Quantitative Finance*, *22*, 2079–2091. https://doi.org/10.1080/14697688.2022.2109989
Hu, Y., Hou, Y. G., & Oxley, L. (2020). What role do futures markets play in bitcoin pricing? causality, cointegration and price discovery from a time-varying perspective? *International Review of Financial Analysis*, *72*. https://doi.org/10.1016/j.irfa.2020.101569
Hull, J. (2014). *Options, futures and other derivatives* (9th ed.). Pearson.
Jarrow, R. A., & Oldfield, G. S. (1981). Forward contracts and futures contracts. *Journal of Financial Economics*, *9*, 373–382.
Johansen, S. (2015). *Time series: Cointegration*. https://doi.org/10.1016/B978-0-08-097086-8.42086-6
Kapar, B., & Olmo, J. (2019). *An analysis of price discovery between bitcoin futures and spot markets*.
Kim, D. H., & Wright, J. H. (2005). *An arbitrage-free three-factor term structure model and the recent behavior of long-term yields and distant-horizon forward rates*.
Lammer, D., Hanspal, T., & Hackethal, A. (2019). Who are the bitcoin investors? evidence from indirect cryptocurrency investments. *SSRN Electronic Journal*. https://doi.org/10.2139/ssrn.3501549

Levy, A. (1989). A note on the relationship between forward and futures contracts. *The Journal of Futures Markets*, *9*, 171–173.

Lian, Y.-M., Cheng, C.-H., Lin, S.-H., & Lin, J.-H. (2019). A cost of carry-based framework for the bitcoin futures price modeling. *Journal of Mathematical Finance*, *09*, 42–53. https://doi.org/10.4236/jmf.2019.91004

Litzenberger, R., & Rabinowitz, N. (1995). Backwardation in oil futures markets: Theory and empirical evidence. *Journal of Finance*, *50*, 1517–1545.

Mackinnon, J. G. (2010). *Critical values for cointegration tests*. http://www.econ.queensu.ca/faculty/mackinnon/

Maslyuk, S., & Smyth, R. (2009). Cointegration between oil spot and future prices of the same and different grades in the presence of structural change. *Energy Policy*, *37*, 1687–1693. https://doi.org/10.1016/j.enpol.2009.01.013

Miltersen, K. R., Nielsen, J. A., & Sandmann, K. (2004). *The futures market model and no-arbitrage conditions on the volatility long-term investment strategies view project book: Einführung in die stochastik der finanzmärkte view project*. https://www.researchgate.net/publication/228950573

MorningConsult. (2022). The state of consumer banking & payments: How consumers are managing their financial relationships during the covid-19 pandemic.

Movassagh, N., & Modjtahedi, B. (2005). Bias and backwardation in natural gas futures prices. *Journal of Futures Markets*, *25*, 281–308. https://doi.org/10.1002/fut.20151

Nakamoto, S. (2008). Bitcoin: A peer-to-peer electronic cash system. www.bitcoin.org

Neusser, K. (2016). *Time series econometrics*. Springer. http://www.springer.com/series/10099

Nimmagadda, S. S., & Ammanamanchi, P. S. (2019). Bitmex funding correlation with bitcoin exchange rate. http://arxiv.org/abs/1912.03270

Phillips, P. C. B. (1987). Time series regression with a unit root. *Econometrica*, *55*, 277–301.

Pinkdyck, R. S. (2001). The dynamics of commodity spot and futures markets: A primer. *The Energy Journal*, *22*.

Pirrong, C. (2011). *Commodity price dynamics a structural approach*. Cambridge University Press.

Quan, J. (1992). Two-step testing procedure for price discovery role of futures prices. *The Journal of Futures Markets*, *12*, 139–149.

Rau-Bredow, H. (2022). Rau-bredow, hans standard-nutzungsbedingungen: Contango and backwardation in arbitrage-free futures-markets. http://hdl.handle.net/10419/249292

REFCO PRIVATE CLIENT GROUP. (2005). *The complete guide to futures trading what you need to know about the risks and rewards*. John Wiley & Sons.

Riley, E. M. (2014). The cost-of-carry model and volatility : An analysis of gold futures contracts pricing. http://scholarship.richmond.edu/honors-theses

Schmeling, M., Schrimpf, A., & Todorov, K. (2022). Crypto carry. https://ssrn.com/abstract=4268371

Schroder, M. (1999). Changes of numeraire for pricing futures, forwards, and options. *The Review of Financial Studies*, *12*, 1143–1163.

Schumacher, J. M. (2020). *Introduction to financial derivatives*. Open Press TiU. https://digicourses.com/openpresstiu-introduction-to-financial-derivatives/

Schwert, G. W., & Simon, W. E. (1989). Tests for unit roots: A monte carlo investigation. *Journal of Business and Economic Statistics*, *7*, 147–159.

Sheikh, H., Azmathullah, R. M., & Rizwan, F. (2018). Proof-of-work vs proof-of-stake: A comparative analysis and an approach to blockchain consensus mechanism. *International Journal for Research in Applied Science & Engineering Technology (IJRASET)*, *887*, 2321–9653. www.ijraset.com

Shiller, R. (1993). Measuring asset values for cash settlement in derivative markets: Hedonic repeated measures indices and perpetual futures. *The Journal of Finance*, *48*, 911–931.

Stadnytska, T. (2010). Deterministic or stochastic trend: Decision on the basis of the augmented dickey-fuller test. *Methodology*, *6*, 83–92. https://doi.org/10.1027/1614-2241/a000009

Viehmann, J. (2011). Risk premiums in the german day-ahead electricity market. *Energy Policy*, *39*, 386–394. https://doi.org/10.1016/j.enpol.2010.10.016

Werner, A. (2022). *What does strong backwardation tell us about where crude oil prices are headed?* https://wernerantweiler.ca/blog.php?item=2022-03-09

Whelan, K. (2011). *Ma advanced econometrics: Spurious regressions and cointegration.*

White, L. H. (2015). The market for cryptocurrencies. *Cato Journal*, *35*.

Wu, J., Xu, K., Zheng, X., & Chen, J. (2021). Fractional cointegration in bitcoin spot and futures markets. *Journal of Futures Markets*, *41*, 1478–1494. https://doi.org/10.1002/fut.22216

Zeckhauser, R., & Niederhoffer, V. (1983). The performance of market index futures contracts. *Source: Financial Analysts Journal*, *39*, 59–65.

A Appendix

A.1 Quarterly Futures Section

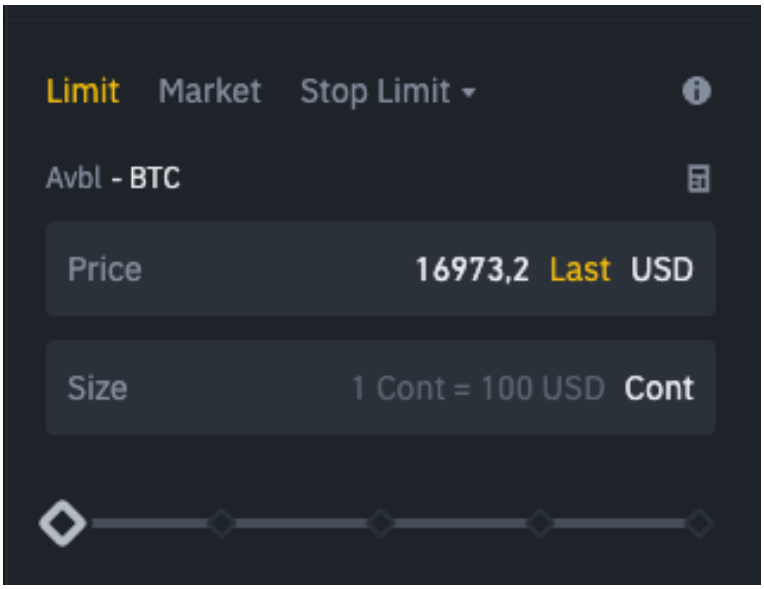

Figure 25: Visual representation of the Binance Coin-M contract size for BTC in the Binance user-interface. We see that $F(t,T)$ is 16793.2, and the contract size is 100 USD. Thus in order to buy 1 unit of $F(t,T)$ we need to long $\frac{16973,2}{100} = 167.932 \approx 168$ contracts. Screenshot from: https://www.binance.com/en/delivery/btcusd_quarter on the 6th of December 2022.

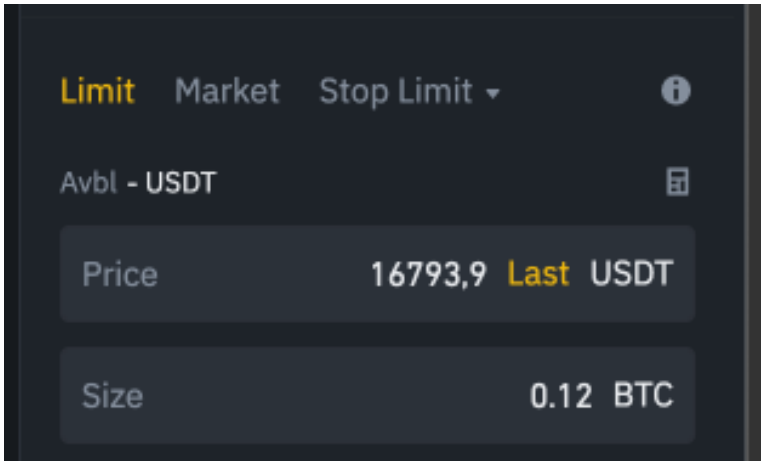

Figure 26: Visual representation of the Binance USD-M contract size for BTC in the Binance user-interface. We see that $F(t,T)$ is 16793.9. If a trader wants to buy 0.12 units worth of $F(t,T)$, that is possible. There is no standardized contract size. The only requirement is that the minimum size is 0.001 BTC. Screenshot from: https://www.binance.com/en/futures/BTCUSDT on the 6th of December 2022.

t	F(t,T)	Futures Type	Position Size (BTC)	Position Size (USD)	Collateral	PnL
0	10000	Coin-M	1 BTC	10000	10000	0
1	12500	Coin-M	1 BTC	12500	15000	5000
2	9000	Coin-M	1 BTC	9000	8000	-2000
3	7500	Coin-M	1 BTC	7500	5000	-5000
4	5000	Coin-M	1 BTC	5000	0	-10000

Table 25: Profit-and-loss (PnL) in USD of a Coin-M position. Note that we make the assumption here that $F(t,T) = S_t$ for $t = 0, 1, 2, 3, 4$.

Tier	Position Bracket (Notional Value in USDT)	Max Leverage	Maintenance Margin Rate	Maintenance Amount (USDT)
1	0 - 375,000	25x	2.00%	0
2	375,000 - 2,000,000	10x	5.00%	11,250
3	2,000,000 - 4,000,000	5x	10.00%	111,250
4	4,000,000 - 10,000,000	4x	12.50%	211,250
5	10,000,000 - 20,000,000	3x	15.00%	461,250
6	20,000,000 - 40,000,000	2x	25.00%	2,461,250
7	40,000,000 - 400,000,000	1x	50.00%	12,461,250

Figure 27: Maximum leverage and maintenance margin per position size interval for BTC USD-M Quarterly Futures. Retrieved from Binance

Tier	Position Bracket (Notional Value in USDT)	Max Leverage	Maintenance Margin Rate	Maintenance Amount (USDT)
1	0 - 50,000	125x	0.40%	0
2	50,000 - 250,000	100x	0.50%	50
3	250,000 - 3,000,000	50x	1.00%	1,300
4	3,000,000 - 15,000,000	20x	2.50%	46,300
5	15,000,000 - 30,000,000	10x	5.00%	421,300
6	30,000,000 - 80,000,000	5x	10.00%	1,921,300
7	80,000,000 - 100,000,000	4x	12.50%	3,921,300
8	100,000,000 - 200,000,000	3x	15.00%	6,421,300
9	200,000,000 - 300,000,000	2x	25.00%	26,421,300
10	300,000,000 - 500,000,000	1x	50.00%	101,421,300

Figure 28: Maximum leverage and maintenance margin per position size interval for BTC USD-M Perpetual Futures. Retrieved from Binance

Figure 29: BTC perpetual futures price and total Coin-M open interest (perpetual and quarterly futures) in 2021 highlighted. The solid (blue) line represents the BTC price, and the candlesticks represent the total Coin-M open interest of BTC perpetual and quarterly futures. Retrieved from https://www.coinalyze.net

Figure 30: BTC perpetual futures prices and total USD-M open interest (perpetual and quarterly futures) in 2021 highlighted. The solid (blue) line represents the BTC price, and the candlesticks represent the total USD-M open interest of BTC perpetual and quarterly futures. Retrieved from https://www.coinalyze.net

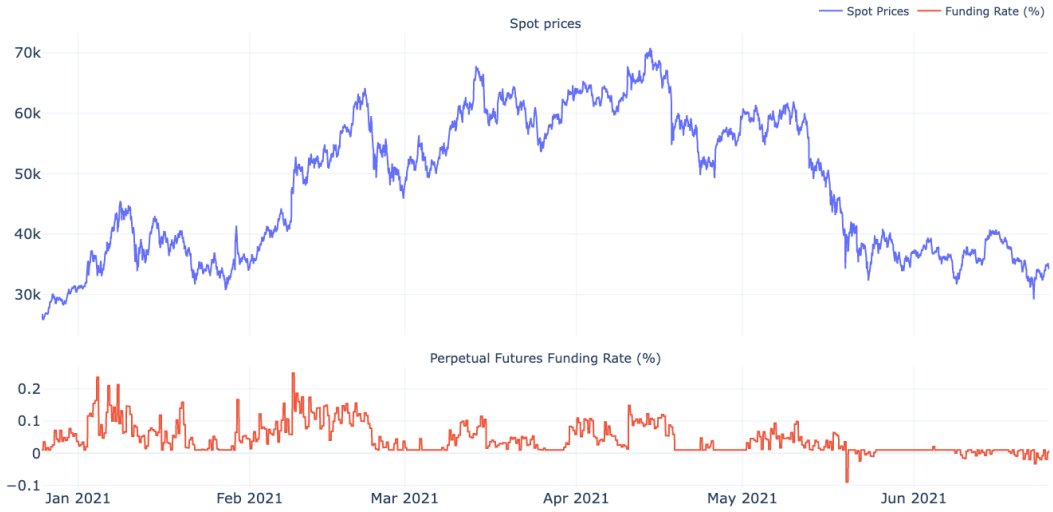

Figure 31: Perperual futures funding rate and Bitcoin spot prices

Component	Explanation
Market Momentum	Price of the S&P 500 above or below its 125-day moving average
Stock Price Strength	Number of stocks at 52-week highs versus those at 52-week lows
Stock Price Breadth	Volume of shares rising versus declining
Put and Call Options	5-day put/call ratio
Market Volatility	Level of the Volatility Index (VIX) above or below its 50-day moving average
Safe Haven Demand	Difference in returns between shocks and bonds over the last 20 days
Junk Bond Demand	Spread in yields of junk bonds versus investment grade

Table 26: Components of the Fear and Greed Index. Each component has an equal weight, from which a value from 0 to 100 is calculated. Retrieved from CNN (2023) https://https://edition.cnn.com/markets/fear-and-greed

Interval	Classification
[0-24]	Extreme Fear
[25-49]	Fear
[50-74]	Greed
[75-100]	Extreme Greed

Table 27: Classification per interval for the Crypto Fear and Greed Index (CFNGI). Retrieved from https://www.alternative.me

Component	Weight
Volatility	29.41%
Market Momentum and Volume	29.41%
Social Media	17.66%
BTC Dominance	11.76%
Google Trends	11.76%

Table 28: Weight per component for the Crypto Fear and Greed Index (CFNGI). Retrieved from https://www.alternative.me

Figure 32: Crypto Fear and Greed Index (CNGI) overlaid with Bitcoin prices. The bar on the right y-axis represents the scores (0-100) of the CFNGI. Red colors imply low values, and green colors imply high values. Retrieved from https://www.lookintobitcoin.com

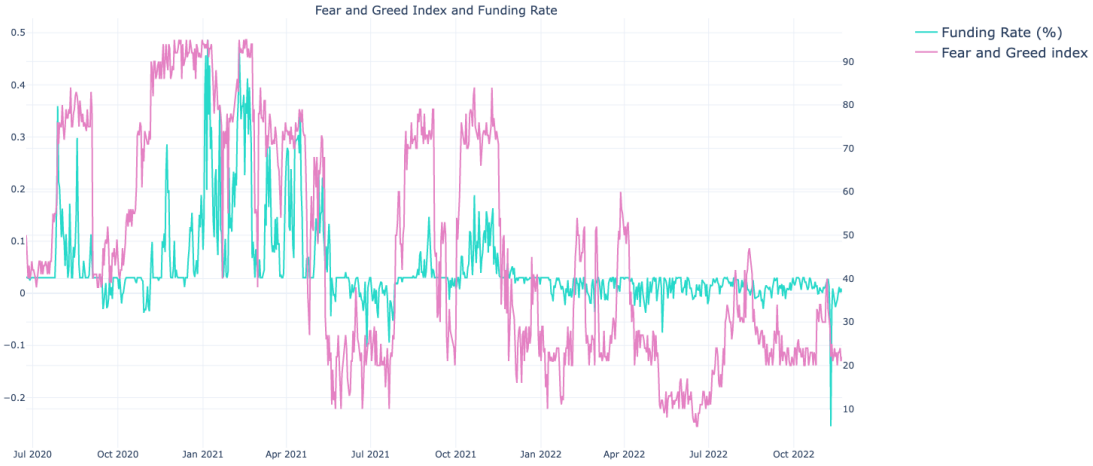

Figure 33: Bitcoin perpetual futures funding rate and Crypto Fear and Greed Index (CFNG).

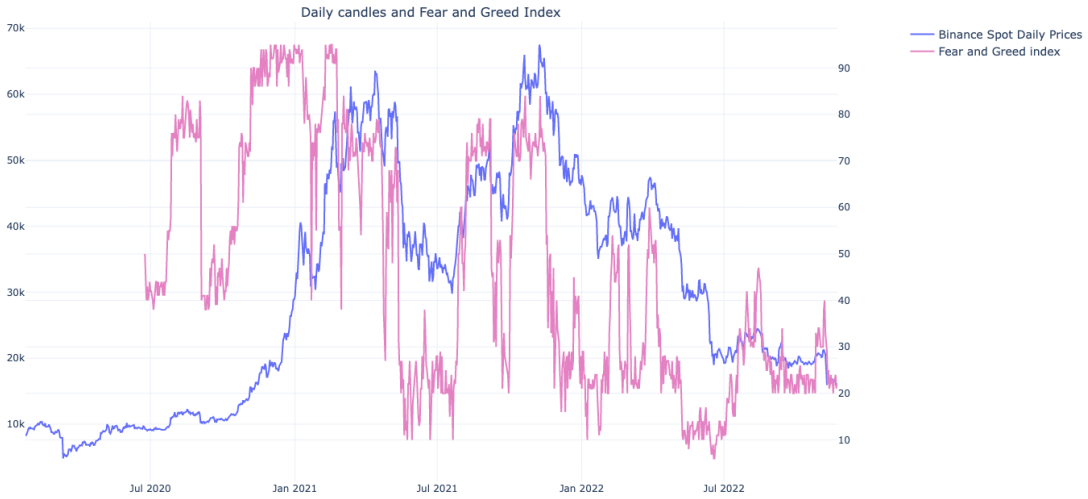

Figure 34: Bitcoin daily spot prices Crypto Fear and Greed Index (CFNG).

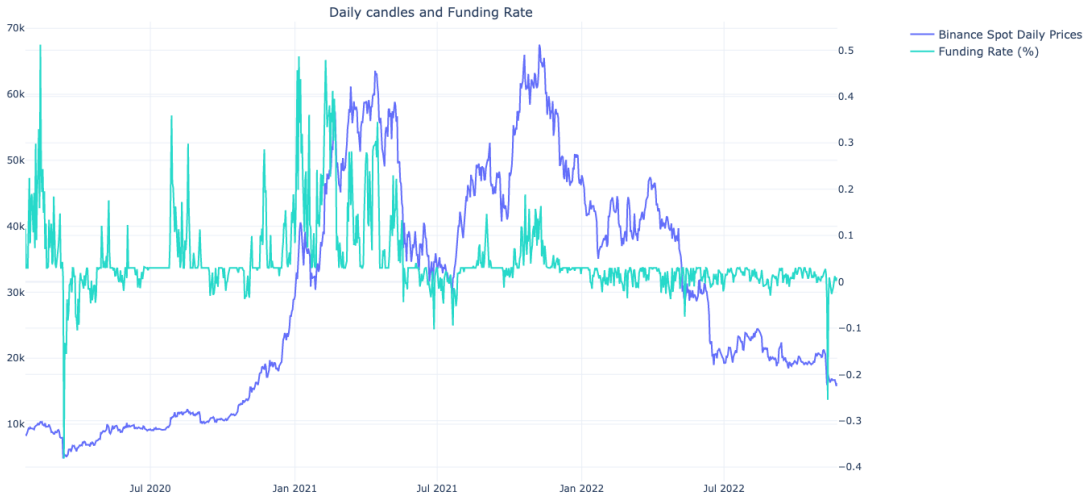

Figure 35: Bitcoin daily spot prices and Bitcoin perpetual futures funding rate plotted.

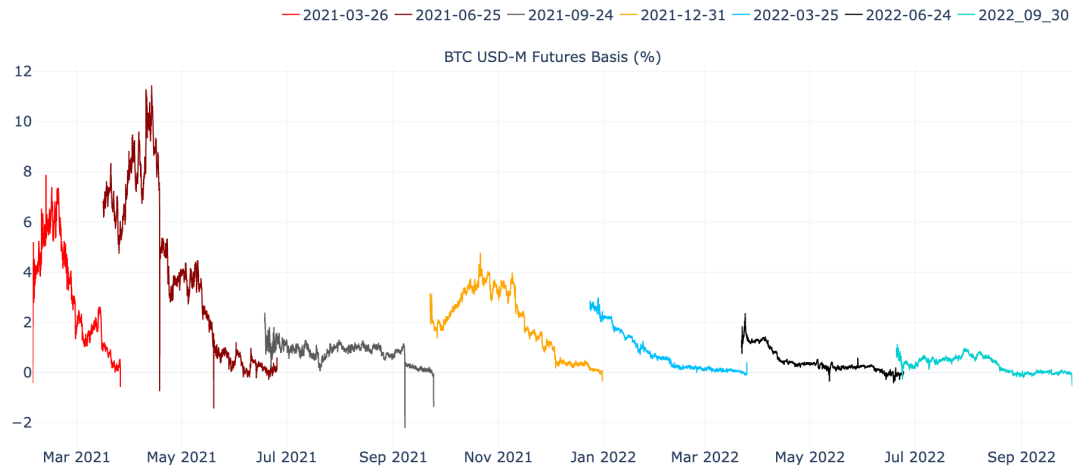

Figure 36: BTC USD-M quarterly futures basis

A.2 Time Series Theory

Figure 37: Swiss Market Index (SWI) price over time as shown by Neusser (2016) (page 8).

Table 10.A.2. Empirical Cumulative Distribution of $\hat{\tau}$ for $\rho = 1$

Sample Size	Probability of a Smaller Value								
n	0.01	0.025	0.05	0.10	0.50	0.90	0.95	0.975	0.99
				$\hat{\tau}$					
25	−2.65	−2.26	−1.95	−1.60	−0.47	0.92	1.33	1.70	2.15
50	−2.62	−2.25	−1.95	−1.61	−0.49	0.91	1.31	1.66	2.08
100	−2.60	−2.24	−1.95	−1.61	−0.50	0.90	1.29	1.64	2.04
250	−2.58	−2.24	−1.95	−1.62	−0.50	0.89	1.28	1.63	2.02
500	−2.58	−2.23	−1.95	−1.62	−0.50	0.89	1.28	1.62	2.01
∞	−2.58	−2.23	−1.95	−1.62	−0.51	0.89	1.28	1.62	2.01
				$\hat{\tau}_\mu$					
25	−3.75	−3.33	−2.99	−2.64	−1.53	−0.37	0.00	0.34	0.71
50	−3.59	−3.23	−2.93	−2.60	−1.55	−0.41	−0.04	0.28	0.66
100	−3.50	−3.17	−2.90	−2.59	−1.56	−0.42	−0.06	0.26	0.63
250	−3.45	−3.14	−2.88	−2.58	−1.56	−0.42	−0.07	0.24	0.62
500	−3.44	−3.13	−2.87	−2.57	−1.57	−0.44	−0.07	0.24	0.61
∞	−3.42	−3.12	−2.86	−2.57	−1.57	−0.44	−0.08	0.23	0.60
				$\hat{\tau}_\tau$					
25	−4.38	−3.95	−3.60	−3.24	−2.14	−1.14	−0.81	−0.50	−0.15
50	−4.16	−3.80	−3.50	−3.18	−2.16	−1.19	−0.87	−0.58	−0.24
100	−4.05	−3.73	−3.45	−3.15	−2.17	−1.22	−0.90	−0.62	−0.28
250	−3.98	−3.69	−3.42	−3.13	−2.18	−1.23	−0.92	−0.64	−0.31
500	−3.97	−3.67	−3.42	−3.13	−2.18	−1.24	−0.93	−0.65	−0.32
∞	−3.96	−3.67	−3.41	−3.13	−2.18	−1.25	−0.94	−0.66	−0.32

Figure 38: Critical values of the Dickey-Fuller distribution. Retrieved from Fuller (1994) (page 641)

A.3 Cointegration Tests

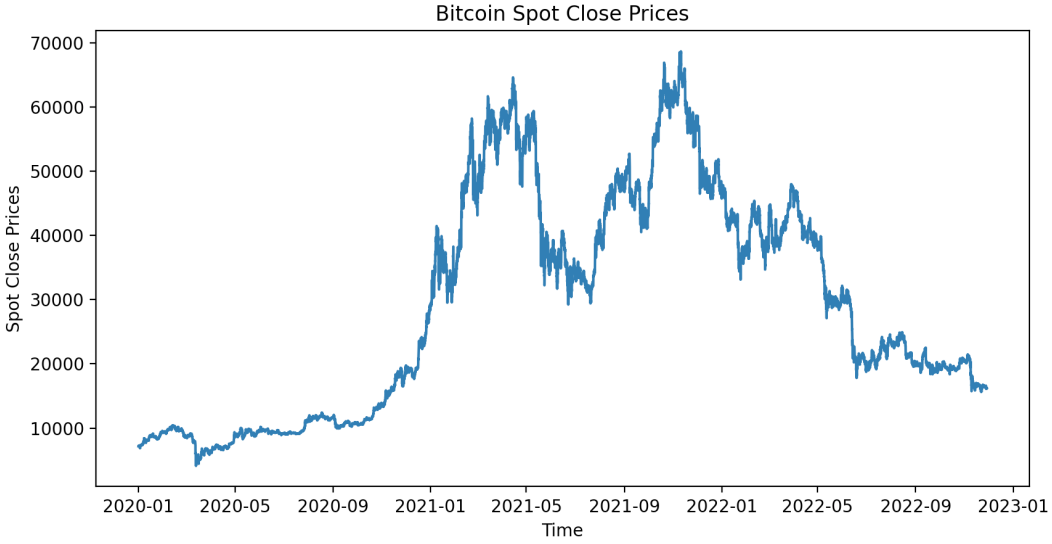

Figure 39: Bitcoin hourly closing prices over our entire testing period

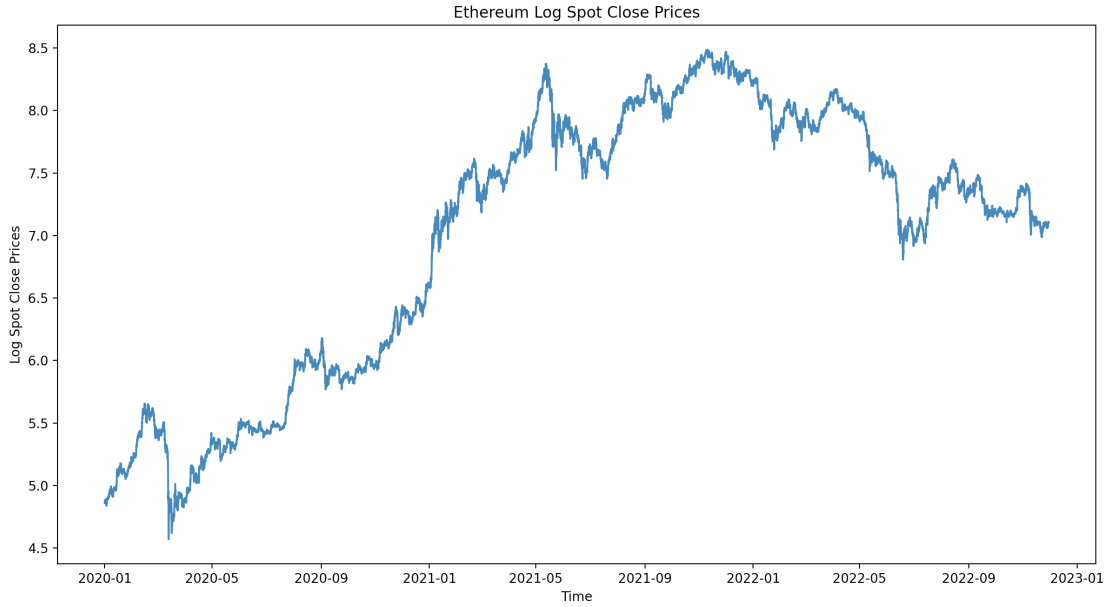

Figure 40: Ethereum hourly log closing prices over our entire testing period

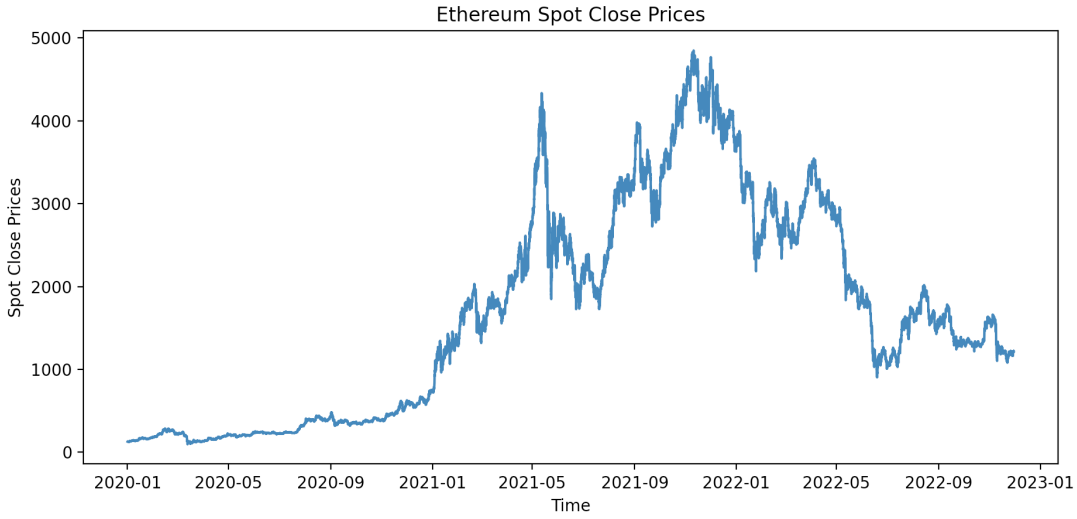

Figure 41: Ethereum hourly closing prices over our entire testing period

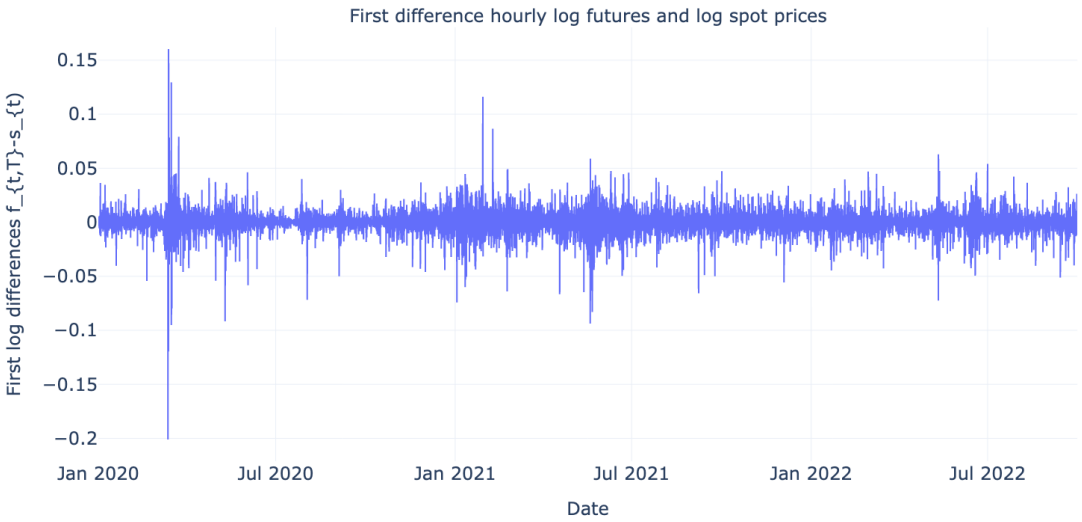

Figure 42: Hourly first differences of BTC log spot prices s, Δs.

Bitcoin Coin-M log price f								
Start Date	End Date	N	γ_{AIC}	$\hat{t}_{AIC}$	p_{AIC}	γ_{BIC}	$\hat{t}_{BIC}$	p_{BIC}
2020-06-30	2020-09-25	2006	1	-1.552	0.508	1	-1.552	0.508
2020-07-01	2020-12-25	3928	2	0.580	0.987	1	0.498	0.985
2020-09-25	2021-03-26	4062	11	-0.979	0.761	0	-0.996	0.754
2020-12-25	2021-06-25	4160	24	-2.018	0.279	0	-2.230	0.195
2021-03-26	2021-09-24	4161	19	-1.482	0.543	4	-1.455	0.555
2021-06-25	2021-12-31	4343	2	-1.791	0.385	0	-1.744	0.408
2021-09-24	2022-03-25	4183	1	-1.242	0.655	0	-1.208	0.670
2021-12-31	2022-06-24	4018	5	-0.051	0.954	0	-0.085	0.951
2022-03-25	2022-09-30	4367	27	-1.519	0.524	0	-1.482	0.542
Bitcoin USD-M log price f								
Start Date	End Date	N	γ_{AIC}	$\hat{t}_{AIC}$	p_{AIC}	γ_{BIC}	$\hat{t}_{BIC}$	p_{BIC}
2021-02-03	2021-03-26	1171	4	-2.737	0.068*	0	-3.176	0.021**
2021-03-16	2021-06-25	2323	11	-0.735	0.838	0	-0.801	0.819
2021-06-18	2021-09-24	2263	0	-1.168	0.687	0	-1.168	0.687
2021-09-22	2021-12-31	2304	2	-1.606	0.481	0	-1.614	0.476
2021-12-24	2022-03-25	2097	0	-2.635	0.086*	0	-2.635	0.086*
2022-03-22	2022-06-24	2166	18	0.304	0.978	0	0.138	0.969
2022-06-20	2022-09-30	2403	2	-2.018	0.278	0	-2.042	0.268
Ethereum Coin-M log price f								
Start Date	End Date	N	γ_{AIC}	$\hat{t}_{AIC}$	p_{AIC}	γ_{BIC}	$\hat{t}_{BIC}$	p_{BIC}
2020-07-24	2020-09-25	1447	1	-3.016	0.033**	0	-3.097	0.027**
2020-08-05	2020-12-25	1954	0	-1.490	0.583	0	-1.490	0.583
2020-09-25	2021-03-26	3331	12	-1.653	0.455	0	-1.755	0.403
2020-12-25	2021-06-25	4157	24	-3.132	0.024**	0	-2.949	0.040**
2021-03-26	2021-09-24	4153	27	-2.151	0.225	0	-2.426	0.135
2021-06-25	2021-12-31	4343	2	-2.163	0.220	0	-2.067	0.258
2021-09-24	2022-03-25	4183	0	-1.407	0.579	0	-1.407	0.579
2021-12-31	2022-06-24	4007	0	0.172	0.971	0	0.172	0.971
2022-03-25	2022-09-30	4367	27	-1.439	0.564	0	-1.470	0.548
Ethereum USD-M log price f								
Start Date	End Date	N	γ_{AIC}	$\hat{t}_{AIC}$	p_{AIC}	γ_{BIC}	$\hat{t}_{BIC}$	p_{BIC}
2021-02-04	2021-03-26	1147	0	-2.033	0.272	0	-2.033	0.272
2021-03-16	2021-06-25	2298	27	-1.490	0.537	0	-1.673	0.445
2021-06-18	2021-09-24	2263	0	-1.039	0.739	0	-1.039	0.739
2021-09-22	2021-12-31	2302	0	-2.480	0.120	0	-2.480	0.120
2021-12-24	2022-03-25	2097	20	-2.476	0.121	0	-2.376	0.149
2022-03-22	2022-06-24	2166	15	0.543	0.986	0	0.349	0.979
2022-06-20	2022-09-30	2403	2	-1.877	0.343	0	-1.869	0.347

Table 29: Results of performing the ADF test on f on Coin-M and USD-M for both Bitcoin and Ethereum. *,** and*** imply a significant test statistic at confidence levels of 0.1,0.05 and 0.01, respectively.

Engle-Granger Test Ethereum Coin-M futures											
$\hat{\alpha}$	$\hat{\beta}$	$\sigma_{\hat{\beta}}$	t_β	p_β	R^2	γ_{AIC}	$\hat{t}_{AIC}$	p_{AIC}	γ_{BIC}	$\hat{t}_{BIC}$	p_{BIC}
2020-07-24 - 2020-09-25 ($N = 1449$)											
-0.026	1.007	0.004	286.253	0.000***	0.983	15	-1.134	0.233	7	-2.358	0.018**
2020-08-05 - 2020-12-25 ($N = 3949$)											
0.364	0.944	0.002	568.879	0.000***	0.994	0	-2.856	0.004***	0	-2.856	0.004***
2020-09-25 - 2021-03-26 ($N = 4062$)											
0.056	0.996	0.000	2187.335	0.000***	0.999	2	-2.777	0.005***	2	-2.777	0.005***
2020-12-25 - 2021-06-25 ($N = 4178$)											
0.385	0.956	0.001	905.433	0.000***	0.995	2	-2.599	0.009***	2	-2.599	0.009**
2021-03-26 - 2021-09-24 ($N = 4176$)											
0.329	0.963	0.003	307.505	0.000***	0.958	31	-1.138	0.232	5	-1.264	0.190
2021-06-25 - 2021-12-31 ($N = 4340$)											
0.089	0.992	0.001	1445.614	0.000***	0.998	6	-1.847	0.062*	5	-1.913	0.053*
2021-09-24 - 2022-03-25 ($N = 4183$)											
-0.710	1.090	0.001	924.960	0.000***	0.995	2	-2.022	0.041**	1	-2.141	0.031**
2021-12-31 - 2022-06-24 ($N = 4009$)											
-0.169	1.023	0.000	2116.475	0.000***	0.999	21	-2.924	0.003***	7	-2.813	0.005***
2022-03-25 - 2022-09-30 ($N = 4395$)											
-0.155	1.021	0.000	2754.753	0.000***	0.999	21	-1.876	0.058*	2	-1.951	0.049**

Table 30: Results of performing the Engle-Granger test on each interval of ETH Coin-M log futures and log spot prices. The left hand side of the table $\hat{\beta}$,$\sigma_{\hat{\beta}}$, t_β and R^2 are parameters corresponding to the OLS regression $f = \beta_1 s + \epsilon$, and the parameters γ_{AIC}, $\hat{t}_{AIC}$, p_{AIC}, γ_{BIC}, $\hat{t}_{BIC}$ and p_{BIC} are parameters corresponding to the Augmented Dickey Fuller (ADF) test. Notice that *, ** and *** imply significant t-statistics at the 10,5, and 1% level, respectively.

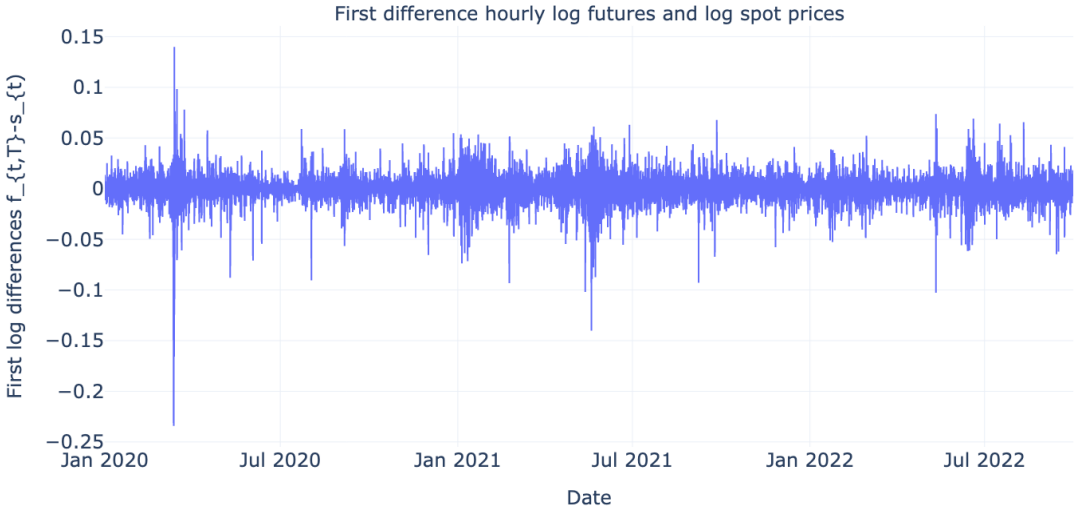

Figure 43: Hourly first differences of log ETH spot prices f_t, Δs_t.

Engle-Granger Test on Bitcoin USD-M futures											
$\hat{\alpha}$	$\hat{\beta}$	$\sigma_{\hat{\beta}}$	t_β	p_β	R^2	γ_{AIC}	$\hat{t}_{AIC}$	p_{AIC}	γ_{BIC}	$\hat{t}_{BIC}$	p_{BIC}
2021-02-03 - 2021-03-26 ($N = 1169$)											
0.792	0.933	0.005	216.411	0.000***	0.976	2	-1.628	0.098	2	-1.628	0.098
2021-03-16 - 2021-06-25 ($N = 2318$)											
-1.335	1.127	0.001	842.000	0.000***	0.997	3	-2.514	0.015**	3	-2.514	0.015**
2021-06-18 - 2021-09-24 ($N = 2259$)											
0.061	0.995	0.000	2187.412	0.000***	1.000	14	-1.795	0.069*	4	-3.674	0.000***
2021-09-22 - 2021-12-31 ($N = 2302$)											
-0.661	1.062	0.001	695.204	0.000***	0.995	8	-1.426	0.144	3	-1.637	0.096*
2021-12-24 - 2022-03-25 ($N = 2097$)											
-0.608	1.0579	0.002	649.394	0.000***	0.995	2	-1.581	0.121	2	-1.581	0.121
2021-03-22 - 2022-06-24 ($N = 2166$)											
-0.152	1.015	0.000	4194.066	0.000***	1.000	15	-2.119	0.033**	5	-2.206	0.026**
2022-06-20 - 2022-09-30 ($N = 2403$)											
-0.249	1.025	0.001	1711.151	0.000***	0.999	3	-3.488	0.000**	3	-3.488	0.000***

Table 31: Results of performing the Engle-Granger test on each interval of BTC USD-M log futures prices and log spot prices. The left hand side of the table $\hat{\beta}$,$\sigma_{\hat{\beta}}$, t_β and R^2 are parameters corresponding to the OLS regression $f = \beta_1 s + \epsilon$, and the parameters γ_{AIC}, $\hat{t}_{AIC}$, p_{AIC}, γ_{BIC}, $\hat{t}_{BIC}$ and p_{BIC} are parameters corresponding to the Augmented Dickey Fuller (ADF) test. Notice that *, ** and *** imply significant t-statistics at the 10,5, and 1% level, respectively.

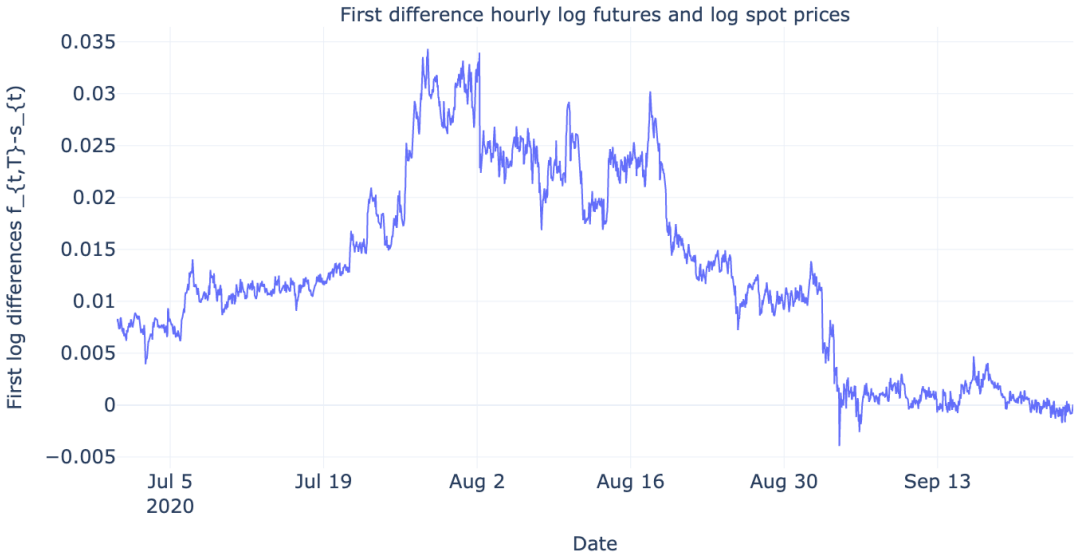

Figure 44: Hourly first differences of Bitcoin Coin-M futures log prices (f) and spot prices s on the interval 2020-06-30 - 2020-09-25

Engle-Granger Test Ethereum USD-M futures											
$\hat{\alpha}$	$\hat{\beta}$	$\sigma_{\hat{\beta}}$	t_β	p_β	R^2	γ_{AIC}	$\hat{t}_{AIC}$	p_{AIC}	γ_{BIC}	$\hat{t}_{BIC}$	p_{BIC}
2021-02-04 - 2021-03-26 ($N = 1147$)											
-0.842	1.118	0.007	128.723	0.000***	0.935	23	-0.546	0.478	3	-1.479	0.130
2021-03-16 - 2021-06-25 ($N = 2318$)											
0.514	0.939	0.003	337.916	0.000***	0.980	3	-1.238	0.198	3	-1.186	0.215
2021-06-18 - 2021-09-24 ($N = 2259$)											
0.040	0.996	0.000	2981.712	0.000***	1.000	13	-3.304	0.001***	3	-4.885	1.768e-6***
2021-09-22 - 2021-12-31 ($N = 2302$)											
0.044	0.997	0.002	466.083	0.000***	0.990	20	-0.376	0.546	1	-0.858	0.346
2021-12-24 - 2022-03-25 ($N = 2097$)											
-0.384	1.049	0.001	1239.101	0.000***	0.999	4	-1.676	0.088*	2	-1.798	0.068*
2021-03-22 - 2022-06-24 ($N = 2166$)											
-0.725	1.010	0.000	4768.318	0.000***	1.000	14	-2.044	0.039**	6	-2.901	0.004***
2022-06-20 - 2022-09-30 ($N = 2403$)											
0.1327	0.981	0.001	1559.43	0.000***	0.999	2	-2.391	0.016**	1	-2.577	0.01***

Table 32: Results of performing the Engle-Granger test on each interval of ETH USD-M log futures prices and log spot prices. The left hand side of the table $\hat{\beta}$,$\sigma_{\hat{\beta}}$, t_β and R^2 are parameters corresponding to the OLS regression $f = \beta_1 s + \epsilon$, and the parameters γ_{AIC}, $\hat{t}_{AIC}$, p_{AIC}, γ_{BIC}, $\hat{t}_{BIC}$ and p_{BIC} are parameters corresponding to the Augmented Dickey Fuller (ADF) test. Notice that *, ** and *** imply significant t-statistics at the 10,5, and 1% level, respectively.

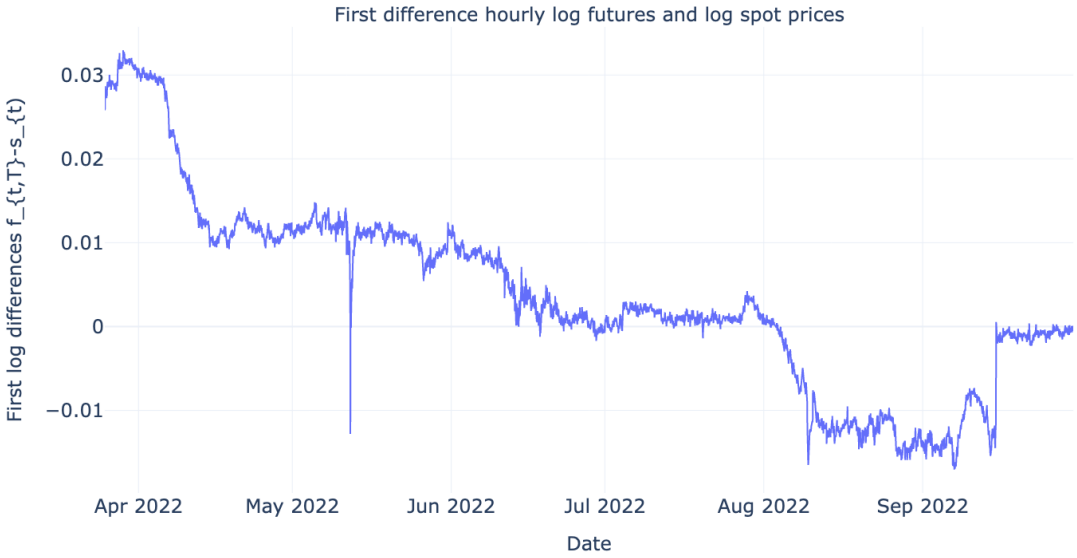

Figure 45: Hourly first differences of Ethereum Coin-M futures log prices (f) and spot prices s on the interval 2022-03-25 - 2022-09-30

ADF test $f-s$ Bitcoin Coin-M futures								
Start Date	End Date	N	γ_{AIC}	$\hat{t}_{AIC}$	p_{AIC}	γ_{BIC}	$\hat{t}_{BIC}$	p_{BIC}
2020-06-30	2020-09-25	2006	12	-0.544	0.883	1	-1.042	0.738
2020-07-01	2020-12-25	3928	18	-1.837	0.362	2	-2.021	0.277
2020-09-25	2021-03-26	4062	18	-1.572	0.498	1	-2.659	0.081*
2020-12-25	2021-06-25	4160	24	-0.919	0.782	2	-1.431	0.567
2021-03-26	2021-09-24	4161	9	-1.084	0.721	7	-1.126	0.704
2021-06-25	2021-12-31	4343	8	-1.382	0.591	3	-1.581	0.492
2021-09-24	2022-03-25	4183	6	-1.051	0.734	2	-1.129	0.703
2021-12-31	2022-06-24	4018	16	-3.152	0.023**	7	-2.841	0.052*
2022-03-25	2022-09-30	4367	26	-2.482	0.120	7	-2.520	0.111
ADF test $f-s$ Bitcoin USD-M futures								
Start Date	End Date	N	γ_{AIC}	$\hat{t}_{AIC}$	p_{AIC}	γ_{BIC}	$\hat{t}_{BIC}$	p_{BIC}
2021-02-03	2021-03-26	1171	9	-0.753	0.832	2	-1.056	0.732
2021-03-16	2021-06-25	2323	4	-1.026	0.743	3	-1.118	0.707
2021-06-18	2021-09-24	2263	14	-2.249	0.188	4	-4.150	0.000***
2021-09-22	2021-12-31	2304	8	-0.231	0.935	2	-0.793	0.821
2021-12-24	2022-03-25	2097	13	-2.417	0.137	3	-2.261	0.185
2022-03-22	2022-06-24	2166	15	-1.620	0.473	5	-1.645	0.459
2022-06-20	2022-09-30	2403	7	-1.855	0.353	3	-2.337	0.160
ADF test $f-s$ Ethereum Coin-M futures								
Start Date	End Date	N	γ_{AIC}	$\hat{t}_{AIC}$	p_{AIC}	γ_{BIC}	$\hat{t}_{BIC}$	p_{BIC}
2020-07-24	2020-09-25	1447	15	-1.043	0.737	0	-2.314	0.167
2020-08-05	2020-12-25	1954	8	-1.626	0.469	1	-1.722	0.419
2020-09-25	2021-03-26	3331	2	-2.912	0.044**	2	-2.912	0.044**
2020-12-25	2021-06-25	4157	2	-1.547	0.510	2	-1.547	0.510
2021-03-26	2021-09-24	4153	29	-1.109	0.712	5	-1.158	0.691
2021-06-25	2021-12-31	4343	6	-1.509	0.529	5	-1.584	0.491
2021-09-24	2022-03-25	4183	5	-1.104	0.713	2	-1.182	0.681
2021-12-31	2022-06-24	4007	16	-3.642	0.005***	10	-3.638	0.012**
2022-03-25	2022-09-30	4367	28	-2.314	0.167	2	-2.201	0.206
ADF test $f-s$ Ethereum USD-M futures								
Start Date	End Date	N	γ_{AIC}	$\hat{t}_{AIC}$	p_{AIC}	γ_{BIC}	$\hat{t}_{BIC}$	p_{BIC}
2021-02-04	2021-03-26	1147	3	-1.278	0.639	0 3	-1.278	0.639
2021-03-16	2021-06-25	2298	12	-0.770	0.827	3	-1.135	0.700
2021-06-18	2021-09-24	2263	13	-2.606	0.092	6	-3.624	0.005
2021-09-22	2021-12-31	2302	20	-0.586	0.874	1	-1.089	0.719
2021-12-24	2022-03-25	2097	16	-3.368	0.012**	10	-2.914	0.044**
2022-03-22	2022-06-24	2166	14	-1.784	0.388	6	-2.396	0.143
2022-06-20	2022-09-30	2403	2	-1.984	0.294	2	-1.984	0.294

Table 33: Results of performing the ADF test on $f-s$ for both assets on Coin-M and USD-M futures. *,** and*** imply a significant test statistic at confidence levels of 0.1,0.05 and 0.01, respectively.

ADF test $\tilde{r}$ on Coin-M intervals								
Start Date	End Date	N	γ_{AIC}	$\hat{t}_{AIC}$	p_{AIC}	γ_{BIC}	$\hat{t}_{BIC}$	p_{BIC}
2020-06-30	2020-09-25	2006	0	- 2.480	0.120	0	- 2.480	0.120
2020-07-01	2020-12-25	3928	23	-2.121	0.236	23	-2.121	0.236
2020-09-25	2021-03-26	4062	23	-1.041	0.738	23	-1.041	0.738
2020-12-25	2021-06-25	4160	23	-1.613	0.476	23	-1.613	0.476
2021-03-26	2021-09-24	4161	23	-1.480	0.543	0	-1.693	0.435
2021-06-25	2021-12-31	4343	23	-1.329	0.616	23	-1.329	0.616
2021-09-24	2022-03-25	4183	0	-0.671	0.854	0	-0.671	0.854
2021-12-31	2022-06-24	4018	0	0.168	0.970	0	0.168	0.970
2022-03-25	2022-09-30	4367	24	2.485	0.999	0	2.361	0.999
ADF test $\tilde{r}$ on USD-M intervals								
Start Date	End Date	N	γ_{AIC}	$\hat{t}_{AIC}$	p_{AIC}	γ_{BIC}	$\hat{t}_{BIC}$	p_{BIC}
2021-02-03	2021-03-26	1171	23	-0.899	0.788	23	-0.899	0.788
2021-03-16	2021-06-25	2323	23	-2.145	0.225	23	-2.145	0.225
2021-06-18	2021-09-24	2263	0	-0.892	0.791	4 0	-0.892	0.791
2021-09-22	2021-12-31	2304	23	0.360	0.980	23	0.360	0.980
2021-12-24	2022-03-25	2097	23	-0.08	0.951	0	-0.602	0.871
2022-03-22	2022-06-24	2166	0	1.078	0.995	0	1.078	0.995
2022-06-20	2022-09-30	2403	24	1.765	0.998	0	1.705	0.998

Table 34: Results of performing the ADF test on $\tilde{r}$ on the corresponding intervals for Coin-M and USD-M futures. *,** and*** imply a significant test statistic at confidence levels of 0.1,0.05 and 0.01, respectively.

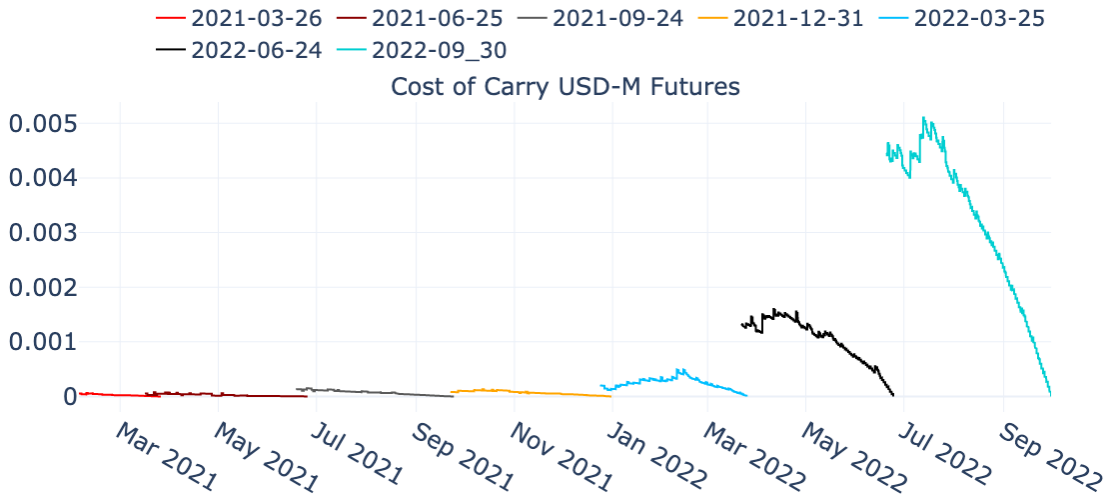

Figure 46: Cost of Carry ($r_{t,T}(T-t)$) per interval of USD-M futures. The declining cost of carry throughout the interval can be explained by $(T-t)$ getting smaller as t increases.

Ethereum Coin-M futures Engle Granger test using cost-of-carry for investment assets											
$\hat{\alpha}$	$\hat{\beta}$	$\sigma_{\hat{\beta}}$	t_β	p_β	R^2	γ_{AIC}	$\hat{t}_{AIC}$	p_{AIC}	γ_{BIC}	$\hat{t}_{BIC}$	p_{BIC}
2020-06-30 - 2020-09-25 ($N = 2008$)											
-0.004	186.893	3.158	59.172	0.000***	0.708	12	-3.311	0.001***	0	-4.879	1.816e-06***
2020-08-05 - 2020-12-25 ($N = 3949$)											
0.002	99.770	0.937	106.494	0.000***	0.853	8	-3.405	0.001***	0	-4.445	1.19e-5***
2020-09-25 - 2021-03-26 ($N = 4062$)											
0.028	23.404	1.737	13.473	0.000***	0.051	2	-2.946	0.003***	2	-2.946	0.003***
2020-12-25 - 2021-06-25 ($N = 4178$)											
0.033	124.396	2.667	46.648	0.000***	0.343	2	-2.455	0.013**	2	-2.455	0.013**
2021-03-26 - 2021-09-24 ($N = 4176$)											
-0.028	627.731	9.363	67.046	0.000***	0.518	7	-2.048	0.038**	3	-2.340	0.018**
2021-06-25 - 2021-12-31 ($N = 4340$)											
0.009	96.237	2.133	45.128	0.000***	0.319	06	-2.839	0.004***	5	-2.864	0.004***
2021-09-24 - 2022-03-25 ($N = 4183$)											
0.057	-75.253	1.686	-44.631	0.000***	0.323	5	-0.023	0.677	1	-0.0224	0.605
2021-12-31 - 2022-06-24 ($N = 4024$)											
0.010	0.331	0.280	1.185	0.236	0.000	16	-2.859	0.004***	2	-2.097	0.034**
2022-03-25 - 2022-09-30 ($N = 4395$)											
-0.013	3.475	0.087	39.721	0.000***	0.264	28	-2.146	0.031**	2	-2.225	0.025**

Table 35: Results of performing the Engle-Granger test on ETH Coin-M futures using the cost of carry model for investment assets. The left hand side of the table $\hat{\beta}$,$\sigma_{\hat{\beta}}$, t_β and R^2 are parameters corresponding to the OLS regression $f - s = \alpha + \beta\tilde{r} + \epsilon$, and the parameters γ_{AIC}, $\hat{t}_{AIC}$, p_{AIC}, γ_{BIC}, $\hat{t}_{BIC}$ and p_{BIC} are parameters corresponding to the Augmented Dickey Fuller (ADF) test. Notice that *, ** and *** imply significant t-statistics at the 10,5, and 1% level, respectively.

Bitcoin USD-M futures Engle Granger test using cost-of-carry for investment assets											
$\hat{\alpha}$	$\hat{\beta}$	$\sigma_{\hat{\beta}}$	t_β	p_β	R^2	γ_{AIC}	$\hat{t}_{AIC}$	p_{AIC}	γ_{BIC}	$\hat{t}_{BIC}$	p_{BIC}
2021-02-03 - 2021-03-26 ($N = 1169$)											
0.004	954.113	19.166	49.781	0.000***	0.680	3	-3.378	0.001***	1	-3.931	9.593e-5***
2021-03-16 - 2021-06-25 ($N = 2318$)											
0.002	1269.269	21.449	59.175.000	0.000***	0.602	24	-3.300	0.0001***	23	-3.424	0.001***
2021-06-18 - 2021-09-24 ($N = 2259$)											
0.004	58.718	1.421	41.331	0.000***	0.431	14	-2.905	0.004***	4	-4.937	1.400e-6***
2021-09-22 - 2021-12-31 ($N = 2302$)											
-0.003	318.375	3.733	85.285	0.000***	0.760	23	-2.605	0.009***	1	-3.336	0.001***
2021-12-24 - 2022-03-25 ($N = 2097$)											
0.010	-9.922	1.736	-5.715	0.000***	0.015	12	-2.002	0.043**	3	-2.200	0.026**
2021-03-22 - 2022-06-24 ($N = 2166$)											
-0.003	6.801	0.191	35.628	0.000***	0.370	15	-2.020	0.042**	4	-2.153	0.030**
2022-06-20 - 2022-09-30 ($N = 2403$)											
-0.002	1.604	0.028	57.803	0.000***	0.582	6	-3.098	0.002***	3	-3.563	0.000***

Table 36: Results of performing the Engle-Granger test on each interval of BTC USD-M futures using the cost of carry model for investment assets. The left hand side of the table $\hat{\beta}$,$\sigma_{\hat{\beta}}$, t_β and R^2 are parameters corresponding to the OLS regression $f - s = \alpha + \beta\tilde{r} + \epsilon$, and the parameters γ_{AIC}, $\hat{t}_{AIC}$, p_{AIC}, γ_{BIC}, $\hat{t}_{BIC}$ and p_{BIC} are parameters corresponding to the Augmented Dickey Fuller (ADF) test. Notice that *, ** and *** imply significant t-statistics at the 10,5, and 1% level, respectively.

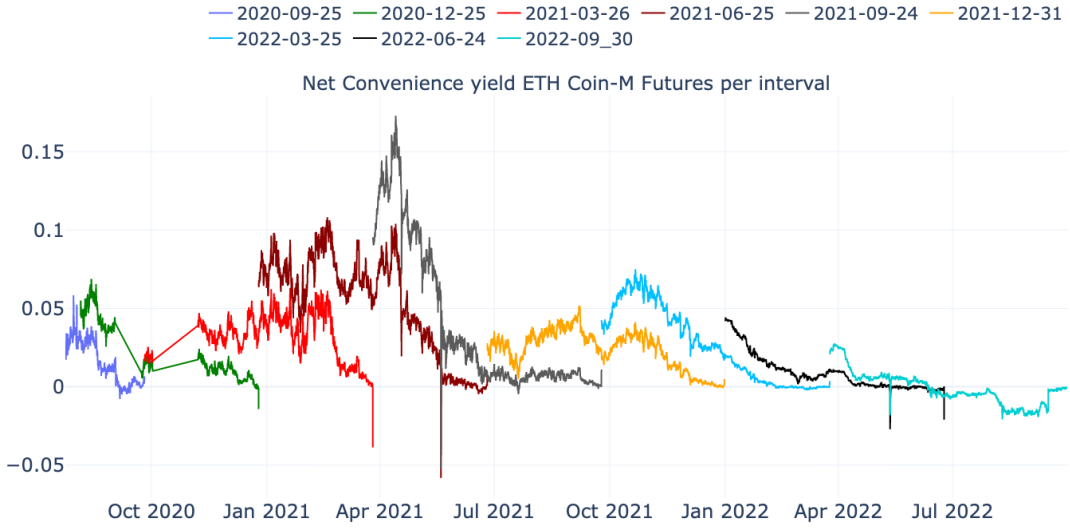

Figure 47: Plot of the net convenience yield for Ethereum Coin-M futures

Ethereum USD-M futures Engle-Granger test using cost-of-carry for investment assets											
$\hat{\alpha}$	$\hat{\beta}$	$\sigma_{\hat{\beta}}$	t_β	p_β	R^2	γ_{AIC}	$\hat{t}_{AIC}$	p_{AIC}	γ_{BIC}	$\hat{t}_{BIC}$	p_{BIC}
2021-02-04 - 2021-03-26 ($N = 1147$)											
0.001	1216.249	27.956	43.506	0.000***	0.623	3	-2.912	0.003***	2	-3.086	0.002***
2021-03-16 - 2021-06-25 ($N = 2318$)											
-0.001	1429.699	23.524	60.775	0.000***	0.615	24	-3.346	0.001***	23	-3.514	0.000***
2021-06-18 - 2021-09-24 ($N = 2259$)											
0.005	55.803	1.590	35.096	0.000***	0.353	12	-4.102	4.873e-05	3	-5.717	3.717e-8***
2021-09-22 - 2021-12-31 ($N = 2302$)											
-0.003	339.693	3.401	99.881	0.000***	0.813	23	-3.357	0.001***	1	-4.117	4.592
2021-12-24 - 2022-03-25 ($N = 2097$)											
0.011	-14.226	1.857	-7.659	0.000***	0.027	16	-2.534	0.011**	4	-2.263	0.022*
2021-03-22 - 2022-06-24 ($N = 2166$)											
-0.003	6.979	0.3214	32.602	0.000***	0.329	6	-2.724	0.006***	5	-2.434	0.014**
2022-06-20 - 2022-09-30 ($N = 2403$)											
-0.01	1.815	0.082	22.075	0.000***	0.169	2	-2.007	0.0428**	2	-2.007	0.042**

Table 37: Results of performing the Engle-Granger test on each interval of Ethereum USD-M futures using the cost of carry model for investment assets. The left hand side of the table $\hat{\beta}$,$\sigma_{\hat{\beta}}$, t_β and R^2 are parameters corresponding to the OLS regression $f - s = \alpha + \beta\tilde{r} + \epsilon$, and the parameters γ_{AIC}, $\hat{t}_{AIC}$, p_{AIC}, γ_{BIC}, $\hat{t}_{BIC}$ and p_{BIC} are parameters corresponding to the Augmented Dickey Fuller (ADF) test. Notice that *, ** and *** imply significant t-statistics at the 10,5, and 1% level, respectively.

Figure 48: Plot of the net convenience yield for Bitcoin USD-M futures

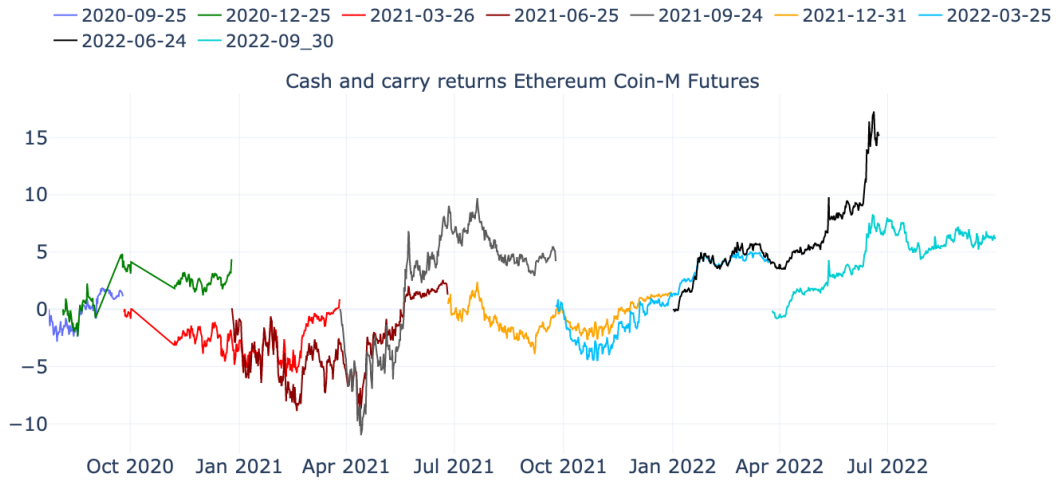

Figure 49: Returns in percentage of the cash and carry strategy for Ethereum Coin-M futures

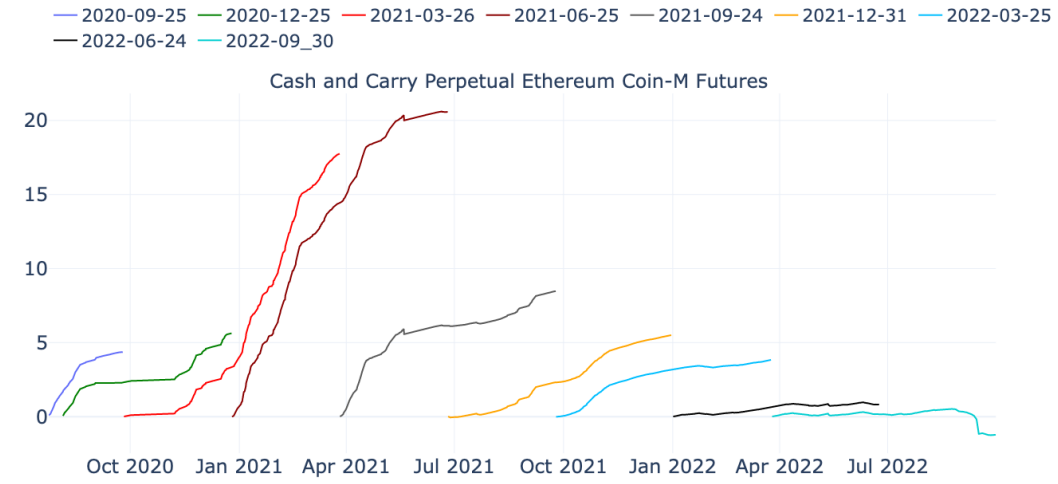

Figure 50: Returns in percentage of the cash and carry strategy for Ethereum Coin-M perpetual futures

Bitcoin Coin-M			*Ethereum Coin-M*		
2020-06-30 - 2020-09-25			**2020-06-30 - 2020-09-25**		
Type	Return (%)	Max Drawdown (%)	Type	Return (%)	Max Drawdown (%)
Quarterly	0.763	2.698	Quarterly	1.131	2.824
Perpetual	3.378	0.997	Perpetual	4.366	0.978
2020-08-05 - 2020-12-25			**2020-08-05 - 2020-12-25**		
Type	Return (%)	Max Drawdown (%)	Type	Return (%)	Max Drawdown (%)
Quarterly	1.046	4.800	Quarterly	4.378	2.355
Perpetual	6.045	0.998	Perpetual	5.632	0.990
2020-09-25 - 2021-03-26			**2020-09-25 - 2021-03-26**		
Type	Return (%)	Max Drawdown (%)	Type	Return (%)	Max Drawdown (%)
Quarterly	1.245	5.207	Quarterly	0.876	5.892
Perpetual	14.247	0.998	Perpetual	17.758	0.999
2020-12-25 - 2021-06-25			**2020-12-25 - 2021-06-25**		
Type	Return (%)	Max Drawdown (%)	Type	Return (%)	Max Drawdown (%)
Quarterly	5.813	7.234	Quarterly	1.274	8.896
Perpetual	16.767	0.998	Perpetual	20.585	0.999
2021-03-26 - 2021-09-24			**2021-03-26 - 2021-09-24**		
Type	Return (%)	Max Drawdown (%)	Type	Return (%)	Max Drawdown (%)
Quarterly	12.000	9.410	Quarterly	4.200	10.999
Perpetual	6.528	0.998	Perpetual	8.472	0.998
2021-06-25 - 2021-12-31			**2021-06-25 - 2021-12-31**		
Type	Return (%)	Max Drawdown (%)	Type	Return (%)	Max Drawdown (%)
Quarterly	2.217	2.570	Quarterly	1.378	3.911
Perpetual	4.869	1.048	Perpetual	5.503	1.010
2021-09-24 - 2022-03-25			**2021-09-24 - 2022-03-25**		
Type	Return (%)	Max Drawdown (%)	Type	Return (%)	Max Drawdown (%)
Quarterly	3.992	4.680	Quarterly	4.029	4.505
Perpetual	4.268	0.999	Perpetual	3.834	1.003
2021-12-31 - 2022-06-24			**2021-12-31 - 2022-06-24**		
Type	Return (%)	Max Drawdown (%)	Type	Return (%)	Max Drawdown (%)
Quarterly	10.236	0.071	Quarterly	15.254	-0.164
Perpetual	1.445	0.993	Perpetual	0.807	0.989
2022-03-25 - 2022-09-30			**2022-03-25 - 2022-09-30**		
Type	Return (%)	Max Drawdown (%)	Type	Return (%)	Max Drawdown (%)
Quarterly	5.722	0.844	Quarterly	6.122	0.812
Perpetual	1.648	1.000	Perpetual	-1.228	3.314

Table 38: Comparison between cash-and-carry strategies for Quarterly and Perpetual Coin-M futures for each interval (note that the perpetual has no interval but it is analyzed in the same time periods as the quarterly futures to give a more fair comparison).

Bitcoin USD-M			*Ethereum USD-M*		
2021-02-04 - 2021-03-26			**2021-02-04 - 2021-03-26**		
Type	Return (%)	Max Drawdown (%)	Type	Return (%)	Max Drawdown (%)
Quarterly	-0.725	-7.549	Quarterly	6.171	3.742
Perpetual	6.485	0.998	Perpetual	7.545	0.982
2021-03-16 - 2021-06-25			**2021-03-16 - 2021-06-25**		
Type	Return (%)	Max Drawdown (%)	Type	Return (%)	Max Drawdown (%)
Quarterly	11.073	4.733	Quarterly	6.898	5.711
Perpetual	5.8755	0.994	Perpetual	6.877	0.964
2021-06-18 - 2021-09-24			**2021-06-18 - 2021-09-24**		
Type	Return (%)	Max Drawdown (%)	Type	Return (%)	Max Drawdown (%)
Quarterly	2.217	2.570	Quarterly	1.225	-0.209
Perpetual	4.869	1.048	Perpetual	2.379	1.019
2021-09-22 - 2021-12-31			**2021-09-22 - 2021-12-31**		
Type	Return (%)	Max Drawdown (%)	Type	Return (%)	Max Drawdown (%)
Quarterly	2.217	2.570	Quarterly	3.377	1.744
Perpetual	4.869	1.048	Perpetual	3.222	0.996
2021-12-24 - 2022-03-25			**2021-12-24 - 2022-03-25**		
Type	Return (%)	Max Drawdown (%)	Type	Return (%)	Max Drawdown (%)
Quarterly	3.274	0.084	Quarterly	4.06	0.033
Perpetual	0.843	0.999	Perpetual	0.765	0.987
2022-03-22 - 2022-06-24			**2022-03-22 - 2022-06-24**		
Type	Return (%)	Max Drawdown (%)	Type	Return (%)	Max Drawdown (%)
Quarterly	2.263	1.289	Quarterly	3.016	-0.838
Perpetual	0.789	0.986	Perpetual	0.211	0.973
2022-06-20 - 2022-09-30			**2022-06-20 - 2022-09-30**		
Type	Return (%)	Max Drawdown (%)	Type	Return (%)	Max Drawdown (%)
Quarterly	1.556	0.170	Quarterly	1.247	0.053
Perpetual	0.926	1.001	Perpetual	-1.376	4.645

Table 39: Comparison between cash-and-carry strategies for Quarterly and Perpetual USD-M futures for each interval (note that the perpetual has no interval but it is analyzed in the same time periods as the quarterly futures to give a more fair comparison).

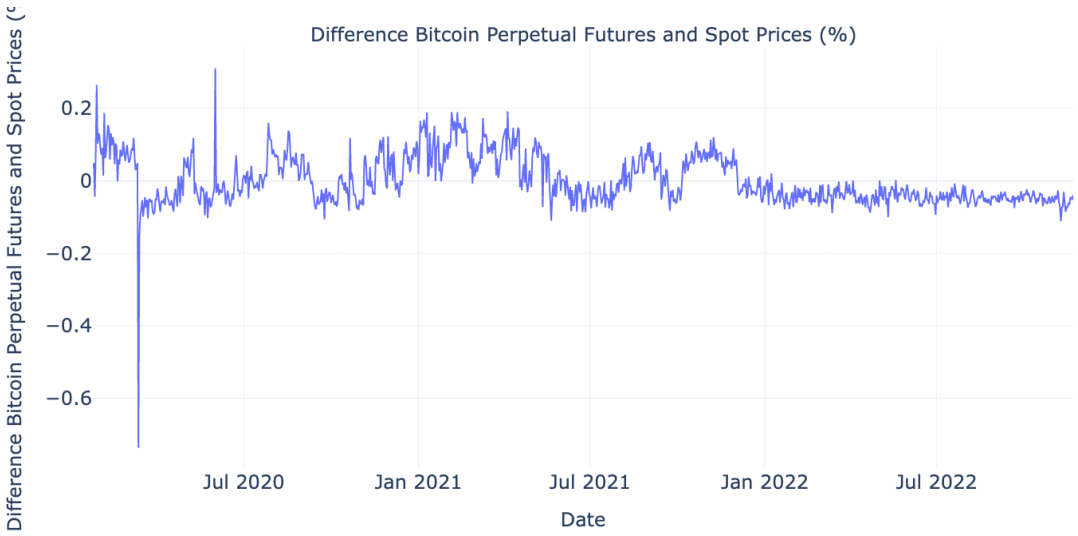

Figure 51: Difference in percentage between Bitcoin Perpetual Futures and Spot Price.

First Difference Bitcoin Perpetual Futures Funding Rate (Δr^f)								
Start Date	End Date	N	γ_{AIC}	$\hat{t}_{AIC}$	p_{AIC}	γ_{BIC}	$\hat{t}_{BIC}$	p_{BIC}
2020-01-01	2022-09-30	2982	28	-14.414	8.120e-27***	7	-27.905	0.000***
First Difference Ethereum Perpetual Futures Funding Rate (Δr^f)								
Start Date	End Date	N	γ_{AIC}	$\hat{t}_{AIC}$	p_{AIC}	γ_{BIC}	$\hat{t}_{BIC}$	p_{BIC}
2020-01-01	2022-09-30	2982	28	-15.656	1.571e-28***	9	-25.117	0.000***

Table 40: Augmented Dickey-Fuller test on the first difference of Bitcoin and Ethereum funding rates for the entire sample period. The test is used to assess whether a unit root is present in funding rates. The null hypothesis (H0) is a unit root present, where the alternative (H1), is that no unit root is present. Note that for the p-value, we have that *** is statistically significant at the 1% level.

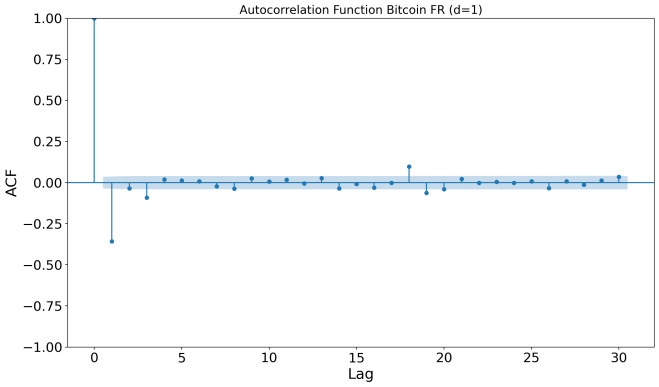

(a) Autocorrelation Function (ACF) for the first-differenced Bitcoin funding rate

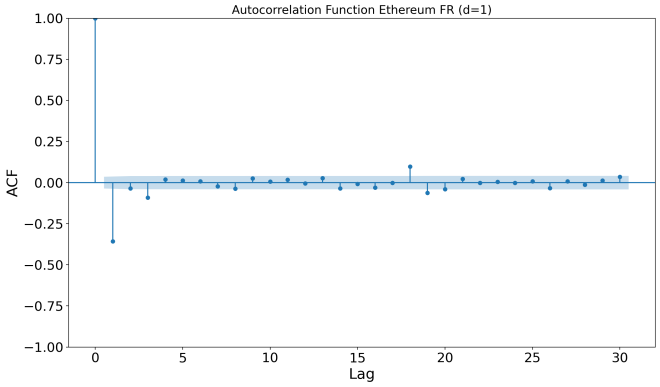

(b) Autocorrelation Function (ACF) for the first-differenced Ethereum funding rate

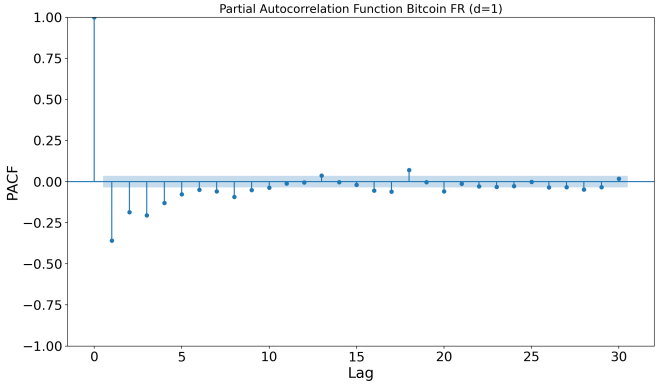

(c) Partial Autocorrelation Function (PACF) for the first-differenced Bitcoin funding rate

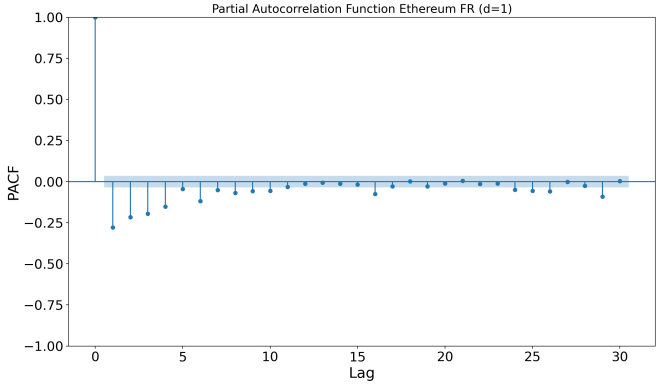

(d) Partial Autocorrelation Function (PACF) for the first-differenced Ethereum funding rate

Figure 52: (Partial) Autocorrelation Function for the Bitcoin and Ethereum USD-M first-differenced funding rate

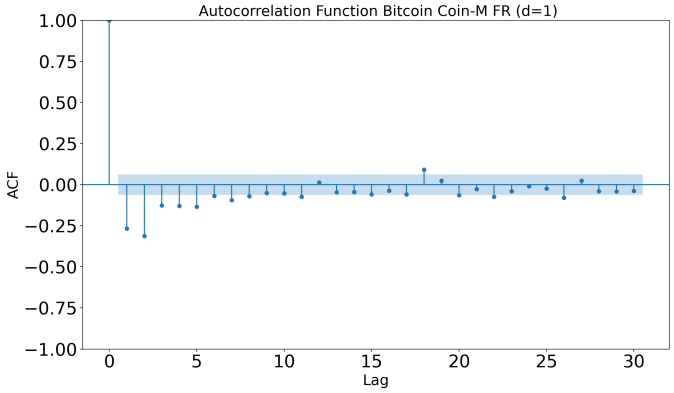

(a) Autocorrelation Function (ACF) for the first-differenced Bitcoin Coin-M funding rate

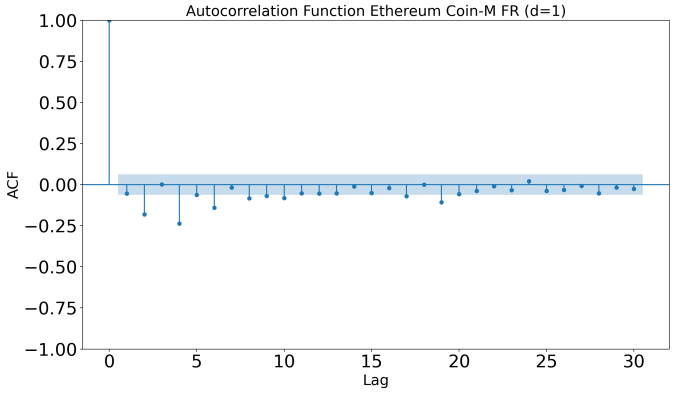

(b) Autocorrelation Function (ACF) for the first-differenced Ethereum Coin-M funding rate

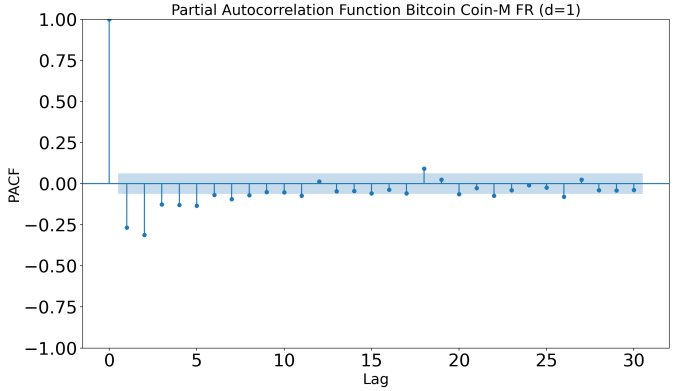

(c) Partial Autocorrelation Function (PACF) for the first-differenced Bitcoin Coin-M funding rate

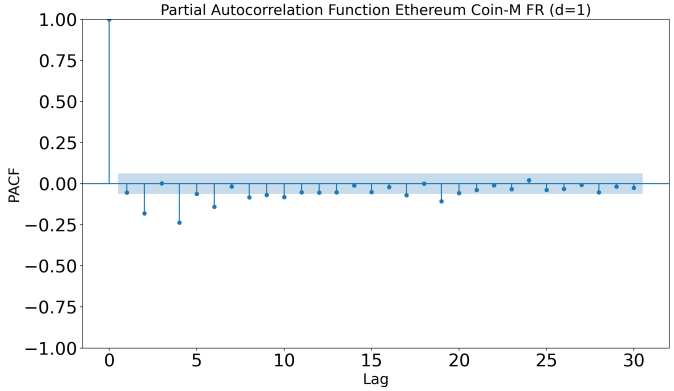

(d) Partial Autocorrelation Function (PACF) for the first-differenced Ethereum Coin-M funding rate

Figure 53: (Partial) Autocorrelation Function for the Bitcoin and Ethereum Coin-M first-differenced funding rate

ADF test $(r^{p_f} - \tilde{r})$ *on Coin-M intervals*								
Start Date	End Date	N	γ_{AIC}	$\hat{t}_{AIC}$	p_{AIC}	γ_{BIC}	$\hat{t}_{BIC}$	p_{BIC}
2020-06-30	2020-09-25	2006	8	- 2.161	0.221	0	- 1.908	0.328
2020-07-01	2020-12-25	3928	15	-2.852	0.051*	15	-2.852	0.051*
2020-09-25	2021-03-26	4062	23	-3.095	0.027**	8	-3.972	0.001***
2020-12-25	2021-06-25	4160	23	-2.727	0.069	23	-2.727	0.069
2021-03-26	2021-09-24	4161	0	-2.400	0.142	0	-2.400	0.142
2021-06-25	2021-12-31	4343	0	-2.127	0.185	0	-2.127	0.185
2021-09-24	2022-03-25	4183	0	-2.542	0.106	0	-2.542	0.106
2021-12-31	2022-06-24	4018	15	-5.032	1.914e-5***	0	-5.311	5.207e-6***
2022-03-25	2022-09-30	4367	24	-2.432	0.107	0	-2.532	0.101
ADF test $(r^{p_f} - \tilde{r})$ *on USD-M intervals*								
Start Date	End Date	N	γ_{AIC}	$\hat{t}_{AIC}$	p_{AIC}	γ_{BIC}	$\hat{t}_{BIC}$	p_{BIC}
2021-02-03	2021-03-26	1171	8	-2.161	0.221	0	-1.908	0.328
2021-03-16	2021-06-25	2323	15	-1.876	0.328	15	-1.876	0.328
2021-06-18	2021-09-24	2263	0	-0.761	0.853	0	-0.761	0.853
2021-09-22	2021-12-31	2304	0	-2.312	0.153	0	-2.312	0.153
2021-12-24	2022-03-25	2097	23	-1.986	0.274	0	-1.912	0.253
2022-03-22	2022-06-24	2166	24	1.765	0.998	0	1.705	0.998
2022-06-20	2022-09-30	2403	24	-2.102	0.076*	0	-2.076	0.079*

Table 41: Results of performing the ADF test on $(r^{p_f} - \tilde{r})$ on the corresponding intervals for Coin-M and USD-M futures. *,** and*** imply a significant test statistic at confidence levels of 0.1,0.05 and 0.01, respectively.

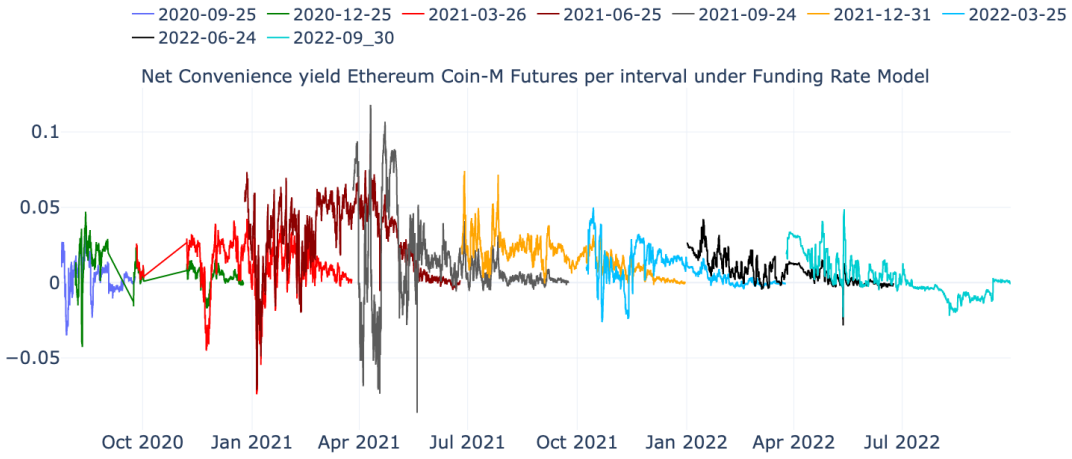

Figure 54: Net convenience yield δ Ethereum Coin-M futures under the funding rate cost-of-carry model.

Engle-Granger test Ethereum Coin-M futures funding rate model											
$\hat{\alpha}$	$\hat{\beta}$	$\sigma_{\hat{\beta}}$	t_β	p_β	R^2	γ_{AIC}	$\hat{t}_{AIC}$	p_{AIC}	γ_{BIC}	$\hat{t}_{BIC}$	p_{BIC}
2020-06-30 - 2020-09-25 ($N = 2008$)											
0.008	0.636	0.017	36.565	0.000***	0.483	10	-2.947	0.003***	3	-3.015	0.002***
2020-08-05 - 2020-12-25 ($N = 3949$)											
0.009	0.9311	0.017	54.144	0.000***	0.603	15	-3.664	0.001***	0	-4.797	1.161e-6***
2020-09-25 - 2021-03-26 ($N = 4062$)											
0.023	0.422	0.01	42.776	0.000***	0.355	2	-4.483	1.014e-5***	1	-4.695	4.079e-6***
2020-12-25 - 2021-06-25 ($N = 4178$)											
0.034	0.798	0.013	61.835	0.000***	0.479	24	-3.092	0.002***	2	-3.921	9.965e-5***
2021-03-26 - 2021-09-24 ($N = 4176$)											
0.018	0.800	0.008	96.954	0.000***	0.694	28	-4.666	4.604e-6***	2	-4.477	1.039e-5***
2021-06-25 - 2021-12-31 ($N = 4340$)											
0.02	0.582	0.016	36.265	0.000***	0.234	2	-3.238	0.001***	2	-3.238	0.001***
2021-09-24 - 2022-03-25 ($N = 4183$)											
0.007	1.054	0.02	52.416	0.000***	0.408	16	-4.106	4.792e-5***	1	-4.698	4.028e-6***
2021-12-31 - 2022-06-24 ($N = 4024$)											
0.008	1.074	0.02	53.152	0.000***	0.414	15	-4.157	3.909e-5**	0	-4.939	1.392e-6***
2022-03-25 - 2022-09-30 ($N = 4395$)											
0.004	0.089	0.025	3.509	0.000***	0.003	28	-2.294	0.021**	2	-2.174	0.028**

Table 42: Results of performing the Engle-Granger test on each interval of ETH Coin-M futures using the funding rate cost-of-carry model. The left hand side of the table $\hat{\beta}$,$\sigma_{\hat{\beta}}$, t_β and R^2 are parameters corresponding to the OLS regression $f - s = \beta(r^{p_f} - \tilde{r}) + \epsilon$, and the parameters γ_{AIC}, $\hat{t}_{AIC}$, p_{AIC}, γ_{BIC}, $\hat{t}_{BIC}$ and p_{BIC} are parameters corresponding to the Augmented Dickey Fuller (ADF) test. Notice that *, ** and *** imply significant t-statistics at the 10,5, and 1% level, respectively.

EG-Test Bitcoin USD-M futures under the funding rate cost of carry model											
$\hat{\alpha}$	$\hat{\beta}$	$\sigma_{\hat{\beta}}$	t_β	p_β	R^2	γ_{AIC}	$\hat{t}_{AIC}$	p_{AIC}	γ_{BIC}	$\hat{t}_{BIC}$	p_{BIC}
2021-02-03 - 2021-03-26 ($N = 1169$)											
0.0123	0.743	0.011	65.374	0.000***	0.788	6	-4.147	4.080e-5***	1	-4.731	3.483e-6***
2021-03-16 - 2021-06-25 ($N = 2318$)											
0.014	0.988	0.013	76.322	0.000***	0.717	27	-4.331	1.919e-5***	2	-4.068	5.588e-5***
2021-06-18 - 2021-09-24 ($N = 2259$)											
0.008	0.051	0.012	4.306	0.000***	0.008	14	-2.251	0.023**	4	-4.4118	4.575e-5***
2021-09-22 - 2021-12-31 ($N = 2302$)											
0.006	1.118	0.013	88.414	0.000***	0.774	1	-4.845	2.116e-6***	1	-4.845	2.116e-6***
2021-12-24 - 2022-03-25 ($N = 2097$)											
0.003	1.765	0.027	66.068	0.000***	0.677	2	-4.311	2.089e-5***	1	-4.491	9.821e-6***
2021-03-22 - 2022-06-24 ($N = 2166$)											
0.004	0.073	0.032	2.270	0.023**	0.002	15	-1.571	0.109	4	-1.712	0.082*
2022-06-20 - 2022-09-30 ($N = 2403$)											
0.003	0.529	0.011	47.926	0.000***	0.490	3	-4.453	1.152e-5***	3	-4.453	1.152e-5***

Table 43: Results of performing the Engle-Granger test on each interval of BTC USD-M futures using the cost of carry model for investment assets. The left hand side of the table $\hat{\beta}$,$\sigma_{\hat{\beta}}$, t_β and R^2 are parameters corresponding to the OLS regression $f - s = \beta(r^{p_f} - \tilde{r}) + \epsilon$, and the parameters γ_{AIC}, $\hat{t}_{AIC}$, p_{AIC}, γ_{BIC}, $\hat{t}_{BIC}$ and p_{BIC} are parameters corresponding to the Augmented Dickey Fuller (ADF) test. Notice that *, ** and *** imply significant t-statistics at the 10,5, and 1% level, respectively.

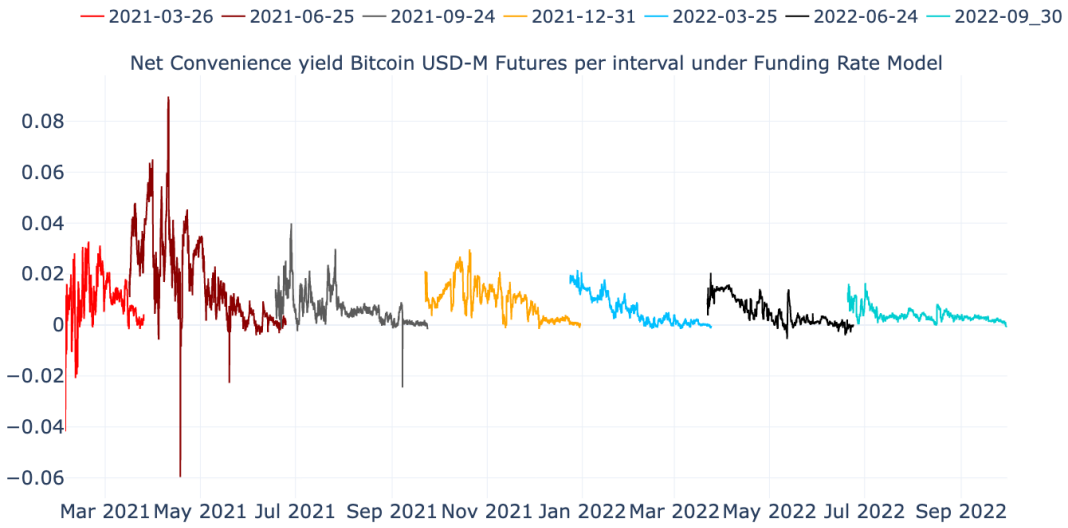

Figure 55: Net convenience yield δ Bitcoin USD-M futures under the funding rate cost of carry model.

EG-Test Ethereum USD-M futures under the funding rate cost of carry model											
$\hat{\alpha}$	$\hat{\beta}$	$\sigma_{\hat{\beta}}$	t_β	p_β	R^2	γ_{AIC}	$\hat{t}_{AIC}$	p_{AIC}	γ_{BIC}	$\hat{t}_{BIC}$	p_{BIC}
2021-02-03 - 2021-03-26 ($N = 1169$)											
0.0114	0.979	0.015	66.854	0.000***	0.798	21	-2.561	0.010***	2	-4.200	3.287e-5***
2021-03-16 - 2021-06-25 ($N = 2318$)											
0.014	1.077	0.015	71.003	0.000***	0.687	2	-3.704	0.000***	1	-3.908	0.001***
2021-06-18 - 2021-09-24 ($N = 2259$)											
0.046	0.009	0.012	3.747	0.000***	0.006	13	-2.500	0.012**	6	-3.624	0.001***
2021-09-22 - 2021-12-31 ($N = 2302$)											
0.006	1.128	0.014	81.319	0.000***	0.776	1	-3.824	0.001***	1	-3.824	0.001***
2021-12-24 - 2022-03-25 ($N = 2097$)											
0.002	1.885	0.029	66.107	0.000***	0.678	15	-3.709	0.001***	1	-4.555	7.465e-6***
2021-03-22 - 2022-06-24 ($N = 2166$)											
0.004	0.241	0.035	6.951	0.000**	0.022	6	-2.155	0.029**	6	-2.155	0.029**
2022-06-20 - 2022-09-30 ($N = 2403$)											
-0.0043	0.718	0.028	25.334	0.000***	0.212	2	-2.783	0.005***	1	-2.910	0.003***

Table 44: Results of performing the Engle-Granger test on each interval of ETH USD-M futures using the cost of carry model for investment assets. The left hand side of the table $\hat{\beta}$,$\sigma_{\hat{\beta}}$, t_β and R^2 are parameters corresponding to the OLS regression $f - s = \beta(r^{p_f} - \tilde{r}) + \epsilon$, and the parameters γ_{AIC}, $\hat{t}_{AIC}$, p_{AIC}, γ_{BIC}, $\hat{t}_{BIC}$ and p_{BIC} are parameters corresponding to the Augmented Dickey Fuller (ADF) test. Notice that *, ** and *** imply significant t-statistics at the 10,5, and 1% level, respectively.